Volume 4

MICROWAVE AND RF DESIGN
MODULES

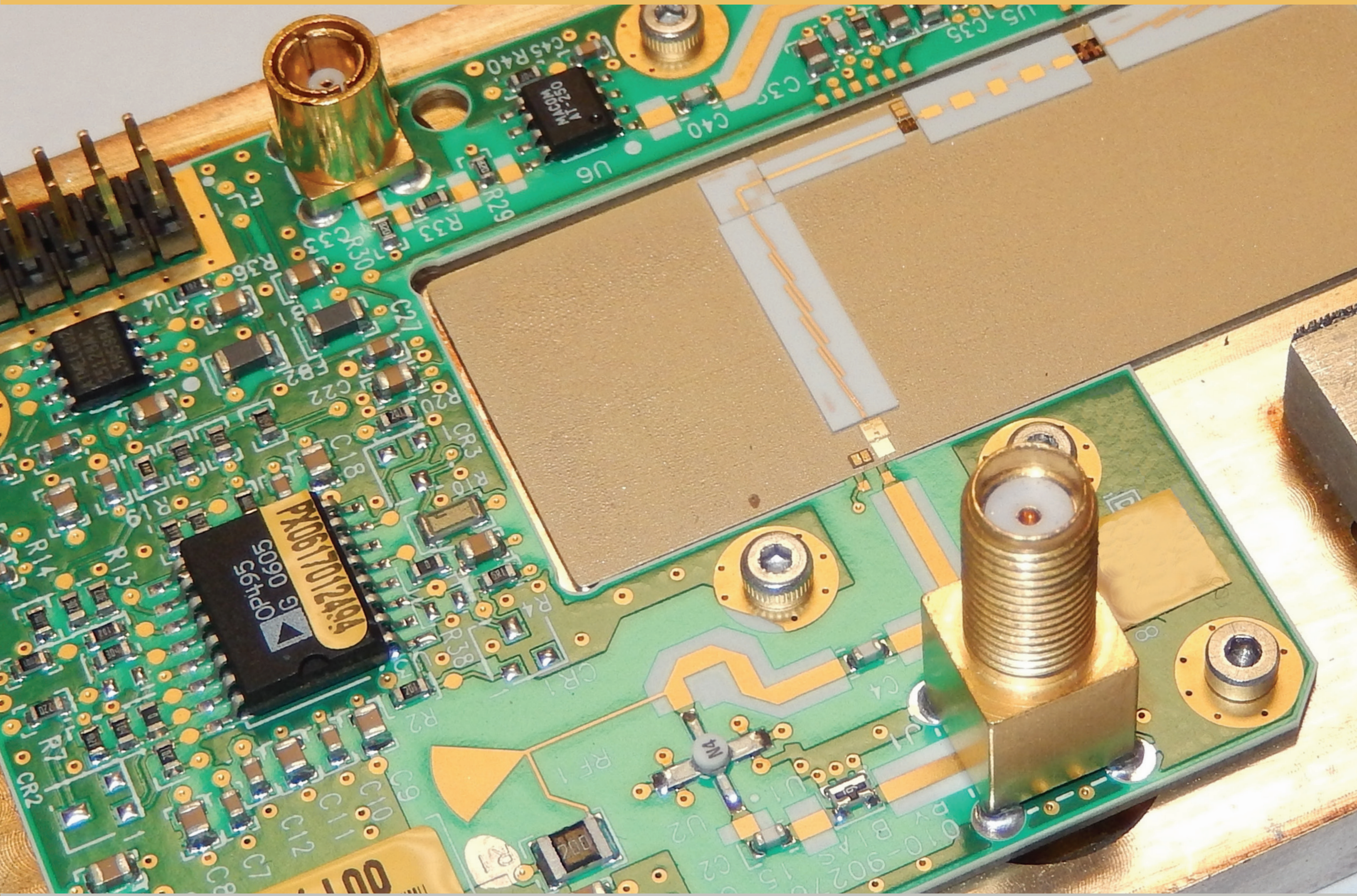

Michael Steer

Third Edition

Microwave and RF Design
Modules

Volume 4

Third Edition

Michael Steer

Microwave and RF Design
Modules

Volume 4

Third Edition

Michael Steer

Citation: Steer, Michael. *Microwave and RF Design: Modules*. Volume 4. (Third Edition), NC State University, 2019. doi: https//doi.org/10.5149/9781469656977_Steer

ISBN 978-1-4696-5696-0 (paperback)
ISBN 978-1-4696-5697-7 (open access ebook)

Published by NC State University

NC STATE UNIVERSITY

Distributed by the University of North Carolina Press
www.uncpress.org

Printing: 1

To my Son- and Daughter-in-Laws

Claudio and Tracy

Preface

The book series *Microwave and RF Design* is a comprehensive treatment of radio frequency (RF) and microwave design with a modern "systems-first" approach. A strong emphasis on design permeates the series with extensive case studies and design examples. Design is oriented towards cellular communications and microstrip design so that lessons learned can be applied to real-world design tasks. The books in the Microwave and RF Design series are:

- Microwave and RF Design: Radio Systems, Volume 1
- Microwave and RF Design: Transmission Lines, Volume 2
- Microwave and RF Design: Networks, Volume 3
- Microwave and RF Design: Modules, Volume 4
- Microwave and RF Design: Amplifiers and Oscillators, Volume 5

The length and format of each is suitable for automatic printing and binding.

Rationale

The central philosophy behind this series's popular approach is that the student or practicing engineer will develop a full appreciation for RF and microwave engineering and gain the practical skills to perform system-level design decisions. Now more than ever companies need engineers with an ingrained appreciation of systems and armed with the skills to make system decisions. One of the greatest challenges facing RF and microwave engineering is the increasing level of abstraction needed to create innovative microwave and RF systems. This book series is organized in such a way that the reader comes to understand the impact that system-level decisions have on component and subsystem design. At the same time, the capabilities of technologies, components, and subsystems impact system design. The book series is meticulously crafted to intertwine these themes.

Audience

The book series was originally developed for three courses at North Carolina State University. One is a final-year undergraduate class, another an introductory graduate class, and the third an advanced graduate class. Books in the series are used as supplementary texts in two other classes. There are extensive case studies, examples, and end of chapter problems ranging from straight-forward to in-depth problems requiring hours to solve. A companion book, *Fundamentals of Microwave and RF Design*, is more suitable for an undergraduate class yet there is a direct linkage between the material in this book and the series which can then be used as a career-long reference text. I believe it is completely understandable for senior-level students where a microwave/RF engineering course is offered. The book series is a comprehensive RF and microwave text and reference, with detailed index, appendices, and cross-references throughout. Practicing engineers will find the book series a valuable systems primer, a refresher as needed, and a reference tool in the field. Additionally, it can serve as a valuable, accessible resource for those outside RF circuit engineering who need to understand how they can work with RF hardware engineers.

Organization

This book is a volume in a five volume series on RF and microwave design. The first volume in the series, *Microwave and RF Design: Radio Systems*, addresses radio systems mainly following the evolution of cellular radio. A central aspect of microwave engineering is distributed effects considered in the second volume of this book series, *Microwave and RF Design: Transmission Lines*. Here transmission lines are treated as supporting forward- and backward-traveling voltage and current waves and these are related to electromagnetic effects. The third volume, *Microwave and RF Design: Networks*, covers microwave network theory which is the theory that describes power flow and can be used with transmission line effects. Topics covered in *Microwave and RF Design: Modules*, focus on designing microwave circuits and systems using modules introducing a large number of different modules. Modules is just another term for a network but the implication is that is is packaged and often available off-the-shelf. Other topics that are important in system design using modules are considered including noise, distortion, and dynamic range. Most microwave and RF designers construct systems using modules developed by other engineers who specialize in developing the modules. Examples are filter and amplifier modules which once designed can be used in many different systems. Much of microwave design is about maximizing dynamic range, minimizing noise, and minimizing DC power consumption. The fifth volume in this series, *Microwave and RF Design: Amplifiers and Oscillators*, considers amplifier and oscillator design and develops the skills required to develop modules.

Volume 1: Microwave and RF Design: Radio Systems

The first book of the series covers RF systems. It describes system concepts and provides comprehensive knowledge of RF and microwave systems. The emphasis is on understanding how systems are crafted from many different technologies and concepts. The reader gains valuable insight into how different technologies can be traded off in meeting system requirements. I do not believe this systems presentation is available anywhere else in such a compact form.

Volume 2: Microwave and RF Design: Transmission Lines

This book begins with a chapter on transmission line theory and introduces the concepts of forward- and backward-traveling waves. Many examples are included of advanced techniques for analyzing and designing transmission line networks. This is followed by a chapter on planar transmission lines with microstrip lines primarily used in design examples. Design examples illustrate some of the less quantifiable design decisions that must be made. The next chapter describes frequency-dependent transmission line effects and describes the design choices that must be taken to avoid multimoding. The final chapter in this volume addresses coupled-lines. It is shown how to design coupled-line networks that exploit this distributed effect to realize novel circuit functionality and how to design networks that minimize negative effects. The modern treatment of transmission lines in this volume emphasizes planar circuit design and the practical aspects of designing around unwanted effects. Detailed design of a directional coupler is used to illustrate the use of coupled lines. Network equivalents of coupled lines are introduced as fundamental building blocks that are used later in the synthesis of coupled-line filters. The text, examples, and problems introduce the often hidden design requirements of designing to mitigate parasitic effects and unwanted modes of operation.

Volume 3: Microwave and RF Design: Networks

Volume 3 focuses on microwave networks with descriptions based on S parameters and $ABCD$ matrices, and the representation of reflection and transmission information on polar plots called Smith charts. Microwave measurement and calibration technology are examined. A sampling of the wide variety of microwave elements based on transmission lines is presented. It is shown how many of these have lumped-element equivalents and how lumped elements and transmission lines can be combined as a compromise between the high performance of transmission line structures and the compactness of lumped elements. This volume concludes with an in-depth treatment of matching for maximum power transfer. Both lumped-element and distributed-element matching are presented.

Volume 4: Microwave and RF Design: Modules

Volume 4 focuses on the design of systems based on microwave modules. The book considers the wide variety of RF modules including amplifiers, local oscillators, switches, circulators, isolators, phase detectors, frequency multipliers and dividers, phase-locked loops, and direct digital synthesizers. The use of modules has become increasingly important in RF and microwave engineering. A wide variety of passive and active modules are available and high-performance systems can be realized cost effectively and with stellar performance by using off-the-shelf modules interconnected using planar transmission lines. Module vendors are encouraged by the market to develop competitive modules that can be used in a wide variety of applications. The great majority of RF and microwave engineers either develop modules or use modules to realize RF systems. Systems must also be concerned with noise and distortion, including distortion that originates in supposedly linear elements. Something as simple as a termination can produce distortion called passive intermodulation distortion. Design techniques are presented for designing cascaded systems while managing noise and distortion. Filters are also modules and general filter theory is covered and the design of parallel coupled line filters is presented in detail. Filter design is presented as a mixture of art and science. This mix, and the thought processes involved, are emphasized through the design of a filter integrated throughout this chapter.

Volume 5: Microwave and RF Design: Amplifiers and Oscillators

The fifth volume presents the design of amplifiers and oscillators in a way that enables state-of-the-art designs to be developed. Detailed strategies for amplifiers and voltage-controlled oscillators are presented. Design of competitive microwave amplifiers and oscillators are particularly challenging as many trade-offs are required in design, and the design decisions cannot be reduced to a formulaic flow. Very detailed case studies are presented and while some may seem quite complicated, they parallel the level of sophistication required to develop competitive designs.

Case Studies

A key feature of this book series is the use of real world case studies of leading edge designs. Some of the case studies are designs done in my research group to demonstrate design techniques resulting in leading performance. The case studies and the persons responsible for helping to develop them are as follows.

1. Software defined radio transmitter.
2. High dynamic range down converter design. This case study was developed with Alan Victor.
3. Design of a third-order Chebyshev combline filter. This case study was developed with Wael Fathelbab.
4. Design of a bandstop filter. This case study was developed with Wael Fathelbab.
5. Tunable Resonator with a varactor diode stack. This case study was developed with Alan Victor.
6. Analysis of a 15 GHz Receiver. This case study was developed with Alan Victor.
7. Transceiver Architecture. This case study was developed with Alan Victor.
8. Narrowband linear amplifier design. This case study was developed with Dane Collins and National Instruments Corporation.
9. Wideband Amplifier Design. This case study was developed with Dane Collins and National Instruments Corporation.
10. Distributed biasing of differential amplifiers. This case study was developed with Wael Fathelbab.
11. Analysis of a distributed amplifier. This case study was developed with Ratan Bhatia, Jason Gerber, Tony Kwan, and Rowan Gilmore.
12. Design of a WiMAX power amplifier. This case study was developed with Dane Collins and National Instruments Corporation.
13. Reflection oscillator. This case study was developed with Dane Collins and National Instruments Corporation.
14. Design of a C-Band VCO. This case study was developed with Alan Victor.
15. Oscillator phase noise analysis. This case study was developed with Dane Collins and National Instruments Corporation.

Many of these case studies are available as captioned YouTube videos and qualified instructors can request higher resolution videos from the author.

Course Structures

Based on the adoption of the first and second editions at universities, several different university courses have been developed using various parts of what was originally one very large book. The book supports teaching two or three classes with courses varying by the selection of volumes and chapters. A standard microwave class following the format of earlier microwave texts can be taught using the second and third volumes. Such a course will benefit from the strong practical design flavor and modern treatment of measurement technology, Smith charts, and matching networks. Transmission line propagation and design is presented in the context of microstrip technology providing an immediately useful skill. The subtleties of multimoding are also presented in the context of microstrip lines. In such a class the first volume on microwave systems can be assigned for self-learning.

Another approach is to teach a course that focuses on transmission line effects including parallel coupled-line filters and module design. Such a class would focus on Volumes 2, 3 and 4. A filter design course would focus on using Volume 4 on module design. A course on amplifier and oscillator design would use Volume 5. This course is supported by a large number of case studies that present design concepts that would otherwise be difficult to put into the flow of the textbook.

Another option suited to an undergraduate or introductory graduate class is to teach a class that enables engineers to develop RF and microwave systems. This class uses portions of Volumes 2, 3 and 4. This class then omits detailed filter, amplifier, and oscillator design.

The fundamental philosophy behind the book series is that the broader impact of the material should be presented first. Systems should be discussed up front and not left as an afterthought for the final chapter of a textbook, the last lecture of the semester, or the last course of a curriculum.

The book series is written so that all electrical engineers can gain an appreciation of RF and microwave hardware engineering. The body of the text can be covered without strong reliance on this electromagnetic theory, but it is there for those who desire it for teaching or reader review. The book is rich with detailed information and also serves as a technical reference.

The Systems Engineer

Systems are developed beginning with fuzzy requirements for components and subsystems. Just as system requirements provide impetus to develop new base technologies, the development of new technologies provides new capabilities that drive innovation and new systems. The new capabilities may arise from developments made in support of other systems. Sometimes serendipity leads to the new capabilities. Creating innovative microwave and RF systems that address market needs or provide for new opportunities is the most exciting challenge in RF design. The engineers who can conceptualize and architect new RF systems are in great demand. This book began as an effort to train RF systems engineers and as an RF systems resource for practicing engineers. Many RF systems engineers began their careers when systems were simple. Today, appreciating a system requires higher levels of abstraction than in the past, but it also requires detailed knowledge or the ability to access detailed knowledge and expertise. So what makes a systems engineer? There is not a simple answer, but many partial answers. We know that system engineers have great technical confidence and broad appreciation for technologies. They are both broad in their knowledge of a large swath of technologies and also deep in knowledge of a few areas, sometimes called the “T” model. One book or course will not make a systems engineer. It is clear that there must be a diverse set of experiences. This book series fulfills the role of fostering both high-level abstraction of RF engineering and also detailed design skills to realize effective RF and microwave modules. My hope is that this book will provide the necessary background for the next generation of RF systems engineers by stressing system principles immediately, followed by core RF technologies. Core technologies are thereby covered within the context of the systems in which they are used.

Supplementary Materials

Supplementary materials available to qualified instructors adopting the book include PowerPoint slides and solutions to the end-of-chapter problems. Requests should be directed to the author. Access to downloads of the books, additional material and YouTube videos of many case studies are available at `https://www.lib.ncsu.edu/do/open-education`

Acknowledgments

Writing this book has been a large task and I am indebted to the many people who helped along the way. First I want to thank the more than 1200 electrical engineering graduate students who used drafts and the first two editions at NC State. I thank the many instructors and students who have provided feedback. I particularly thank Dr. Wael Fathelbab, a filter expert, who co-wrote an early version of the filter chapter. Professor Andreas Cangellaris helped in developing the early structure of the book. Many people have reviewed the book and provided suggestions. I thank input on the structure of the manuscript: Professors Mark Wharton and Nuno Carvalho of Universidade de Aveiro, Professors Ed Delp and Saul Gelfand of Purdue University, Professor Lynn Carpenter of Pennsylvania State University, Professor Grant Ellis of the Universiti Teknologi Petronas, Professor Islam Eshrah of Cairo University, Professor Mohammad Essaaidi and Dr. Otman Aghzout of Abdelmalek Essaadi Univeristy, Professor Jianguo Ma of Guangdong University of Technology, Dr. Jayesh Nath of Apple, Mr. Sony Rowland of the U.S. Navy, and Dr. Jonathan Wilkerson of Lawrence Livermore National Laboratories, Dr. Josh Wetherington of Vadum, Dr. Glen Garner of Vadum, and Mr. Justin Lowry who graduated from North Carolina State University.

Many people helped in producing this book. In the first edition I was assisted by Ms. Claire Sideri, Ms. Susan Manning, and Mr. Robert Lawless who assisted in layout and production. The publisher, task master, and chief coordinator, Mr. Dudley Kay, provided focus and tremendous assistance in developing the first and second editions of the book, collecting feedback from many instructors and reviewers. I thank the Institution of Engineering and Technology, who acquired the original publisher, for returning the copyright to me. This open access book was facilitated by John McLeod and Samuel Dalzell of the University of North Carolina Press, and by Micah Vandergrift and William Cross of NC State University Libraries. The open access ebooks are host by NC State University Libraries.

The book was produced using LaTeX and open access fonts, line art was drawn using xfig and inkscape, and images were edited in gimp. So thanks to the many volunteers who developed these packages.

My family, Mary, Cormac, Fiona, and Killian, gracefully put up with my absence for innumerable nights and weekends, many more than I could have ever imagined. I truly thank them. I also thank my academic sponsor, Dr. Ross Lampe, Jr., whose support of the university and its mission enabled me to pursue high risk and high reward endeavors including this book.

Michael Steer
North Carolina State University
Raleigh, North Carolina
mbs@ncsu.edu

List of Trademarks

3GPP® is a registered trademark of the European Telecommunications Standards Institute.

802® is a registered trademark of the Institute of Electrical & Electronics Engineers .

APC-7® is a registered trademark of Amphenol Corporation.

AT&T® is a registered trademark of AT&T Intellectual Property II, L.P.

AWR® is a registered trademark of National Instruments Corporation.

AWRDE® is a trademark of National Instruments Corporation.

Bluetooth® is a registered trademark of the Bluetooth Special Interest Group.

GSM® is a registered trademark of the GSM MOU Association.

Mathcad® is a registered trademark of Parametric Technology Corporation.

MATLAB® is a registered trademark of The MathWorks, Inc.

NEC® is a registered trademark of NEC Corporation.

OFDMA® is a registered trademark of Runcom Technologies Ltd.

Qualcomm® is a registered trademark of Qualcomm Inc.

Teflon® is a registered trademark of E. I. du Pont de Nemours.

RFMD® is a registered trademark of RF Micro Devices, Inc.

SONNET® is a trademark of Sonnet Corporation.

Smith is a registered trademark of the Institute of Electrical and Electronics Engineers.

Touchstone® is a registered trademark of Agilent Corporation.

WiFi® is a registered trademark of the Wi-Fi Alliance.

WiMAX® is a registered trademark of the WiMAX Forum.

All other trademarks are the properties of their respective owners.

Contents

CHAPTER 1

Introduction to RF and Microwave Modules

1.1 Introduction to Microwave Modules

Most microwave design develops microwave systems using modules such amplifiers, integrated circuits (ICs), filters, frequency multipliers, and passive components. Economics necessitate that since modules are expensive to design, e.g RF integrated circuits, that they be developed for multiple applications. In system design modules are chosen for their dynamic range, noise performance, DC power consumption, and cost. Foremost the system designer must have knowledge of available modules and be prepared to design a module itself if this results in competitive performance and manages cost. Modules are interconnected by transmission lines, bias settings and matching networks must be designed, and a system frequency plan must be developed that trades-off cost and performance while avoiding interference. All these topics are addressed on this book which develops the knowledge of modules, and the skills required to design microwave systems.

Most RF systems are composed of a cascade of modules each of which is separately designed and characterized. They often have $50\ \Omega$ input and output impedances so that modules can be freely interconnected. Just as often matching networks must be design by the user as otherwise operating frequencies are pre-determined by the module vendor as a matching network usually has a narrower bandwidth than that of the functional core of the module. In high volume applications, several modules could be monolithically integrated, but even then, design is based on the concept of modules. Many modules are available "off the shelf" and high-performance RF systems can be constructed using them.

Examples of commercially available modules are shown in Figure 1-1. They can range in complexity from the surface mount resistor of Figure 1-1(a) and the transformer of Figure 1-1(d), up to the mixer and synthesizer modules shown in Figures 1-1(b and c). Modules can have very good performance as it is cost effective to put considerable design effort into a module that can be used in many applications and thus design costs shared.

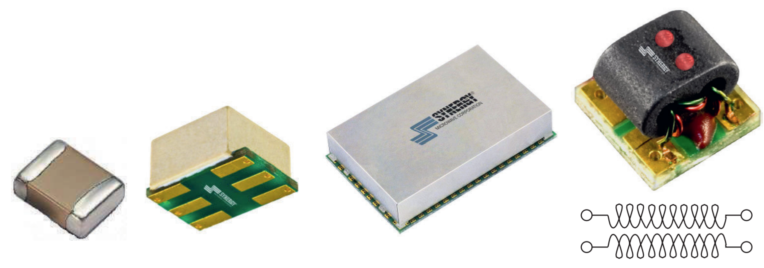

(a) Resistor (b) Mixer (c) Synthesizer (d) Transformer

Figure 1-1: Modules in surface-mount packages. Copyright Synergy Microwave Corporation, used with permission [1].

1.2 A 15 GHz Receiver Subsystem

An example of a microwave subsystem designed using modules is the 15 GHz receiver subsystem shown in Figure 1-2 with details of the frequency conversion section shown in Figure 1-3. This receiver subsystem is itself a module used in building a complete transceiver system for a point-to-point microwave link connecting two basestations. The modules of the receiver include amplifiers, frequency multipliers, a mixers, an isolator, and a waveguide adaptor. These modules are available as off-the-shelf components from companies that specialize in developing them, and selling them to a large user base. This receiver is the subject of a case study in Section 7.6 where more details of the modules, frequency planning, and signal flow are given.

1.3 Book Outline

This book describes modules and tools required to design microwave systems using modules. A large number of modules are presented with the aim of building a 'module vocabulary.' An engineer must know what modules are available before a microwave system can be designed using modules.

The first set of modules examined are filters in Chapter 2. These have the important task of only letting wanted signals through a circuit while blocking noise and unwanted signals. Then parallel coupled line (PCL) filters are considered in Chapter 3. A PCL filter is the most common type of microwave filter and is based on the inherent filtering properties of a pair of coupled transmission lines.

Chapter 4 introduces metrics for noise, distortion, and dynamic range and introduces the tools that are required to design systems of cascaded modules that minimize noise and distortion, and maximize dynamic range.

Chapter 5 develops knowledge of passive modules, particular ones that use diodes and switches. The final chapter, Chapter 6, considers mixer and source modules.

This book is the fourth volume in a series on microwave and RF design. The first volume in the series addresses radio systems [2] mainly following the evolution of cellular radio. A central aspect of microwave engineering is distributed effects considered in the second volume of the series [3]. Here the transmission lines are treated as supporting forward- and backward-traveling voltage and current waves and these are related to electromagnetic effects. The third volume [4] covers microwave network theory which is the theory that describes power flow in microwave circuits and can be used to describe transmission line effects. Topics covered in this volume include scattering parameters, Smith charts, and matching networks that

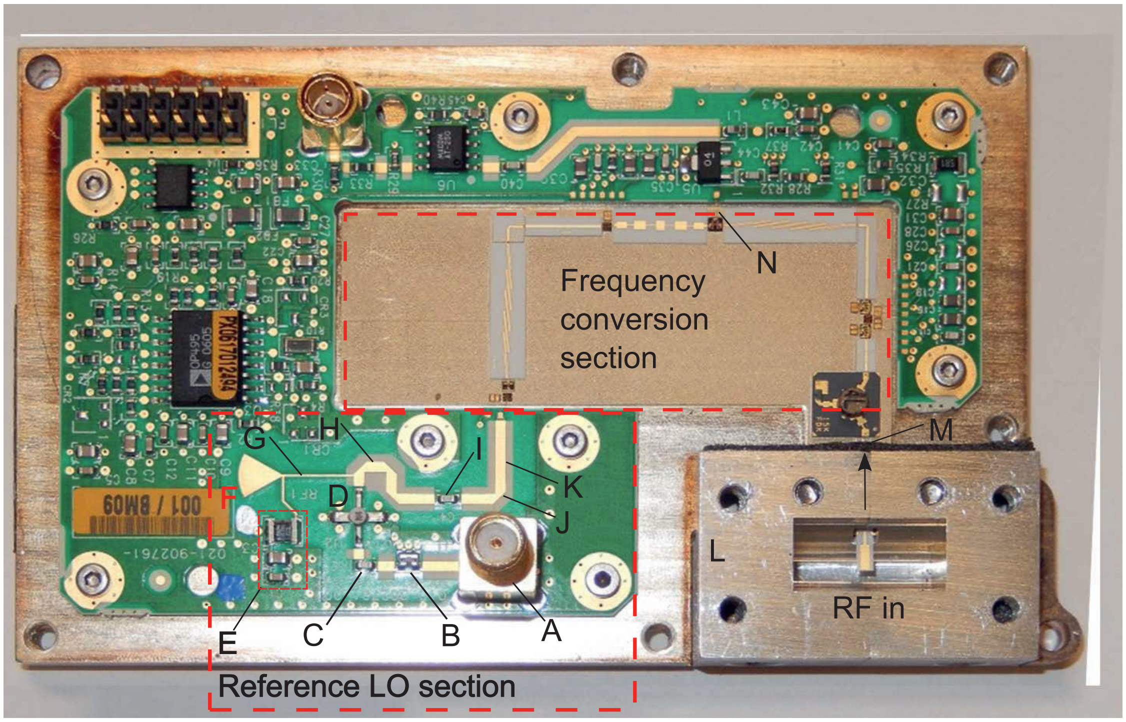

A	SMA connector, Reference LO in	**H**	50 Ω transmission line
B	Attenuator	**I**	DC blocking capacitor
C	DC blocking capacitor	**J**	Mitered bend
D	Reference LO amplifier	**K**	50 Ω transmission line
E	Bias line	**L**	Waveguide-to-microstrip adaptor, RF in
F	Radial stub	**M**	Interface to frequency conversion section
G	High-impedance transmission line	**N**	Interface to IF section

Figure 1-2: A 14.4–15.35 GHz receiver module itself consisting of cascaded modules interconnected by microstrip transmission lines. Surrounding the microwave circuit are DC conditioning and control circuitry. RF in is 14.4 GHz to 15.35 GHz, LO in is 1600.625 MHz to 1741.875 MHz. The frequency of the IF is 70–1595 MHz. Detail of the frequency conversion section mounted on the mat is shown in Figure 1-3. The silk-screened mat provides a strain-relieving surface for mounting ceramic- and semiconductor-based modules.

enable maximum power transfer. The fifth volume in this series [5] considers amplifier and oscillator design and develops the skills required to develop modules.

The books in the Microwave and RF Design series are:

- Microwave and RF Design: Radio Systems
- Microwave and RF Design: Transmission Lines
- Microwave and RF Design: Networks
- Microwave and RF Design: Modules
- Microwave and RF Design: Amplifiers and Oscillators

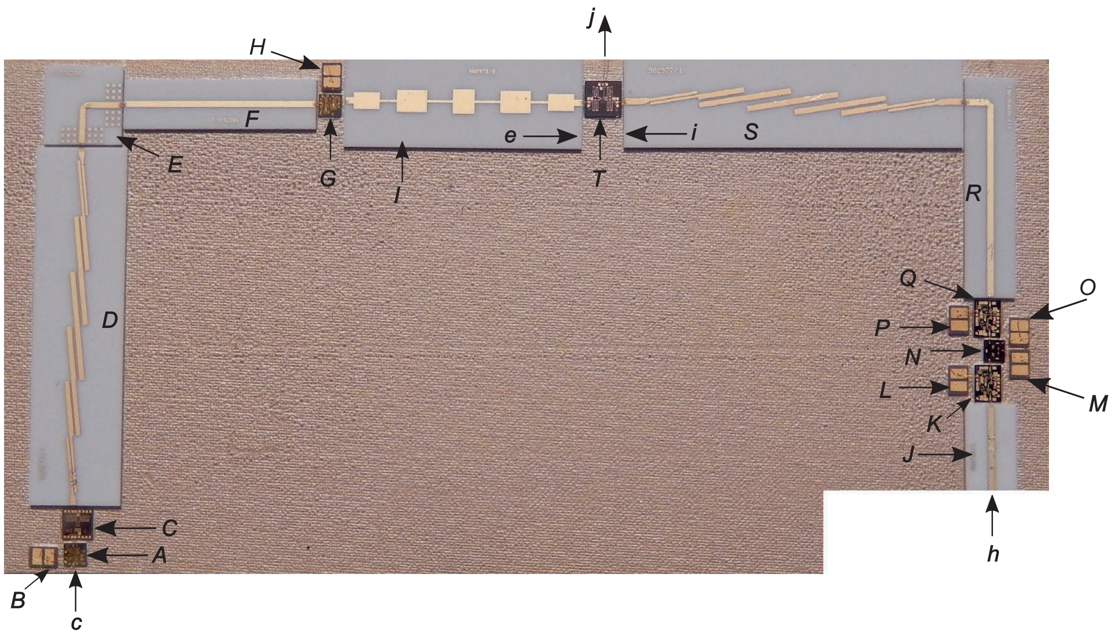

A	Reference LO amplifier	*K*	RF amplifier
B	Power supply decoupling capacitor	*L*	Power supply decoupling capacitor
C	×2 frequency multiplier	*M*	Power supply decoupling capacitor
D	Edge-coupled PCL bandpass filter	*N*	Voltage variable attenuator
E	Microstrip bend	*O*	Power supply decoupling capacitor
F	Microstrip transmission line	*P*	Power supply decoupling capacitor
G	×2 frequency multiplier	*Q*	RF amplifier
H	Power supply decoupling capacitor	*R*	Microstrip transmission line and bend
I	stepped impedance lowpass filter	*S*	Edge-coupled PCL bandpass filter
J	Microstrip transmission line	*T*	Subharmonic mixer

Figure 1-3: Frequency conversion section of the receiver module shown in Figure 1-2. The reference LO is applied to the frequency conversion section at *c*, the RF is applied at *h* following the isolator. The IF is output at *j*.

1.4 References

[1] http://www.synergymwave.com.

[2] M. Steer, *Microwave and RF Design, Radio Systems*, 3rd ed. North Carolina State University, 2019.

[3] ——, *Microwave and RF Design, Transmission Lines*, 3rd ed. North Carolina State University, 2019.

[4] ——, *Microwave and RF Design, Networks*, 3rd ed. North Carolina State University, 2019.

[5] ——, *Microwave and RF Design, Amplifiers and Oscillators*, 3rd ed. North Carolina State University, 2019.

[6] IEEE Standard 315-1975, Graphic Symbols for Electrical and Electronics Diagrams (Including Reference Designation Letters), Adopted Sept. 1975, Reaffirmed Dec. 1993. Approved by American National Standards Institute, Jan. 1989. Approved adopted for mandatory use, Department of Defense, United States of America, Oct. 1975. Approved by Canadian Standards Institute, Oct. 1975.

[7] R. Baker, *CMOS Circuit Design, Layout, and Simulation*, 2nd ed. Wiley-Interscience, IEEE Press, 2008.

Appendix

1.A RF and Microwave Circuit Schematic Symbols

This appendix lists the symbols commonly used with RF and microwave circuits. Symbols are from IEEE Standard 315-1975 [6]. Up until the 1970s IEEE was active in establishing standard symbols for all electrical engineering fields and in particular circuit schematic symbols to be used with microwave circuits. Since then vendors of microwave computer-aided design tools have developed their own symbols but very often a vendor tends to adopt symbols similar to those used by other vendors. However there are differences and as a result there has not been a consensus to adopt a more modern standard for microwave symbols. What is presented in this chapter follows the earlier IEEE standard where possible and for components that are not in the standard, an attempt has been made to select symbols that are in common use in technical papers.

1.A.1 Element and Circuit Symbols

Table 1-1: IEEE standard qualifying properties added to schematic symbols to identify a particular property.

Qualifying property	Symbol
Adjustable	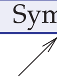
Adjustable, continuously adjustable	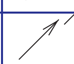
Adjustable, stepped	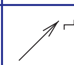
Linear	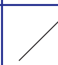
Nonlinear	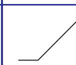
Positive	+
Negative	–

Table 1-2: Standard schematic symbols of RF and microwave components.

Component	Symbol	Alternate
Analog to digital converter		
Attenuator, fixed		
Attenuator, balanced		
Attenuator, unbalanced		
Attenuator, variable		
Attenuator, continuously variable		
Attenuator, stepped		
Amplifier		
Antenna, general		
Antenna, balanced		
Antenna, dipole		
Antenna, loop		
Balun		
Balun with coaxial line and dipole antenna		
Capacitor, general		
Capacitor, polarized	+	
Capacitor, variable		
Capacitor, nonlinear		
Capacitor, shielded		
Circulator		
Coaxial cable		
Conductive path		
Connector, female		
Connector, male		
Contact, fixed		
Contact, closed		
Contact, open		
Delay		
Digital-to-analog converter (DAC)		
Element, linear (* to be replaced by designation)	*	*
Ground, general		
Ground, chassis		
Coupler		
Filter, bandpass filter (BPF)		
Filter, lowpass filter (LPF)		

Component	Symbol	Alternate
Filter, highpass filter (HPF)		
Filter, bandstop filter (BSF)		
Isolator		
Inductor, general		
Inductor with magnetic core		
Junction		
Junction of paths		
Network, linear (* to be replaced by designation)	*	
Open		
Phase shifter	ϕ	β
Piezoelectric resonator		
Port		
Power divider	P_1 −3 dB P_2 P_3	
Radio link		
Radio link with antennas		
Rectifier		
Resistor, general		
Resistor, variable		
Resistor, nonlinear		
Resistor with open path		
Resistor with short		

Component	Symbol	Alternate
Shield		
Short, movable		
Source, AC		
Source, DC		+ −
Switch, multiposition		
Test, point		
Transformer		
Transformer with magnetic core		
Transformer, center tapped		
Triax		
Twinax		
Twinax with shield showing connection		
Twinax with shield grounded		
Short		
Wire		
Wires, connected		
Wires, unconnected, crossing		

1.A.2 Sources

Commonly used symbols for sources.

Component	Symbol
Voltage source	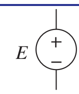
Current source	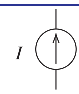
AC source	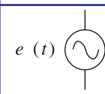
Controlled voltage source	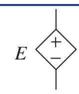

Component	Symbol
Controlled current source	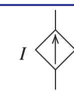
Voltage noise source	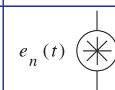
Current noise source	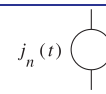

1.A.3 Diodes

IEEE standard symbols for diodes and a rectifier [6]. ([1]In the direction of anode (A) to cathode (K). [2]Use symbol for general diode unless it is essential to show intrinsic region.)

Component	Symbol
Diode, general (including Schottky)[1]	
Gunn diode[1]	
IMPATT diode[1]	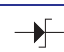
PIN diode[1,2]	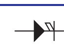
Light emitting diode (LED)[1]	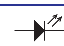

Component	Symbol
Rectifier[1]	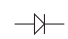
Tunnel diode1	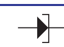
Varactor diode[1]	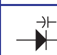 or 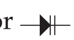
Zener diode[1]	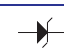

1.A.4 Bipolar Junction Transistor

IEEE standard schematic symbols for bipolar junction transistors (BJT and HBT) [6] and commonly used symbols in layouts [7]. The letters indicate terminals: B (base), C (collector), E (emitter).

Transistor	IEEE symbol	Commonly used symbol
BJT, pnp	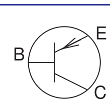	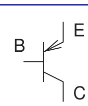

Transistor	IEEE symbol	Commonly used symbol
BJT, npn	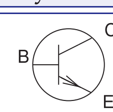	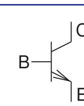

1.A.5 Junction Field Effect Transistor

Table 1-3: IEEE standard schematic symbols for junction field effect transistors (MESFET, HEMT, JFET) [6] and symbols more commonly used in schematics. The letters indicate terminals: G (gate), D (drain), S (source).

Transistor	IEEE symbol	Commonly used symbol
FET, pJFET	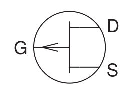	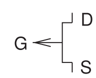
FET, nJFET, MESFET, HEMT	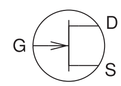	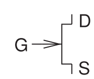

1.A.6 Metal-Oxide-Semiconductor Field Effect Transistor

Table 1-4: IEEE standard schematic symbols for MOSFET transistors [6] and symbols more commonly used in schematics [7]. The MOSFET symbols are for enhancement- and depletion-mode transistors. The letters indicate terminals: G (gate), D (drain), S (source), U (bulk). Four-terminal and three-terminal common symbols are shown. The three-terminal common symbol is most often used when the bulk is connected to the most negative connection in the circuit, and the pMOSFET symbol is used when the bulk is tied to V_{DD} (the most positive connection). The bulk connection is often not shown, as it is assumed to be connected to the most negative voltage point.

Transistor	IEEE symbol	Commonly used symbol (three-terminal)	Commonly used symbol (four-terminal)
FET, nMOS, depletion	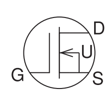	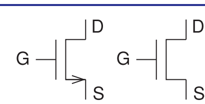	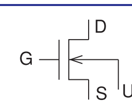
FET, pMOS, depletion	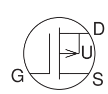	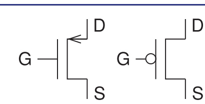	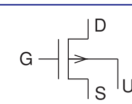
FET, nMOS, enhancement	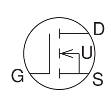	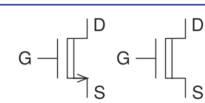	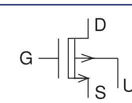
FET, pMOS, enhancement	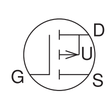	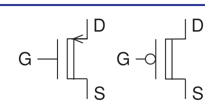	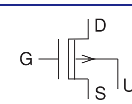

CHAPTER 2

Filters

With Wael Fathelbab

2.1 Introduction

Filters are the most fundamental of signal processing circuits using energy storage elements to obtain frequency-dependent characteristics. Some of the important filter attributes are (1) controlling noise by not allowing out-of-band noise to propagate in a circuit; (2) keeping signals outside the transmit band, especially harmonics, from being transmitted; and (3) presenting only signals in a specified band to active receive circuitry. At microwave frequencies a filter can consist solely of lumped elements, solely of distributed elements, or a mix of lumped and distributed elements. The distributed realizations can be transmission line-based implementations of the components of lumped-element filter prototypes or, preferably, make use of the particular frequency characteristics found with certain distributed structures. Loss in lumped elements, particularly above a few gigahertz, means that the performance of distributed filters nearly always exceeds that of lumped-element filters. However, since the basic component of a distributed filter is a one-quarter wavelength long transmission line, distributed filters can be prohibitively large below a few gigahertz.

Only a few basic types of responses are required of most RF filters as follows:

(a) Lowpass—providing maximum power transfer at frequencies below the corner frequency, f_0. Above f_0, transmission is blocked. See Figure 2-1(a).

(b) Highpass—passing signals at frequencies above f_0. Below f_0, transmission is blocked. See Figure 2-1(b).

(c) Bandpass—passing signals at frequencies between lower and upper corner frequencies (defining the passband) and blocking transmission outside the band. This is the most common type of RF filter. See Figure 2-1(c).

(d) Bandstop (or notch)—which blocks signals between lower and upper corner frequencies (defining the stopband). See Figure 2-1(d).

(e) Allpass—which equalizes a signal by adjusting the phase generally to correct for phase distortion elsewhere. See Figure 2-1(e).

The above list is not comprehensive, as actual operating conditions may mandate specific frequency profiles. For example, WiFi systems operating at 2.45 GHz are susceptible to potentially large signals being transmitted from nearby cellular phones operating in the 1700–2300 MHz range. Thus a front-end filter for a 2.45 GHz system must ensure very high levels of attenuation over the 1700–2300 MHz range. Thus the optimum solution here, probably, will have an asymmetrical frequency response with high rejection on one side of the passband obtained by accepting lower rejection on the other side.

2.1.1 Filter Prototypes

In the 1960s an approach to RF filter design and synthesis was developed and this is still followed. The approach is to translate the mathematical response of a lowpass filter. A filter with the desired lowpass response is then synthesized using lumped elements and the resulting filter is called a lowpass prototype. The lowpass filter is then transformed so that the new lumped-element filter has the desired RF response, such as highpass or bandpass. In the case of a bandpass filter, each inductor and capacitor of the lowpass prototype becomes a resonator that is coupled to another resonator. In distributed form, this basic resonator is a one-quarter wavelength long transmission line.

Filter synthesis is a systematic approach to realizing circuits with desired frequency characteristics. A filter can also be thought of as a hardware implementation of a differential equation producing a specific impulse,

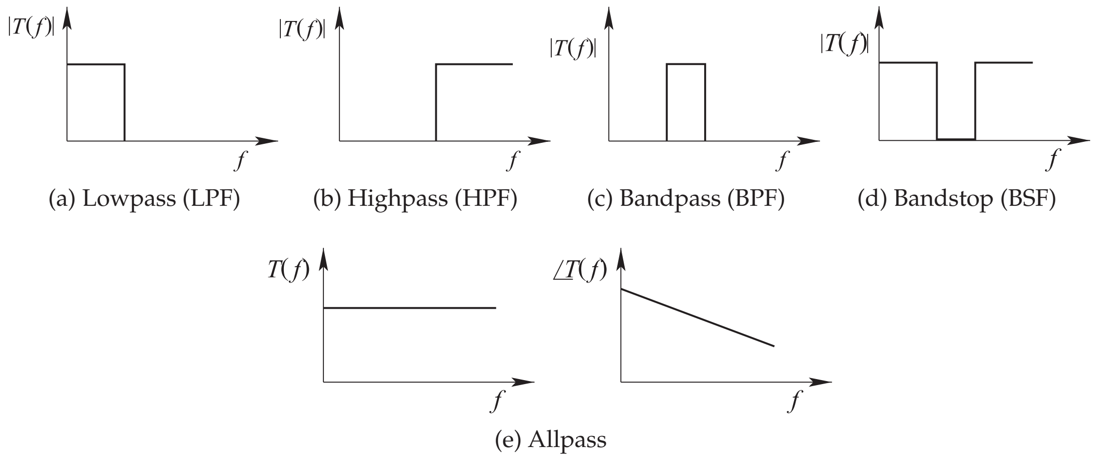

Figure 2-1: Ideal filter transfer function, $T(f)$, responses.

step, or frequency response. It is not surprising that a filter can be described this way as the lumped reactive elements, L and C, describe first-order differential equations and their interconnection describes higher-order differential equations.

The synthesis of a filter response begins by identifying the desired differential equation response. The differential equations are specified using the Laplace variable, s, so that in the frequency domain (with $s = \jmath\omega$) an nth-order differential equation becomes an nth-order polynomial expression in s. If possible, and this is usually the case, a lowpass version of a filter can be developed. The conversion to the final filter shape, say a bandpass response, proceeds mathematically through a number of stages. Each stage has a circuit form and each stage is called a filter prototype.

2.1.2 Image Parameter Versus Insertion loss Methods

Filter networks can be synthesized using the image parameter method or the reflection coefficient (or insertion loss) method [1]. The image parameter measured is based on cascading two-port networks with each two-port having the essential desired filter response [2]. Several of these two-ports are cascaded to achieve a periodic-like structure that has the final desired filter response. This method is restrictive and arbitrary filter responses can not be obtained. It is rarely used in RF and microwave filter design but is useful in analyzing simple structures with cascades of identical elements [3]. A better approach is to use the insertion loss method as used in this chapter.

2.2 Singly and Doubly Terminated Networks

Filters are generally two-port networks and they provide maximum power transfer from a source to a load over a specified frequency range while rejecting the transmission of signals at other frequencies. Two possible filter networks are shown in Figure 2-2. The network in Figure 2-2(a) is known as a doubly terminated network, as both ports are resistively terminated.

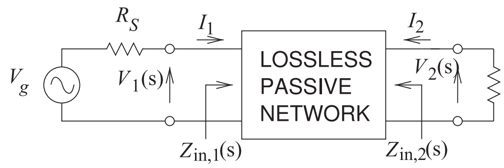

(a) Doubly terminated network

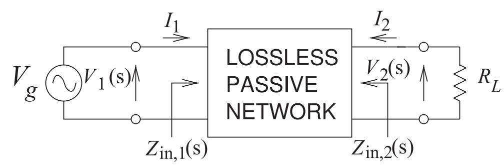

(b) Singly terminated network

Figure 2-2: Terminated networks.

The network in Figure 2-2(b) is called a singly terminated network, as only one port is terminated in a resistor. The doubly terminated network is much closer to the type of network required at RF where loads and source impedances are finite. A singly terminated network is applicable in some RF integrated circuit applications where very little RF power is involved and often when feedback is used. In such cases the output of an RFIC amplifier can approximate an ideal voltage source as the Thevenin equivalent source impedance can be negligible. Most synthesis of singly terminated filter networks uses an analogous procedure to that presented here for doubly terminated filters.

2.2.1 Doubly Terminated Networks

The established filter synthesis procedure for doubly terminated filter networks focuses on realizing the input reflection coefficient. For a lossless filter the square of the reflection coefficient magnitude is one minus the square of the insertion loss and this is the origin of this method being called the insertion loss method.

The input reflection coefficient of the doubly terminated network in Figure 2-2(a) is

$$\Gamma_1\left(s\right) = \frac{Z_{\text{in},1}(s) - R_S}{Z_{\text{in},1}(s) + R_S}, \tag{2.1}$$

where the reference impedance is the source resistance, R_S, and s is the Laplace variable. In the passband of a filter the reflection coefficient is approximately zero.

There are several other parameters used in filter design and these will be introduced now. The **transducer power ratio** (**TPR**) is defined as

$$\begin{aligned}\text{TPR} &= \frac{\text{Maximum power available from the source}}{\text{Power absorbed by the load}} \\ &= \frac{\frac{1}{2}(V_g(s)/2)^2/R_S}{\frac{1}{2}V_2^2(s)/R_L} = \left|\frac{1}{2}\sqrt{\frac{R_L}{R_S}}\frac{V_g(s)}{V_2(s)}\right|^2 .\end{aligned} \tag{2.2}$$

The transmission coefficient, $T(s)$, of the network is

$$T(s) = \frac{1}{\sqrt{\text{TPR}(s)}} = 2\sqrt{\frac{R_S}{R_L}}\frac{V_2(s)}{V_g(s)}, \tag{2.3}$$

IF the filter is lossless, the insertion loss (IL) (or **transducer function**) is

$$\text{IL}(s) = \text{TPR}(s) = \left|1/T(s)\right|^2 . \tag{2.4}$$

The next step in development of the filter synthesis procedure is introduction of the **characteristic function**, defined as the ratio of the reflection and transmission coefficients:

$$K(s) = \frac{\Gamma_1(s)}{T(s)} = \frac{N(s)}{D(s)}, \tag{2.5}$$

where N is the numerator function and D is the denominator function. Ideally the filter network is lossless and so, from the principle of energy conservation, the sum of the magnitudes squared of the transmission and reflection coefficients must be unity:

$$|T(s)|^2 + |\Gamma_1(s)|^2 = 1. \tag{2.6}$$ That is, $$|T(s)|^2 = 1 - |\Gamma_1(s)|^2. \tag{2.7}$$

Dividing both sides of Equation (2.7) by $|T(s)|^2$ results in

$$1 = \frac{1}{|T(s)|^2} - \frac{|\Gamma_1(s)|^2}{|T(s)|^2}, \tag{2.8}$$ or $$1 = |\mathrm{IL}(s)| - |K(s)|^2. \tag{2.9}$$

Rearranging Equation (2.9) leads to

$$|\mathrm{IL}(s)| = 1 + |K(s)|^2 \tag{2.10}$$

and so $$|T(s)|^2 = \frac{1}{1 + |K(s)|^2} \tag{2.11}$$ and $$|\Gamma_1(s)|^2 = \frac{|K(s)|^2}{1 + |K(s)|^2}. \tag{2.12}$$

In the above it is seen that both the reflection and transmission coefficients are functions of the characteristic function of the two-port network. A milestone has been reached. In an RF filter, the frequency-dependent insertion loss or transmission coefficient is of most importance, as these are directly related to power flow. Equation (2.11) shows that this can be expressed in terms of another function, $K(s)$, which, from Equation (2.5), can be expressed as the ratio of $N(s)$ and $D(s)$. For lumped-element circuits, $N(s)$ and $D(s)$ are polynomials.

2.2.2 Lowpass Filter Response

As an example of the relationship of the various filter responses, consider the lossless lowpass filter responses shown in Figure 2-3. This filter has a lowpass response with a corner frequency expressed in radians as $\omega_c = 1$ rad/s. Ideally $T(s)$ for $s \leq \jmath$ (note $s = \jmath\omega$) would be one, and for $s > \jmath$, $T(s)$ would be zero. It is not possible to realize such an ideal response, and the response shown in Figure 2-3(a) is typical of what can be achieved. The reflection coefficient is shown in Figure 2-3(b), with the characteristic function $K(s)$ shown in Figure 2-3(c). If $|K(s)|^2$ is expressed as the ratio of two polynomials (i.e, as $N(s)/D(s)$), then it can be seen from Figure 2-3(e and f) that the zeros of the reflection coefficient, $|\Gamma_1(s)|^2$, are also the zeros of $N(s)$. Also, it is observed that the zeros of the transmission coefficient are also the zeros of $D(s)$, as shown in Figure 2-3(a and c).

The first objective in lumped-element filter design is development of the transfer function of the network in the frequency domain or, equivalently, the s domain.[1] The input-output transfer function of the generic filter in Figure 2-4 is

[1] Care is being taken in the use of terminology as s can be complex with some filter types, but these filters are realized using digital signal processing.

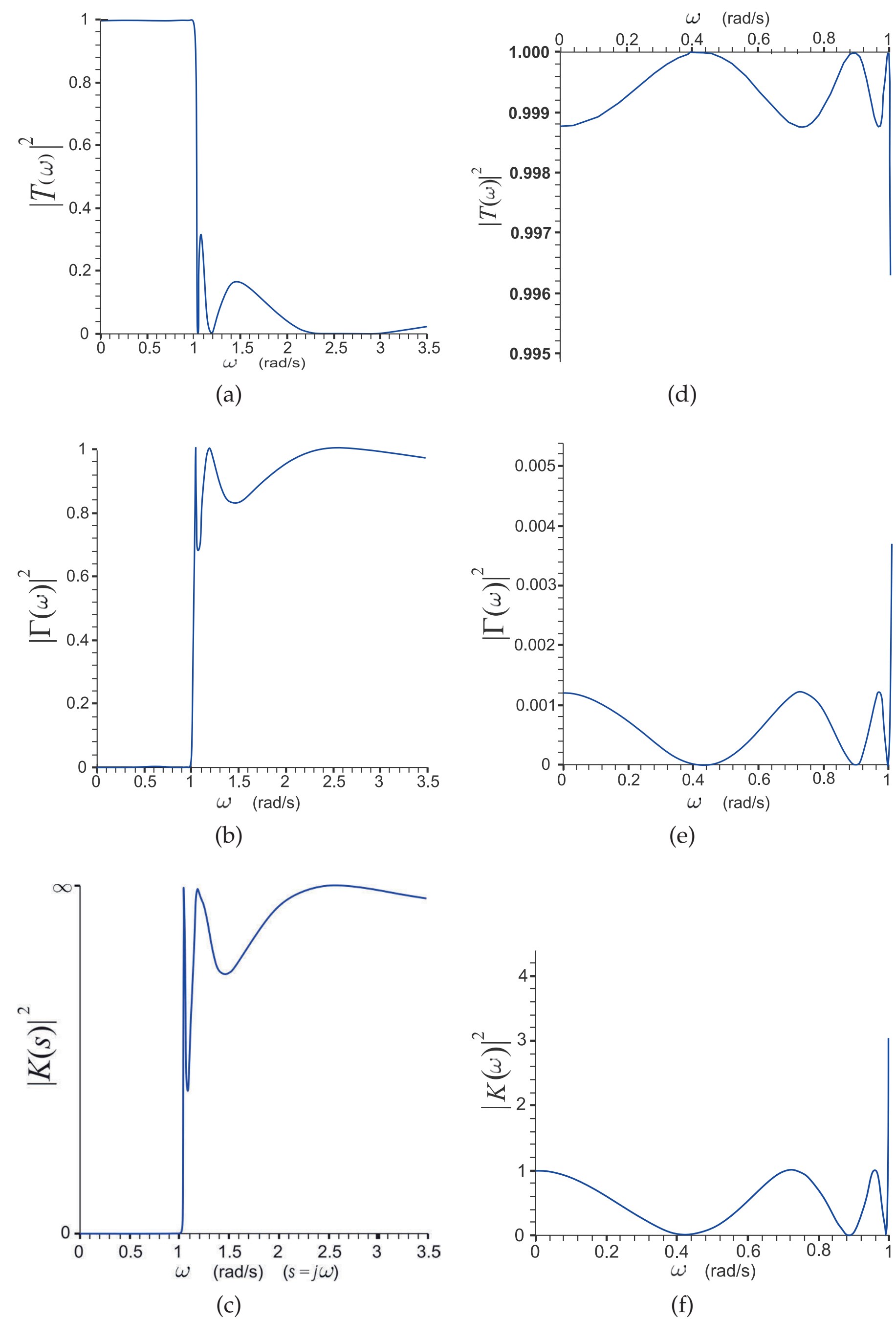

Figure 2-3: An example of a lowpass filter in terms of various responses: (a) transmission coefficient; (b) reflection coefficient response; and (c) characteristic function response. Detailed responses are shown in (d), (e), and (f), respectively.

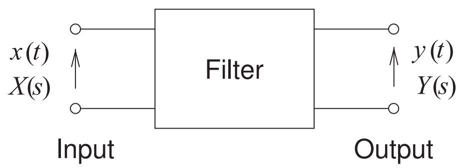

Figure 2-4: Generic filter.

$$T(s) = Y(s)/X(s) \tag{2.13}$$

and the design procedure is to match this response to a response defined by the ratio of two polynomials:

$$T(s) = \frac{N(s)}{D(s)} = \frac{a_m s^m + a_{m-1}s^{m-1} + \cdots + a_1 s + a_0}{s^n + b_{n-1}s^{n-1} + \cdots + b_1 s + b_0}. \tag{2.14}$$

Here N stands for numerator and D for denominator, and these are not the same as those in Equation (2.5) (where they were just labels for numerator and denominator). The filter response using a **pole-zero description** can be synthesized so the design process begins by rewriting Equation (2.14) explicitly in terms of zeros, z_m, and poles, p_n:

$$T(s) = \frac{N(s)}{D(s)} = \frac{a_m(s+z_1)(s+z_2)\cdots(s+z_{m-1})(s+z_m)}{(s+p_1)(s+p_2)\cdots(s+p_{n-1})(s+p_n)}. \tag{2.15}$$

Since only the frequency response is of interest, $s = \jmath\omega$, thus simplifying the analysis for sinusoidal signals.

The poles and zeros can be complex numbers and can be plotted on the complex s plane. Conditions imposed by realizable circuits require that $D(s)$ be a **Hurwitz** polynomial,[2] which ensures that its poles are located in the left-half plane. $N(s)$ determines the location of the transmission zeros of the filter, and the order of $N(s)$ cannot be more than the order of $D(s)$. That is, $n \geq m$ so that the filter has finite or zero response at infinite frequency.

Two strategies can be employed in deriving the filter response. The first is to derive the polynomials $N(s)$ and $D(s)$ in Equation (2.14). This seems like an open-ended problem, but it was discovered in the 1950s and 1960s that in normal situations there are only a few types of useful responses that are described by a few polynomials, including Butterworth, Bessel, Chebyshev, and Cauer polynomials.

2.3 The Lowpass Filter Prototype

Most filter design is based on the synthesis of a lowpass filter equivalent called a lowpass prototype. Transformations are then used to correct for the actual source and load impedances, frequency range, and the desired filter type, such as highpass or bandpass. An ideal lowpass response is shown in Figure 2-5(a), which shows a transmission coefficient of 1 up to a normalized frequency of 1 rad/sec. This type of response defines what is called a **brick-wall filter**, which unfortunately cannot be physically realized. Instead, the response is approximated and specified in terms of a response template (see Figure 2-5(b)).

[2] A Hurwitz polynomial is a polynomial whose coefficients are positive real numbers and whose zeros are located in the left-half of the complex s plane.

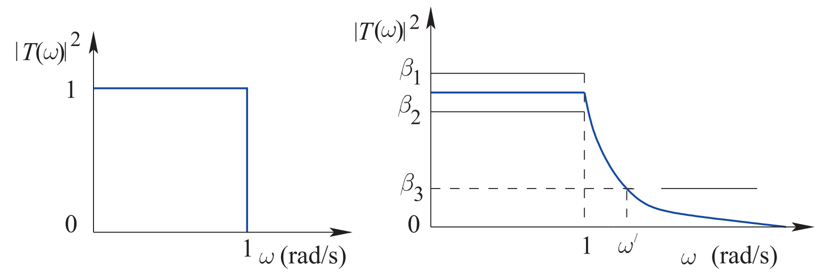

(a) Ideal brick-wall response (b) Response template

Figure 2-5: Lowpass filter response.

The template specifies a passband response that is between β_1 and β_2 at frequencies below the corner radian frequency (at $\omega = 1$), and below β_3 above a radian frequency $\omega' > 1$. The lowpass filter is harder to realize the closer the specified response is to the ideal response shown in Figure 2-5(a), that is, when

$$(\beta_2 - \beta_1) \to 0, \quad \beta_3 \to 0, \quad \text{and} \quad (\omega' - 1) \to 0. \tag{2.16}$$

Several polynomials have particularly interesting characteristics that match the requirements of the response template. At first it may seem surprising that polynomial functions could yield close to ideal filter responses. However, as will be seen, there is something special about these polynomials: they are natural solutions to extreme conditions. For example, the nth-order Butterworth polynomial has the special property that the first n derivatives at $s = 0$ are zero. The other polynomials also have extreme properties, and filters that are synthesized using them also have extreme properties. As well as the maximally flat property resulting from Butterworth polynomials, filter responses obtained using Chebyshev polynomials have the steepest skirts (i.e., fastest transitions from the frequency region where signals are passed to the region where they are blocked). Usually it is one of these extreme cases that is most desirable.

A streamlining of the filter synthesis procedure is obtained by first focusing on the development of normalized lowpass filters having a 1 rad/s corner frequency and 1 Ω reference impedance. Transformations transform a lowpass filter prototype into another filter having the response desired. These transformations give rise to symmetrical responses.

2.4 The Maximally Flat (Butterworth) Lowpass Approximation

Butterworth filters have a maximally flat response (Figure 2-6) that in the time domain corresponds to a critically damped system.

2.4.1 Butterworth Filter Design

Butterworth filters have the transfer function

$$T(s) = \frac{N(s)}{D(s)} = \frac{k}{s^n + b_{n-1}s^{n-1} + \cdots + b_1 s + b_0}. \tag{2.17}$$

This is an all-pole response. The characteristic polynomial of the Butterworth filter is

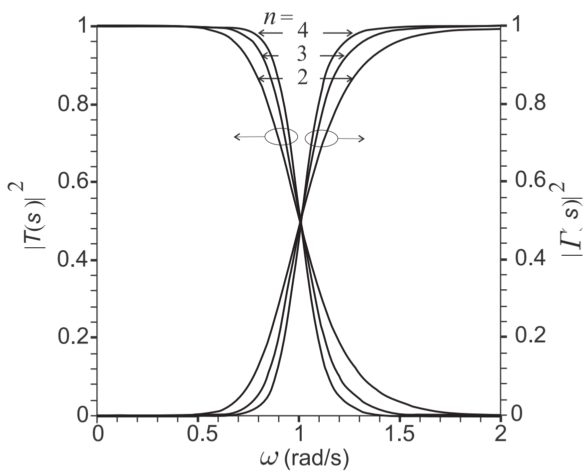

Figure 2-6: Maximally flat, or Butterworth, lowpass filter approximation for various orders, n, of the filter.

Table 2-1: Factors of the $B_n(s)$ polynomial.

n	Factors of $B_n(s)$
1	$(s+1)$
2	$(s^2+1.4142s+1)$
3	$(s+1)(s^2+s+1)$
4	$(s^2+0.7654s+1)(s^2+1.8478s+1)$
5	$(s+1)(s^2+0.6180s+1)(s^2+1.6180s+1)$
6	$(s^2+0.5176s+1)(s^2+1.4142s+1)(s^2+1.9319s+1)$
7	$(s+1)(s^2+0.4450s+1)(s^2+1.2470s+1)(s^2+1.8019s+1)$
8	$(s^2+0.3902+1)(s^2+1.1111s+1)(s^2+1.6629s+1)(s^2+1.9616s+1)$

$$|K(s)|^2 = \left|s^{2n}\right| = \omega^{2n}, \tag{2.18}$$

since $s = \jmath\omega$ and where n is the order of the function. Thus the transmission coefficient is

$$|T(s)|^2 = \frac{1}{1+|K(s)|^2} = \frac{1}{1+|s^{2n}|} = \frac{1}{1+\omega^{2n}}, \tag{2.19}$$

which is often written as

$$|T(s)|^2 = \frac{1}{1+|K(s)|^2} = \frac{1}{B_n(s)B_n(-s)}. \tag{2.20}$$

In the filter community, $B_n(s)$ is called the Butterworth polynomial and has the general form

$$B_n(s) = \begin{cases} \prod_{k=1}^{n/2}\left[s^2 - 2s\cos\left(\dfrac{2k+n-1}{2n}\pi\right)+1\right] & \text{for } n \text{ even} \\ (s+1)\prod_{k=1}^{(n-1)/2}\left[s^2 - 2s\cos\left(\dfrac{2k+n-1}{2n}\pi\right)+1\right] & \text{for } n \text{ odd} \end{cases}. \tag{2.21}$$

$B_n(s)$ is given in factorized form in Table 2-1. Further factorization of the second-order factors results in complex conjugate roots, so they are generally left in the form shown.

Insight is gained by examining the characteristic polynomial for a real radian frequency, ω (where $s = \jmath\omega$), at the following frequency points:

$$\text{at } \omega = 0 \quad \rightarrow \quad |T(0)|^2 = \frac{1}{1+0} = 1 \tag{2.22}$$

$$\text{at } \omega = 1 \quad \rightarrow \quad |T(1)|^2 = \frac{1}{1+1} = \frac{1}{2}. \tag{2.23}$$

Thus the transmission response of the filter is at half power at the corner frequency $\omega = 1$. Another observation is that the transmission coefficient at $\omega = 0$ and $\omega = 1$ are independent of the degree of the characteristic polynomial. This is shown in Figure 2-6, where the responses of Butterworth filters are plotted for three different orders.

2.4.2 Construction of the Transfer Function

Often the characteristic function, K, is specified in terms of the variable ω, and for synthesis purposes the response must be transformed back to the s domain. As an example, consider the maximally flat function of third order with a characteristic polynomial equal to ω^3 (from Equation (2.19)):

$$K(\omega) = \omega^3 \quad \text{and} \quad |T(\omega)|^2 = \frac{1}{1+\omega^6}. \tag{2.24}$$

(Note that here the first six derivatives of $|K(s)|^2$ with respect to s are zero at $s = 0$.) So, from Equation (2.7),

$$|\Gamma_1(\omega)|^2 = 1 - \frac{1}{1+\omega^6} = \frac{\omega^6}{1+\omega^6}. \tag{2.25}$$

At real frequencies (i.e., frequencies lying on the imaginary axis in the s plane)

$$s = \jmath\omega, \quad \text{so} \quad \omega = s/\jmath = -\jmath s. \tag{2.26}$$

Thus, in the s domain, the reflection coefficient becomes

$$|\Gamma_1(\jmath\omega)|^2 = |\Gamma_1(\jmath(-\jmath s))|^2 = |\Gamma_1(s)|^2 = \frac{(-\jmath s)^6}{1+(-\jmath s)^6}. \tag{2.27}$$

That is, $$|\Gamma_1(s)|^2 = \frac{-s^6}{1-s^6} = \Gamma_1(s)\,\Gamma_1(-s)\,. \tag{2.28}$$

Factoring the denominator polynomial yields

$$1 - s^6 = (1-s)(1+s)\left(s^2+s+1\right)\left(s^2-s+1\right). \tag{2.29}$$

By choosing those factors with roots only in the left-half plane (required for a realizable network), the zeros of the denominator are obtained. Now the numerator of $|\Gamma_1(s)|^2$ is easily factored, and since this is third order, it only has three reflection zeros at DC. The resulting function is

$$\Gamma_1(s) = \frac{s^3}{(s+1)(s^2+s+1)}, \tag{2.30}$$

and so $$T(s) = \frac{1}{(s+1)(s^2+s+1)}. \tag{2.31}$$

This example illustrates how $\Gamma_1(s)$ and $T(s)$ can be obtained from $K(s)$. This procedure is generalized in the next section.

2.4.3 nth-Order Reflection Approximation

Following the procedure outlined in the previous section, generalization leads to the nth-order Butterworth response:

$$\begin{aligned} |\Gamma_1(s)|^2 &= \Gamma_1(s)\cdot\Gamma_1(-s) \\ &= \frac{(-s^2)^n}{1+(-s^2)^n} = \frac{(-s^2)^n}{\prod_{i=1}^{n}(s-s_i)\,.\prod_{j=n+1}^{2n}(s-s_j)}. \end{aligned} \tag{2.32}$$

So $|\Gamma_1(s)|^2$ has n roots (these are the s_is) lying in the left-half s plane, and n roots (the s_js) lying in the right-half s plane. Note that j is used as an index and $\jmath$ ($\jmath$, without the dot) represents $\sqrt{-1}$. It is reasonable to group all of the left-half plane roots together (a circuit could not be synthesized if there were a right-half plane root) so that

$$\Gamma_1(s) = \frac{(-s)^n}{\prod_{i=1}^{n}(s-s_i)}. \tag{2.33}$$

Solving for the roots of the denominator of Equation (2.32) (i.e., finding the roots of $1+\left(-s^2\right)^n = 0$) yields the following roots in the left-half s plane:

$$s_i = \exp\left\{\jmath\,(2i-1+n)\frac{\pi}{2n}\right\} \qquad i = 1, 2, ..., n, \tag{2.34}$$

where $\exp(\jmath\theta) = \cos(\theta) + \jmath\sin(\theta)$.

EXAMPLE 2.1 Reflection Coefficient Derivation for Butterworth Filter

Develop the reflection coefficient from the roots of the third-order ($n = 3$) Butterworth lowpass filter prototype.

Solution: From Equation (2.34) the three roots are

$$s_1 = \exp\left\{\jmath\,(2\times 1-1+3)\frac{\pi}{2\times 3}\right\} = \exp\left\{\jmath\,\frac{2}{3}\pi\right\} \tag{2.35}$$

$$s_2 = \exp\left\{\jmath\,(2\times 2-1+3)\frac{\pi}{2\times 3}\right\} = \exp\left\{\jmath\,\pi\right\} \tag{2.36}$$

$$s_3 = \exp\left\{\jmath\,(2\times 3-1+3)\frac{\pi}{2\times 3}\right\} = \exp\left\{\jmath\,\frac{4}{3}\pi\right\} \tag{2.37}$$

and the input reflection coefficient of the filter normalized to $1\,\Omega$ is

$$\Gamma_1(s) = \frac{s^3}{\left(s+\frac{1}{2}-\jmath\frac{\sqrt{3}}{2}\right)(s+1)\left(s+\frac{1}{2}+\jmath\frac{\sqrt{3}}{2}\right)} = \frac{s^3}{(s+1)\left(s^2+s+1\right)}. \tag{2.38}$$

This is the same as Equation (2.30).

2.4.4 Bandwidth Consideration

At the corner frequency of the Butterworth response, that is, at 1 rad/s, the transmission response is 3 dB down from its maximum transfer response.

Table 2-2: Radian frequencies at which the response of a Butterworth filter is 1 dB down for a corner frequency $f_0 = 0.1592$ Hz ($\omega_0 = 1$ rad/s). At f_0 the transmission response is down 3 dB.

Order, n							
$n=3$	4	5	6	7	8	9	10
0.798 rad/s	0.844	0.873	0.901	0.908	0.919	0.928	0.935

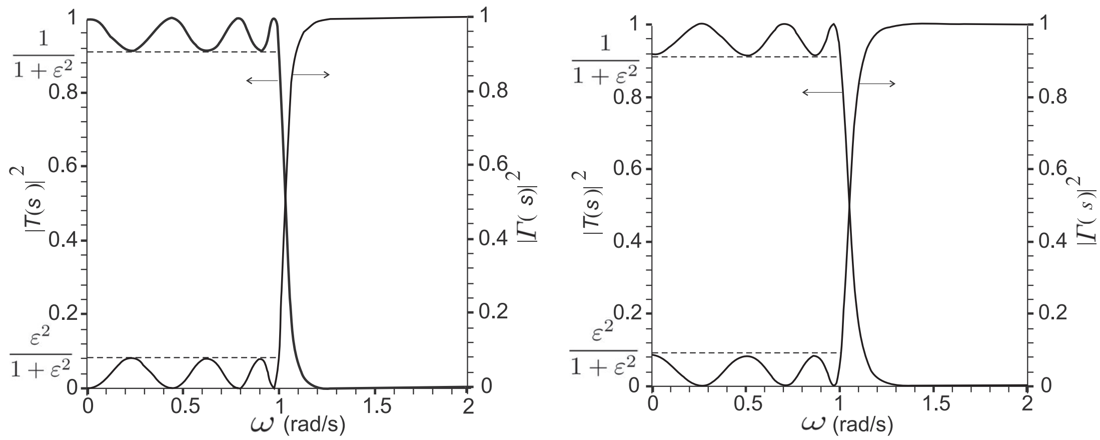

(a) Seventh-order filter, $n=7$ (b) Sixth-order filter, $n=6$

Figure 2-7: Chebyshev lowpass filter responses. In decibels, the ripple is $R_{\rm dB} = -10\log[1/(1+\varepsilon^2)] = 10\log(1+\varepsilon^2)$, ε is called the ripple factor.

Sometimes microwave filters are designed to have 1 dB bandwidths. The radian frequencies at which the responses of various orders of Butterworth filters are 1 dB down are given in Table 2-2. By frequency scaling the Butterworth response the filter can be design for a specified 1 dB bandwidth.

2.5 The Chebyshev Lowpass Approximation

The maximally flat approximation to the ideal lowpass filter response is best near the origin but not so good near the band edge. Chebyshev filters have better responses near the band edge, with lower insertion loss near the edges, but at the cost of ripples in the passband. Example reflection and transmission responses are shown in Figure 2-7 for a seventh-order and a sixth-order Chebyshev lowpass filter.

2.5.1 Chebyshev Filter Design

The general form of the Chebyshev transmission coefficient is

$$|T(s)|^2 = \frac{1}{1+\varepsilon^2|K(s)|^2}, \tag{2.39}$$

where ε is the ripple factor and defines the **passband ripple** (**PBR**):

$$\text{PBR} = 1+\varepsilon^2, \quad \text{or in decibels} \quad R_{\rm dB} = \text{PBR}\,|_{\rm dB} = 10\log\left(1+\varepsilon^2\right). \tag{2.40}$$

The PBR can be seen in the transmission response, $|T(s)|^2$, in Figure 2-7. In the passband the peaks of the lossless filter response have $|T(s)|^2 = 1$ and the minimums of the ripple response all have $|T(s)|^2 = 1/\left(1+\varepsilon^2\right) = 1/\mathrm{PBR}$. Consequently Chebyshev filters are also known as **equiripple** all-pole lowpass filters. Also note that the corner radian frequency, $\omega = 1$ for the lowpass filter prototype, has a transmission response (i.e., insertion loss IL) of $|T(s)|^2 = 1/\left(1+\varepsilon^2\right)$, whereas the Butterworth transmission response was at half power at the corner frequency. For the Chebyshev filter, the insertion loss at the corner frequency is the ripple:

$$\mathrm{IL} = 1R_{\mathrm{dB}} = 10\log(1+\varepsilon^2). \tag{2.41}$$

For the nth-order Chebyshev (lowpass filter) approximation, the square of the characteristic function is

$$|K_n(\omega)|^2 = \begin{cases} \cos^2\left[n\cos^{-1}(\omega)\right], & -1 \le \omega \le 1 \\ \cosh^2\left[n\cosh^{-1}(|\omega|)\right], & \omega \le -1,\ \omega \ge 1 \end{cases}, \tag{2.42}$$

which can be expressed as a polynomial. For example, with $n = 3$,

$$K_3(\omega) = 4\omega^3 - 3\omega, \ \text{ for all } \omega. \tag{2.43}$$

(This equivalence was derived by Pafnuty Chebyshev.) It is surprising that the trigonometric expression has such a simple polynomial equivalence. From Equation (2.11) the transmission coefficient is (for $-1 \le \omega \le 1$)

$$|T(\omega)|^2 = \frac{1}{1+\varepsilon^2\cos^2\left[n\cos^{-1}(\omega)\right]} \tag{2.44}$$

and the reflection coefficient is

$$|\Gamma_1(\omega)|^2 = \frac{\varepsilon^2\cos^2\left[n\cos^{-1}(\omega)\right]}{1+\varepsilon^2\cos^2\left[n\cos^{-1}(\omega)\right]}. \tag{2.45}$$

Factorizing the denominator of either Equation (2.44) or Equation (2.45) yields the following roots (of the denominators of $\Gamma_1(s)$ and $T(s)$):

$$\begin{aligned} s_i = &\sin\left[\frac{(2i-1)\pi}{2n}\right]\sinh\left[\frac{1}{n}\sinh^{-1}\left(\frac{1}{\varepsilon}\right)\right] \\ &+ \jmath\cos\left[\frac{(2i-1)\pi}{2n}\right]\cosh\left[\frac{1}{n}\sinh^{-1}\left(\frac{1}{\varepsilon}\right)\right] \qquad i = 1,2,\ldots,n. \end{aligned} \tag{2.46}$$

The roots of the numerator of $\Gamma_1(s)$ in the s plane are

$$s_k = \jmath\cos\frac{(2k-1)\pi}{2n} \qquad k = 1,2,\ldots,n. \tag{2.47}$$

Equations (2.46) and (2.47) can be used to obtain the reflection and transmission coefficients directly in the s domain.

2.5.2 Chebyshev Approximation and Recursion

The characteristic function of the Chebyshev approximation can be obtained from the recursion formula,

$$K_n(\omega) = 2\omega K_{n-1}(\omega) - K_{n-2}(\omega), \tag{2.48}$$

Table 2-3: Radian frequencies at which the transmission response of an nth Chebyshev filter is down 1 dB and 3 dB for a corner frequency $\omega_0 = 1$ rad/s. (Note that ω_0 is the radian frequency at which the transmission response of a Chebyshev filter is down by the ripple, see Figure 2-7.)

Response 1 dB down				
Ripple	$n=3$	$n=5$	$n=7$	$n=9$
0.01 dB	1.564	1.192	1.097	1.058
0.1 dB	1.202	1.071	1.036	1.022
0.2 dB	1.127	1.045	1.023	1.014
1 dB	1.000	1.000	1.000	1.000
3 dB	–	–	–	–

Response 3 dB down				
Ripple	$n=3$	$n=5$	$n=7$	$n=9$
0.01 dB	1.877	1.291	1.145	1.087
0.1 dB	1.389	1.134	1.068	1.041
0.2 dB	1.284	1.099	1.050	1.030
1 dB	1.095	1.0338	1.017	1.010
3 dB	1.000	1.000	1.000	1.000

$$\text{with} \qquad K_1(\omega) = \omega; \qquad K_2(\omega) = 2\omega^2 - 1. \tag{2.49}$$

For example, with $n = 3$,

$$\begin{aligned} K_3(\omega) &= 2\omega K_{3-1}(\omega) - K_{3-2}(\omega) \\ &= 2\omega\left(2\omega^2 - 1\right) - \omega = 4\omega^3 - 2\omega - \omega = 4\omega^3 - 3\omega. \end{aligned} \tag{2.50}$$

2.5.3 Bandwidth Consideration

At the corner frequency of the Chebyshev filter the transmission response is down by the amount of the ripple. This can be seen in Figure 2-7. However, the bandwidth of a filter is usually specified in terms of its 1 dB or 3 dB bandwidth at which the transmission response is down 1 dB or 3 dB, respectively, from its maximum response. The radian frequencies at which the responses of various orders of Chebyshev filters are 1 dB down and 3 dB down are given in Table 2-3. By frequency scaling the Chebyshev response, the filter can be designed for a specified 1 dB or 3 dB bandwidth.

2.6 Element Extraction

In the previous two sections the mathematical responses of Butterworth and Chebyshev filters were derived for various orders. In this section it will be shown how these filters can be implemented with inductors and capacitors using what is called **ladder synthesis** [4].

2.6.1 Ladder Synthesis

To obtain the element values yielding the desired transfer function, an impedance or admittance function must first be obtained. The impedance or admittance function can be readily obtained from the input reflection coefficient of a network, but for now the focus is on synthesizing a given impedance function. A general impedance function can be expressed as

$$Z(s) = \frac{a_n\left(s^2+\omega_1^2\right)\left(s^2+\omega_3^2\right)\left(s^2+\omega_5^2\right)\ldots}{b_m s\left(s^2+\omega_2^2\right)\left(s^2+\omega_4^2\right)\left(s^2+\omega_6^2\right)\ldots}, \tag{2.51}$$

where a_n and b_m are constants. This can be realized using L and C elements in a network terminated by a resistor, provided that the degree of the numerator and denominator differ by no more than unity (i.e., $|m-n| \leq 1$). In

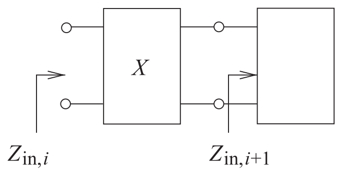

Figure 2-8: Extraction of a network X to reduce an impedance $Z_{\text{in},i}$ to a lower-order impedance $Z_{\text{in},i+1}$.

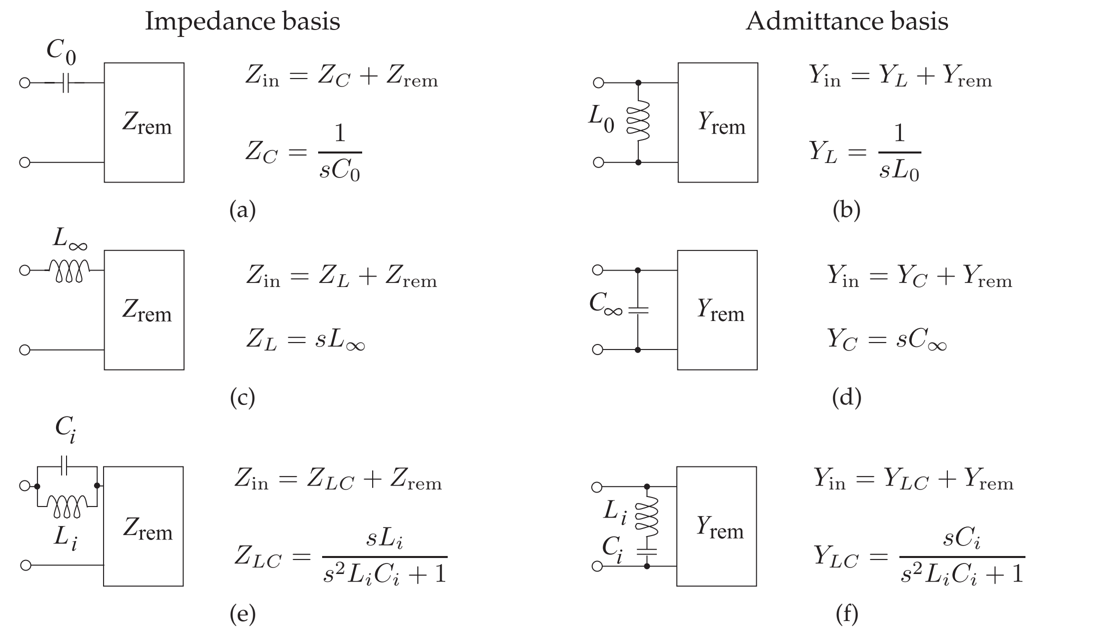

Figure 2-9: Synthesis of impedance and admittance functions. Starting with an impedance function $Z(s)$: (a) extraction of a series capacitor; (c) extraction of a series inductor; and (e) extraction of a series parallel LC block i. Starting with an admittance function $Y(s)$: (b) extraction of a shunt inductor; (d) extraction of a shunt capacitor; and (f) extraction of a shunt series LC block.

the case of a doubly terminated network, this resistor is the load. The element extraction procedure, shown in Figure 2-8, involves extracting a network X from $Z_{\text{in},i}$, leaving a reduced-order impedance $Z_{\text{in},i+1}$.

The extraction of inductors and capacitors is illustrated in Figure 2-9. Thus, following the extraction of an element or a pair of elements an impedance, Z_{rem}, or admittance, Y_{rem}, remains that can be similarly simplified. For example, and referring to Figure 2-9(a), $Z(s) = 1/(sC) + Z_{\text{rem}}$. So a pole of $Z(s)$ at DC requires the extraction of a series capacitor of value (see Figure 2-9(a))

$$C_0 = \left.\frac{1}{sZ(s)}\right|_{s=0}, \tag{2.52}$$

while a pole at infinity requires the extraction of a series inductor of value (see Figure 2-9(c))

$$L_\infty = \left.\frac{Z(s)}{s}\right|_{s=\infty}. \tag{2.53}$$

Another possibility is a pole at a finite frequency (call this ω_0), which requires the extraction of a series parallel LC block, as shown in Figure 2-9(e), with elements of value

$$C_i = \left. \frac{s}{(s^2 + \omega_0^2)\, Z(s)} \right|_{s=\jmath\omega_o} \quad \text{and} \quad L_i = \frac{1}{\omega_0^2 . C_i}. \tag{2.54}$$

The extraction process can also be carried out on an admittance basis. First,

$$Y(s) = \frac{b_m s\,(s^2 + \omega_2^2)\,(s^2 + \omega_4^2)\,(s^2 + \omega_s^2)\dots}{a_n\,(s^2 + \omega_1^2)\,(s^2 + \omega_3^2)\,(s^2 + \omega_5^2)\dots}\,. \tag{2.55}$$

Now a pole at zero requires the extraction of a shunt inductor of value (see Figure 2-9(b))

$$L_0 = \left. \frac{1}{sY(s)} \right|_{s=0} \tag{2.56}$$

and a pole at infinity requires the extraction of a shunt capacitor of value (see Figure 2-9(d))

$$C_\infty = \left. \frac{Y(s)}{s} \right|_{s=\infty}. \tag{2.57}$$

A pole at a finite frequency requires the extraction of a shunt-series LC block (as shown in Figure 2-9(f)) with values

$$L_i = \left. \frac{s}{(s^2 + \omega_o^2)\, Y(s)} \right|_{s=\jmath\omega_o} \quad \text{and} \quad C_i = \frac{1}{\omega_o^2 . L_i}. \tag{2.58}$$

Many aspects of filter synthesis can seem abstract when presented in full generality. Consequently it is common to illustrate filter synthesis concepts using examples. Following this time-honored tradition, an example is now presented.

EXAMPLE 2.2 Element Extraction for a Third-Order Lowpass Filter

A third-order maximally flat filter has the reflection coefficient

$$\Gamma_1(s) = \frac{s^3}{(s+1)\,(s^2+s+1)}. \tag{2.59}$$

Synthesize this filter as a doubly terminated network.

Solution:

The reflection coefficient function (Equation (2.59)) has all its poles located at infinity, so the corresponding network realization must be made of simple L or C elements and terminated in a resistor. Hence, referring to Figure 2-2 and considering a 1 Ω system,

$$Z_{\text{in},1}(s) = \frac{1+\Gamma_1(s)}{1-\Gamma_1(s)} = \frac{2s^3 + 2s^2 + 2s + 1}{2s^2 + 2s + 1}. \tag{2.60}$$

Note that the input impedance approaches infinity as the frequency goes to infinity, hence a series inductor must be extracted. The value of this inductor is

$$L_{\infty 1} = \left. \frac{Z_{\text{in},1}(s)}{s} \right|_{s=\infty} = 1\ \text{H}. \tag{2.61}$$

The filter is developed by extracting one element at a time. Following the extraction of the first element, the second-stage impedance is left. Now the impedance function is

$$\begin{aligned}Z_{\text{in},2}(s) = Z_{\text{in},1}(s) - sL_{\infty 1} &= \frac{2s^3 + 2s^2 + 2s + 1}{2s^2 + 2s + 1} - sL_{\infty 1} \\ &= \frac{2s^3 + 2s^2 + 2s + 1 - s\left(2s^2 + 2s + 1\right)}{2s^2 + 2s + 1} = \frac{s + 1}{2s^2 + 2s + 1}.\end{aligned}$$

Note that the stage impedance above, $Z_{\text{in},2}$, approaches zero as the frequency goes to infinity. There is not a single series element that would cause this. However, the stage admittance function,

$$Y_{\text{in},2}(s) = \frac{1}{Z_{\text{in},2}(s)} = \frac{2s^2 + 2s + 1}{s + 1}, \tag{2.62}$$

goes to infinity as the frequency approaches infinity and so a shunt capacitor is extracted:

$$Y_{\text{in},3}(s) = Y_{\text{in},2}(s) - sC_{\infty 2} = \frac{1}{s + 1}, \tag{2.63}$$

where

$$C_{\infty 2} = 2\ \text{F}. \tag{2.64}$$

So sometimes it is more convenient to consider extraction of an admittance and sometimes it is better to consider extraction of an impedance.

By examining the remaining stage impedance, it is seen that a pole exists at infinity, and so a series inductor, $L_{\infty 3}$, is extracted. The value of this inductor comes from

$$Z_{\text{in},3} = \frac{1}{Y_{\text{in},3}} = s + 1\ \Omega \tag{2.65}$$

and so the inductor value is

$$L_{\infty 3} = \left.\frac{s + 1}{s}\right|_{S=\infty} = 1\ \text{H}. \tag{2.66}$$

The final step is to extract a load of value 1 as follows:

$$Z_{\text{in},4} = Z_{\text{in},3} - sL_{\infty 3} = 1\ \Omega. \tag{2.67}$$

This example synthesized a doubly terminated network. The resulting network, called a ladder circuit, is shown in Figure 2-10. The left-most 1 Ω resistor is part of the source.

This circuit has a dual form consisting of two shunt capacitors separated by a series inductor. The dual circuit derives from realizing the admittance function obtained from the reflection coefficient. Other network extraction techniques are presented in Scanlan and Levy [4, 5] and Matthaei et al. [1].

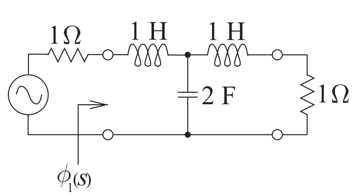

Figure 2-10: Synthesized maximally flat network with a third-order lowpass reflection response.

2.6.2 Summary

The input impedance function of a lumped-element circuit can always be expressed as the ratio of two polynomials in s and the order of the numerator and the denominator polynomials can differ by at most one [5]. If the orders differ by one, then a single inductor or capacitor can always be extracted, however, the remaining impedance function may not be realizable. This indicates that a more complex LC (and possibly R) combination is required. To be able to systematically extract arbitrarily complex circuits, a long list of possible functions, such as those shown in Figure 2-9, is required. For most of the circuits of interest the LC combinations shown in Figure 2-9 are sufficient. The next example describes impedance function extraction that requires an LC combination.

EXAMPLE 2.3 Element Extraction of an Impedance Function

Realize the impedance function $Z_w = \dfrac{4s^3 + 4s^2 + 2s + 2}{4s^2 + 2s + 1}$.

Solution:

The order of the numerator is 1 greater than the order of the denominator and this indicates that a series inductor is perhaps present. The series inductance is

$$L_1 = \left.\frac{Z_w(s)}{(s)}\right|_{z=\infty} = 1\ \text{H}. \tag{2.68}$$

The remaining impedance is

$$Z_{\text{in},2} = Z_w - sL_1 = \frac{4s^3 + 4s^2 + 2s + 2}{4s^2 + 2s + 1} - s = \frac{2s^2 + s + 2}{4s^2 + 2s + 1}. \tag{2.69}$$

The numerator and denominator of $Z_{\text{in},2}$ have the same order. Therefore a simple L or C element cannot be used to reduce the complexity of the impedance function. Thus an initial series inductor was not the right choice and the extraction must backtrack.

Figure 2-9 shows several element combinations that can be used to reduce the complexity of an impedance function. Insight into which alternative to choose comes from factoring z_w, and note that real roots are required, thus

$$Z_w = \frac{4s^3 + 4s^2 + 2s + 2}{4s^2 + 2s + 1} = \frac{(2s^2 + 1)(2s + 2)}{4s^2 + 2s + 1}. \tag{2.70}$$

Examination of Figure 2-9 reveals that a ready fit to Z_w is not found. Instead consider the admittance function

$$Y_w = \frac{1}{Z_w} = \frac{4s^2 + 2s + 1}{(2s^2 + 1)(2s + 2)}. \tag{2.71}$$

So the reduction shown in Figure 2-9(f) looks like the right candidate. The general choice for the element is

$$y_x = \frac{as}{bs^2 + 1}. \tag{2.72}$$

Choosing $b = 2$ now reduces complexity (since part of the factored denominator of Y_w now occurs), so

$$Y_w = \frac{as}{2s^2 + 1} + \left(\frac{4s^2 + 2s + 1}{(2s^2 + 1)(2s + 2)} - \frac{as}{2s^2 + 1}\right) \tag{2.73}$$

$$= \frac{as}{2s^2 + 1} + \left(\frac{(4 - 2a)s^2 + (2 - 2a)s + 1}{(2s^2 + 1)(2s + 2)}\right). \tag{2.74}$$

Choose $a = 1$,
$$Y_w = \frac{s}{(2s^2+1)} + \frac{2s^2+1}{(2s^2+1)(2s+2)} = \frac{s}{2s^2+1} + \frac{1}{2s+2} \tag{2.75}$$
$$= \frac{s}{2s^2+1} + Y_{\text{in},2}. \tag{2.76}$$

So $C_1L_1 = b = 1$, $C_1 = a = 1$ F, $L_1 = 2$ H, and

$$Y_{\text{in},2} = \frac{1}{(2s+2)} \quad \text{or} \quad Z_{\text{in},2} = \frac{1}{Y_{\text{in},2}} = 2s + 2. \tag{2.77}$$

The final network is

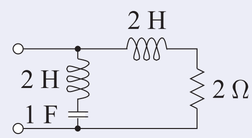

2.7 Butterworth and Chebyshev Filters

The nth-order lowpass filters constructed from the Butterworth and Chebyshev polynomials have the ladder circuit forms of Figure 2-11(a or b). Figure 2-11 uses several shorthand notations commonly used with filters. First, note that there are two prototype forms designated Type 1 and Type 2, and these are referred to as duals of each other. The two prototype forms have identical responses with the same numerical element values $g_1, \ldots, g_n$. Consider the Type 1 prototype of Figure 2-11(a). The right-most element is the resistive load, which is also known as the $(n+1)$th element. The next element to the left of this is either a shunt capacitor (of value g_n) if n is even, or a series inductor (of value g_n) if n is odd. So for the Type 1 prototype, the shunt capacitor next to the load does not exist if n is odd. The same interpretation applies to the circuit in Figure 2-11(b).

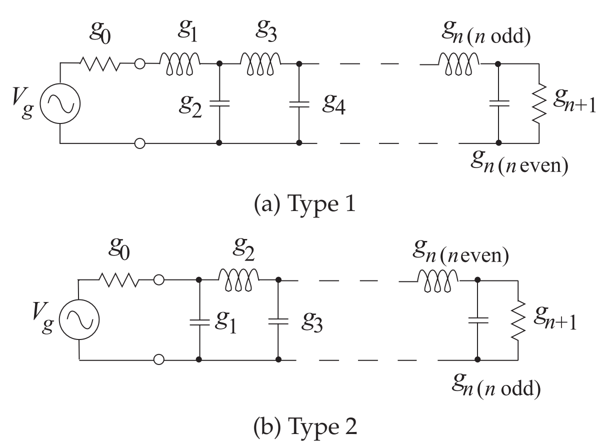

Figure 2-11: Filter prototypes in the Cauer topology. Here n is the order of the filter.

Table 2-4: Coefficients of the Butterworth lowpass prototype filter normalized to a radian corner frequency of 1 rad/s and a 1 Ω system impedance (i.e., $g_0 = 1 = g_{n+1}$).

Order, n	2	3	4	5	6	7	8	9
g_1	1.4142	1	0.7654	0.6180	0.5176	0.4450	0.3902	0.3473
g_2	1.4142	2	1.8478	1.6180	1.4142	1.2470	1.1111	1
g_3	1	1	1.8478	2	1.9318	1.8019	1.6629	1.5321
g_4		1	0.7654	1.6180	1.9318	2	1.9615	1.8794
g_5			1	0.6180	1.4142	1.8019	1.9615	2
g_6				1	0.5176	1.2470	1.6629	1.8794
g_7					1	0.4450	1.1111	1.5321
g_8						1	0.3902	1
g_9							1	0.3473
g_{10}								1

2.7.1 Butterworth Filter

A generalization of the example of the previous section leads to a formula for the element values of a ladder circuit implementing a Butterworth lowpass filter. For a maximally flat or Butterworth response the element values of the circuit in Figure 2-11(a and b) are

$$g_r = 2\sin\left\{(2r-1)\frac{\pi}{2n}\right\} \qquad r = 1, 2, 3, \ldots, n \tag{2.78}$$

and $g_0 = 1 = g_{n+1}$. Table 2-4 lists the coefficients of Butterworth lowpass prototype filters up to ninth order.

EXAMPLE 2.4 Fourth-Order Butterworth Lowpass Filter

Derive the fourth-order Butterworth lowpass prototype of Type 1.

Solution:

From Equation (2.78),

$$g_1 = 2\sin\left[\pi/(2\cdot 4)\right] = 0.765369\ \text{H} \tag{2.79}$$
$$g_2 = 2\sin\left[3\pi/(2\cdot 4)\right] = 1.847759\ \text{F} \tag{2.80}$$
$$g_3 = 2\sin\left[5\pi/(2\cdot 4)\right] = 1.847759\ \text{H} \tag{2.81}$$
$$g_4 = 2\sin\left[7\pi/(2\cdot 4)\right] = 0.765369\ \text{F}. \tag{2.82}$$

Thus the fourth-order Butterworth lowpass prototype circuit with a corner frequency of 1 rad/s is as shown in Figure 2-12.

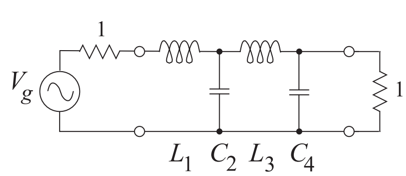

$L_1 = 0.765369$ H $\quad C_2 = 1.847759$ F
$L_3 = 1.847759$ H $\quad C_4 = 0.765369$ F

Figure 2-12: Fourth-order Butterworth lowpass filter prototype.

2.7.2 Chebyshev Filter

For a Chebyshev response, the element values of the lowpass prototype shown in Figure 2-11 are found from the recursive formula [1, 6, 7]:

$$g_0 = 1 \qquad g_1 = \frac{2a_1}{\gamma} \tag{2.83}$$

$$g_{n+1} = \left\{ \begin{array}{ll} 1, & n \text{ odd} \\ \tanh^2(\beta/4), & n \text{ even} \end{array} \right\} \tag{2.84}$$

$$g_k = \frac{4a_{k-1}a_k}{b_{k-1}g_{k-1}}, \quad k = 2,\ 3, \ldots, n \tag{2.85}$$

$$a_k = \sin\left[\frac{(2k-1)\pi}{2n}\right], \quad k = 1,\ 2, \ldots, n\ , \tag{2.86}$$

where
$$\gamma = \sinh\left(\frac{\beta}{2n}\right), \tag{2.87}$$

$$b_k = \gamma^2 + \sin^2\left(\frac{k\pi}{n}\right) \quad k = 1,\ 2, \ldots, n \tag{2.88}$$

$$\beta = \ln\left[\coth\left(\frac{R_{\text{dB}}}{2 \cdot 20\log(\text{e})}\right)\right] = \ln\left[\coth\left(\frac{R_{\text{dB}}}{17.3717793}\right)\right] \tag{2.89}$$

$$R_{\text{dB}} = 10\log\left(1 + \varepsilon^2\right), \tag{2.90}$$

n is the order of the filter, and ε is the ripple factor and defines the level of the ripple in absolute terms. R_{dB} is the ripple expressed in decibels (the ripple is generally specified in decibels).

An interesting point to note here is that the source resistor, the value of which is given by g_0, and terminating resistor, the value of which is given by g_{n+1}, are only equal for odd-order filters. For an even-order Chebyshev filter the terminating resistor, g_{n+1}, will be different and a function of the filter ripple. Because it is generally desirable to have identical source and load impedances, Chebyshev filters are nearly always restricted to odd order. Thus the odd-order Chebyshev prototypes are as shown in Figure 2-13.

Also, for an odd-degree function (n is odd) there is a perfect match at DC,

$$|T(0)|^2 = 1, \tag{2.91}$$

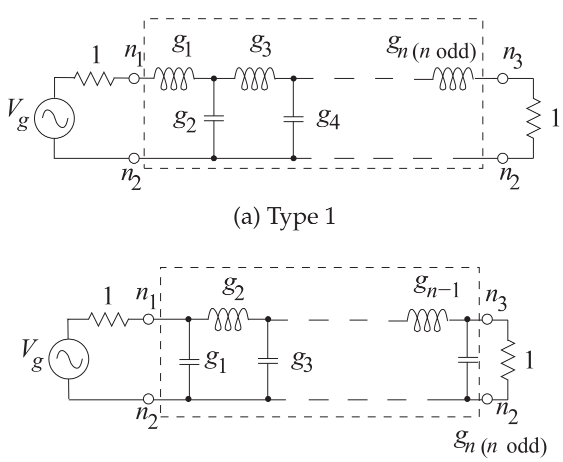

(a) Type 1

(b) Type 2

Figure 2-13: Odd-order Chebyshev lowpass filter prototypes in the Cauer topology. Here n is the order of the filter.

Table 2-5: Coefficients of a Chebyshev lowpass prototype filter normalized to a radian corner frequency of $\omega_0 = 1$ rad/s and a 1 Ω system impedance (i.e., $g_0 = 1 = g_{n+1}$). The ripple factor, ε, is related to the ripple in decibels by Equation (2.90) (e.g., $\varepsilon = 0.1$ is a ripple of 0.0432 dB). (Note that ω_0 is the radian frequency at which the transmission response of a Chebyshev filter is down by the ripple, see Figure 2-7.)

Order	$n = 3$					
Ripple	0.01 dB	0.1 dB	0.2 dB	1.0 dB	3.0 dB	$\varepsilon = 0.1$
g_1	0.62918	1.03156	1.22754	2.02359	3.34874	0.85158
g_2	0.97028	1.14740	1.15254	0.99410	0.71170	1.10316
g_3	0.62918	1.03156	1.22754	2.02359	3.34874	0.85158

Order	$n = 5$					
Ripple	0.01 dB	0.1 dB	0.2 dB	1.0 dB	3.0 dB	$\varepsilon = 0.1$
g_1	0.75633	1.14681	1.33944	2.13488	3.48129	0.97140
g_2	1.30492	1.37121	1.33702	1.09111	0.76192	1.37208
g_3	1.57731	1.97500	2.16605	3.00092	4.53755	1.80136
g_4	1.30492	1.37121	1.33702	1.09111	0.76192	1.37208
g_5	0.75633	1.14681	1.33944	2.13488	3.48129	0.97140

Order	$n = 7$					
Ripple	0.01 dB	0.1 dB	0.2 dB	1.0 dB	3.0 dB	$\varepsilon = 0.1$
g_1	0.79694	1.18118	1.37226	2.16656	3.51852	1.00794
g_2	1.39242	1.42281	1.37820	1.11151	0.77220	1.43678
g_3	1.74813	2.09667	2.27566	3.09364	4.63898	1.93981
g_4	1.63313	1.57340	1.50016	1.17352	0.80381	1.62196
g_5	1.74813	2.09667	2.27566	3.09364	4.63898	1.93981
g_6	1.39242	1.42281	1.37820	1.11151	0.77220	1.43678
g_7	0.79694	1.18118	1.37226	2.16656	3.51852	1.00794

Order	$n = 9$					
Ripple	0.01 dB	0.1 dB	0.2 dB	1.0 dB	3.0 dB	$\varepsilon = 0.1$
g_1	0.81446	1.19567	1.38603	2.17972	3.53394	1.02347
g_2	1.42706	1.44260	1.39389	1.11918	0.76604	1.46186
g_3	1.80436	2.13455	2.30932	3.12143	4.66906	1.98372
g_4	1.71254	1.61672	1.53405	1.18967	0.81181	1.67776
g_5	1.90579	2.20537	2.37280	3.17463	4.72701	2.06485
g_6	1.71254	1.61672	1.53405	1.18967	0.81181	1.67776
g_7	1.80436	2.13455	2.30932	3.12143	4.66906	1.98372
g_8	1.42706	1.44260	1.39389	1.11918	0.76604	1.46186
g_9	0.81446	1.19567	1.38603	2.17972	3.53394	1.02347

while for an even-degree function (i.e., n is even) a mismatch exists of value

$$|T(0)|^2 = \frac{4R_L}{(R_L+1)^2} = \frac{1}{1+\varepsilon^2} \tag{2.92}$$

so that $$R_L = g_{n+1} = \left[\varepsilon + \sqrt{(1+\varepsilon^2)}\right]^2. \tag{2.93}$$

Coefficients of several Chebyshev lowpass prototype filters with different levels of ripple and odd orders up to ninth order are given in Table 2-5.

2.7.3 Summary

A Butterworth filter has a monotonic response without ripple, but a relatively slow transition from the passband to the stopband. A Chebyshev filter has a rapid transition but has ripple in either the stopband or passband. Butterworth and Chebyshev filters are special cases of **elliptical filters**, which are also called **Cauer filters**. In general, an elliptical filter has ripple in both the stopband and the passband. The level of the ripple can be selected

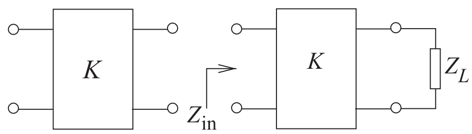

Figure 2-14: Impedance inverter (of impedance K in ohms): (a) represented as a two-port; and (b) the two-port terminated in a load.

independently in each band. With zero ripple in the stopband, but ripple in the passband, an elliptical filter becomes a **Type I Chebyshev filter**. With zero ripple in the passband, but ripple in the stopband, an elliptical filter becomes a **Type II Chebyshev filter**. With no ripple in either band the elliptical filter becomes a Butterworth filter. With ripple in both the passband and stopband, the transition between the passband and stopband can be made more abrupt or alternatively the tolerance to component variations increased.

Another type of filter is the **Bessel filter** which has maximally flat group delay in the passband, which means that the phase response has maximum linearity across the passband. The **Legendre filter** (also known as the **optimum "L" filter**) has a high transition rate from passband to stopband for a given filter order, and also has a monotonic frequency response (i.e., without ripple). It is a compromise between the Butterworth filter, with monotonic frequency response but slower transition and the Chebyshev filter, which has a faster transition but ripples in the frequency response.

More in-depth discussions of a large class of filters along with coefficient tables and coefficient formulas are available in Matthaei et al. [1], Hunter [3], Daniels [8], Lutovac et al. [9], and in most other books dedicated solely to microwave filters.

2.8 Impedance and Admittance Inverters

Inverters are two-port networks used in many RF and microwave filters. The input impedance of an inverter terminated in an impedance Z_L is $1/Z_L$. Impedance and admittance inverters are the same network, with the distinction being whether siemens or ohms are used to define them. An inverter is sometimes called a **unit element** (**UE**). At frequencies of a few hundred megahertz and below an inverter can be realized using operational and transconductance amplifiers. At microwave frequencies the simplest inverter is a one-quarter wavelength long line. In RF and microwave filter design they are used to convert a series element into a shunt element. It is much easier to realize shunt elements in distributed circuits than series elements. Similar circuit transformations enable an inductor to be replaced by a capacitor.

The schematic representation of an impedance inverter is shown in Figure, 2-14(a). The constitutive property of the inverter is that the input impedance of the terminated impedance inverter in Figure 2-14(b) is

$$Z_{\text{in}} = \frac{K^2}{Z_L}. \tag{2.94}$$

So the inverter both inverts the load impedance and scales it. Similarly, if Port 1 is terminated in Z_L the input impedance at Port 2 is Z_{in} as defined above.

An impedance inverter has the value K (in ohms), and sometimes K is called the characteristic impedance of the inverter. Sometimes K is just

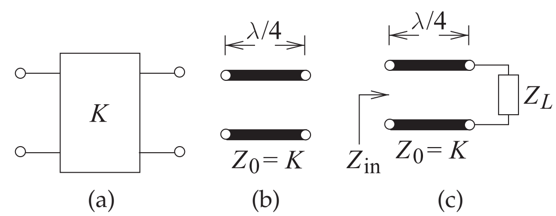

Figure 2-15: Inverter equivalence: (a) two-port impedance inverter (of impedance K): (b) a quarter-wave transmission line of characteristic impedance $Z_0 = K$; and (c) a terminated one-quarter wavelength long line.

called the impedance of the inverter. For an admittance inverter J is used and is called the characteristic admittance of the inverter, and sometimes just the admittance of the inverter. They are related as $J = 1/K$. In Section 2.4.6 of [10] it is shown that a $\lambda/4$ long line with a load has an input impedance that is the inverse of the load, normalized by the square of the characteristic impedance of the line. So an inverter can be realized at microwave frequencies using a one-quarter wavelength long transmission line (see Figure 2-15(b)). For the configuration shown in Figure 2-15(c),

$$Z_{\text{in}} = \frac{K^2}{Z_L}. \tag{2.95}$$

2.8.1 Properties of an Impedance Inverter

An impedance inverter has the $ABCD$ matrix

$$\mathbf{T} = \begin{bmatrix} 0 & \jmath K \\ \jmath/K & 0 \end{bmatrix}, \tag{2.96}$$

where K is called the characteristic impedance of the inverter. With a load impedance, Z_L (at Port 2), the input impedance (at Port 1) is (as expected)

$$Z_{\text{in}}(s) = \frac{AZ_L + B}{CZ_L + D} = \frac{\jmath K}{(\jmath/K)\,Z_L} = \frac{K^2}{Z_L}. \tag{2.97}$$

Now the $ABCD$ matrix of the transmission line of Figure 2-15(b) is

$$\begin{bmatrix} \cos\theta & \jmath Z_0 \sin\theta \\ (\jmath/Z_0)\sin\theta & \cos\theta \end{bmatrix}, \tag{2.98}$$

which is identical to Equation (2.96) when the electrical length is $\theta = \pi/2$ (i.e., when the line is $\lambda/4$ long). The inverter is shown in Figure 2-14(a) as a two-port and its implementation as a $\lambda/4$ long line is shown in Figure 2-14(c). The bandwidth over which the line realizes an impedance inverter is limited, however, as it is an ideal inverter only at the frequency at which it is $\lambda/4$ long.

2.8.2 Replacement of a Series Inductor by a Shunt Capacitor

A series inductor can be replaced by a shunt capacitor surrounded by a pair of inverters followed by a negative unity transformer (i.e., an inverter with $K = 1$). This equivalence is shown in Figure 2-16 and this will now be shown mathematically.

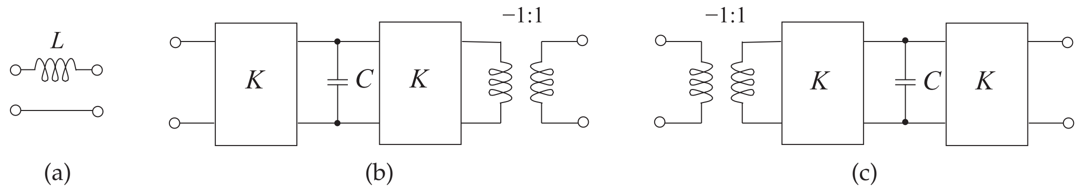

Figure 2-16: Equivalent realizations of a series inductor: (a) as a two-port; (b) its realization using a capacitor, inverters of characteristic impedance K, and a negative unity transformer; and (c) an alternative realization. $C = L/K^2$.

From Table 2-1 of [11], the $ABCD$ matrix of the series inductor shown in Figure 2-16(a) (which has an impedance of sL) is

$$\mathbf{T}_L = \begin{bmatrix} 1 & sL \\ 0 & 1 \end{bmatrix} \tag{2.99}$$

and the $ABCD$ matrix of the shunt capacitor (which has an admittance of sC) is, from Table 2-1 of of [11],

$$\mathbf{T}_1 = \begin{bmatrix} 1 & 0 \\ sC & 1 \end{bmatrix}. \tag{2.100}$$

The $ABCD$ matrix of an inverter with K in ohms (generally the unit is dropped and ohms is assumed) is

$$\mathbf{T}_2 = \begin{bmatrix} 0 & \jmath K \\ \jmath/K & 0 \end{bmatrix}, \tag{2.101}$$

and finally, the $ABCD$ matrix of a negative unity transformer, $n = -1$, is, from Table 2-1 of [11],

$$\mathbf{T}_3 = \begin{bmatrix} -1 & 0 \\ 0 & -1 \end{bmatrix}. \tag{2.102}$$

Then the $ABCD$ matrix of the cascade shown in Figure 2-16(b) is

$$\begin{aligned}
\mathbf{T}_C &= \mathbf{T}_2\mathbf{T}_1\mathbf{T}_2\mathbf{T}_3 \\
&= \begin{bmatrix} 0 & \jmath K \\ \jmath/K & 0 \end{bmatrix}\begin{bmatrix} 1 & 0 \\ sC & 1 \end{bmatrix}\begin{bmatrix} 0 & \jmath K \\ \jmath/K & 0 \end{bmatrix}\begin{bmatrix} -1 & 0 \\ 0 & -1 \end{bmatrix} \\
&= \begin{bmatrix} 0 & \jmath K \\ \jmath/K & 0 \end{bmatrix}\begin{bmatrix} 1 & 0 \\ sC & 1 \end{bmatrix}\begin{bmatrix} 0 & -\jmath K \\ -\jmath/K & 0 \end{bmatrix} \\
&= \begin{bmatrix} \jmath sCK & \jmath K \\ \jmath/K & 0 \end{bmatrix}\begin{bmatrix} 0 & -\jmath K \\ -\jmath/K & 0 \end{bmatrix} \\
&= \begin{bmatrix} 1 & sCK^2 \\ 0 & 1 \end{bmatrix}.
\end{aligned} \tag{2.103}$$

Thus $T_C = T_L$ if $L = CK^2$ (compare Equations (2.99) and (2.103)). Thus a series inductor can be replaced by a shunt capacitor with an inverter before and after it and with a negative unity transformer. The unity transformer

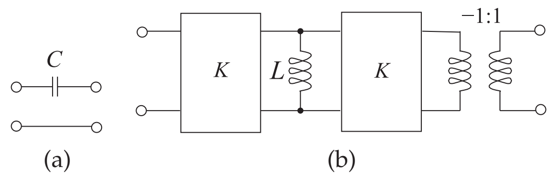

Figure 2-17: A series capacitor: (a) as a two-port; (b) its realization using a shunt inductor, inverters and negative unity transformer' $L = CK^2$.

may also be placed at the first port, as in Figure 2-16(c). Thus the two-ports shown in Figure 2-16 are all electrically identical, with the limitation being the frequency range over which the inverter can be realized. An interesting and important observation is that as a result of the characteristic impedance of the inverter (e.g., 50 Ω), a small shunt capacitor can be used to realize a large series inductance value.

EXAMPLE 2.5 Inductor Synthesis Using an Inverter

Consider the network of Figure 2-16(c) with inverters having a characteristic impedance of 50 Ω. What value of inductance is realized using a 10 pF capacitor?

Solution:

$K = 50$, so $L = CK^2 = 10^{-11} \cdot 2500 = 25$ nH.

2.8.3 Replacement of a Series Capacitor by a Shunt Inductor

A series capacitor can be replaced by a shunt inductor plus inverters and a negative transformer (see Figure 2-17). The $ABCD$ parameters of the series capacitor in Figure 2-17(a) are

$$\mathbf{T} = \begin{bmatrix} 1 & 1/sC \\ 0 & 1 \end{bmatrix}, \tag{2.104}$$

and here it is shown that the cascade in Figure 2-17(b) has the same $ABCD$ parameters. The cascade in Figure 2-17(b) has the $ABCD$ parameters

$$\begin{aligned} \mathbf{T} &= \begin{bmatrix} 0 & \jmath K \\ \jmath/K & 0 \end{bmatrix} \begin{bmatrix} 1 & 0 \\ 1/sL & 1 \end{bmatrix} \begin{bmatrix} 0 & \jmath K \\ \jmath/K & 0 \end{bmatrix} \begin{bmatrix} -1 & 0 \\ 0 & -1 \end{bmatrix} \\ &= \begin{bmatrix} 0 & \jmath K \\ \jmath/K & 0 \end{bmatrix} \begin{bmatrix} 1 & 0 \\ 1/sL & 1 \end{bmatrix} \begin{bmatrix} 0 & -\jmath K \\ -\jmath/K & 0 \end{bmatrix} \\ &= \begin{bmatrix} \jmath K/sL & \jmath K \\ \jmath/K & 0 \end{bmatrix} \begin{bmatrix} 0 & -\jmath K \\ -\jmath/K & 0 \end{bmatrix} \\ &= \begin{bmatrix} 1 & K^2/sL \\ 0 & 1 \end{bmatrix}. \end{aligned} \tag{2.105}$$

So the series capacitor, C, can be realized using a shunt inductor, L, inverters, and a negative unity transformer, and $C = L/K^2$. It is unlikely that this transformation would be exploited, as much better lower-loss capacitors can be realized at RF than inductors.

2.8.4 Ladder Prototype with Impedance Inverters

The transformations discussed in the previous two sections can be used to advantage in simplifying filters. In this section the transformations are

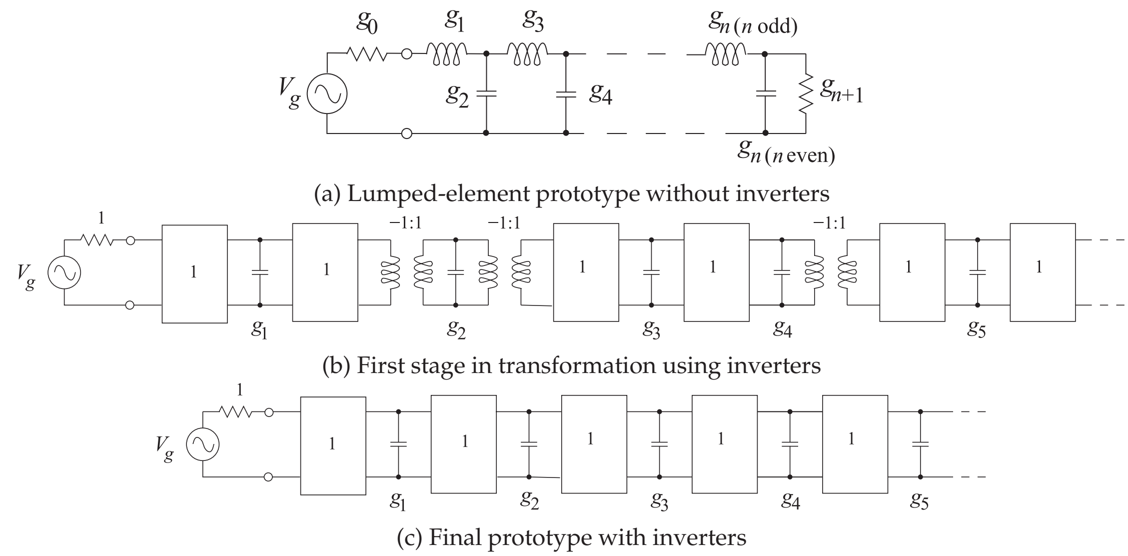

Figure 2-18: Ladder prototype filters using impedance inverters: (a) lumped-element prototype; (b) first stage in transformation using inverters; and (c) final stage.

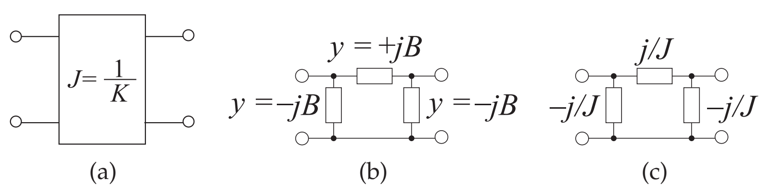

Figure 2-19: Admittance inverter: (a) as a two-port; (b) realized using lumped elements with $B = -J$; and (c) lumped equivalent circuit (the element values in (c) are impedances).

applied to the prototype lowpass ladder filter shown in Figure 2-18(a). The inductors in the ladder circuit are a particular problem as they have considerable resistance at microwave frequencies. The series inductors can be replaced by a circuit with capacitors, inverters, and transformers, as shown in Figure 2-18(b). This simplifies further to the realization shown in Figure 2-18(c), as the negative unity transformers only affect the phase of the transmission coefficient. So a lowpass ladder filter can be realized using just capacitors and inverters.

2.8.5 Lumped-Element Realization of an Inverter

The admittance inverter is functionally the same as the impedance inverter (see Figure 2-14(a)) and the schematic is the same (see Figure 2-19(a)). As will be shown, an inverter can be realized using frequency-invariant lossless elements (i.e., elements whose reactance or susceptance do not vary with frequency) using the network of Figure 2-19(b). Recall that J is used to identify an admittance inverter and K identifies an impedance inverter. If not specified by the context, the inverter (with value specified by a number) defaults to being an impedance inverter. Alternatively units can be used to indicate which type of inverter is being used. The function of

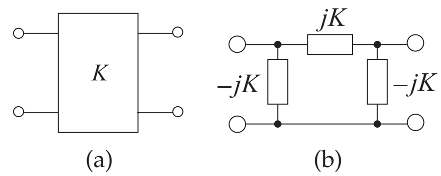

Figure 2-20: Impedance inverter: (a) as a two-port; and (b) its lumped equivalent circuit (the element values in (b) are impedances).

the inverter is the same in any case; both can be realized by one-quarter wavelength long lines, for example. For the remainder of this chapter it will be more convenient, most of the time, to use the admittance inverter, as many calculations will be in terms of admittances since most lumped elements in filters synthesis will be in shunt.

Now it will be shown that the lumped-element network of Figure 2-19(b) realizes an inverter. To do this the inverter and the lumped-element network must have the same two-port parameters. First, the $ABCD$ matrix of an inverter of characteristic admittance J is

$$\mathbf{T}_J = \begin{bmatrix} 0 & \jmath/J \\ \jmath J & 0 \end{bmatrix}. \tag{2.106}$$

Referring to Table 2-1 of [11], the circuit of Figure 2-19(b) has the $ABCD$ matrix

$$\begin{aligned} T &= \begin{bmatrix} 1 & 0 \\ -\jmath B & 1 \end{bmatrix} \begin{bmatrix} 1 & 1/(\jmath B) \\ 0 & 1 \end{bmatrix} \begin{bmatrix} 1 & 0 \\ -\jmath B & 1 \end{bmatrix} \\ &= \begin{bmatrix} 1 & 1/(\jmath B) \\ -\jmath B & 0 \end{bmatrix} \begin{bmatrix} 1 & 0 \\ -\jmath B & 1 \end{bmatrix} = \begin{bmatrix} 0 & -\jmath/B \\ -\jmath B & 0 \end{bmatrix}, \end{aligned} \tag{2.107}$$

where B is the susceptance of the frequency-invariant elements. Equation (2.107) is identical to Equation (2.106) if $B = -J$. More practical equivalents of the circuit of Figure 2-19(b) can be derived, as shown later.

For completeness, the lumped-element equivalent of the impedance inverter is shown in Figure 2-20 (derived from Figure 2-19 with $J = 1/K$).

EXAMPLE 2.6 Lumped Inverter Analysis

Demonstrate that Figure 2-19(b) is a lumped-element admittance inverter.

Solution:

Terminating the network in Figure 2-19(b) results in the network shown in Figure 2-21(a). This is relabeled in Figure 2-21(b), where the elements are admittances. Then

$$y_{\text{in}} = y_3 // (y_1 \$ (y_2 + y_L)), \tag{2.108}$$

where $//$ indicates "in parallel with" and \$ indicates "in series with." These are common shorthand notations in circuit calculations. Continuing on from Equation (2.108),

$$y_{\text{in}} = y_3 + \left[\frac{1}{y_1} + \left(\frac{1}{y_2 + y_L}\right)\right]^{-1} = y_3 + \left[\frac{y_2 + y_L + y_1}{y_1(y_2 + y_L)}\right]^{-1}. \tag{2.109}$$

Substituting $y_1 = \jmath B$ and $y_2 = y_3 = -\jmath B$, this becomes

$$y_{\text{in}} = -\jmath B + \frac{\jmath B(y_L - \jmath B)}{y_L} = \frac{-\jmath B y_L + \jmath B y_L + B^2}{y_L} = \frac{B^2}{y_L}. \tag{2.110}$$

Thus the lumped-element circuit of Figure 2-19(b) is a lumped-element admittance inverter of value B (in siemens).

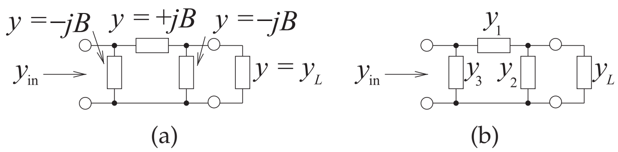

Figure 2-21: Terminated lumped-element admittance inverter.

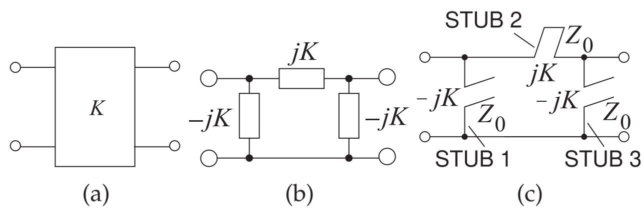

Figure 2-22: Narrowband inverter equivalents at frequency f_0: (a) impedance inverter with characteristic impedance K; (b) lumped-element equivalent network; and (c) inverter realized by short- and open-circuited stubs.

2.8.6 Narrowband Realization of an Inverter Using Transmission Line Stubs

In this section it will be shown that an impedance inverter can be implemented using short- and open-circuited stubs. The match is good over a narrow band centered at frequency f_0. An impedance inverter is shown in Figure 2-22(a) and its equivalent lumped-element network is shown in Figure 2-22(b). A stub-based implementation is shown in Figure 2-22(c), where there are short- and open-circuited stubs of characteristic impedance Z_0. The input impedance of the stubs is shown at the inputs of the stubs. The stubs have an electrical length θ at f_0 and the stubs are one-quarter wavelength long (i.e., resonant) at what is called the commensurate frequency, f_r.

Now it will be shown that the network of Figure 2-22(c) is a good representation of the inverter at f_0. This is done by matching $ABCD$ parameters. The $ABCD$ parameter matrix of an inverter is

$$T = \begin{bmatrix} 0 & \jmath K \\ \jmath/K & 0 \end{bmatrix} \tag{2.111}$$

and, at frequency f_0, the $ABCD$ parameter matrix of the stub circuit of Figure 2-22(c) is

$$\begin{aligned} T &= \begin{bmatrix} 1 & 0 \\ -1/[\jmath Z_0 \tan(\theta)] & 1 \end{bmatrix} \begin{bmatrix} 1 & \jmath Z_0 \tan(\theta) \\ 0 & 1 \end{bmatrix} \begin{bmatrix} 1 & 0 \\ -1/[\jmath Z_0 \tan(\theta)] & 1 \end{bmatrix} \\ &= \begin{bmatrix} 1 & \jmath Z_0 \tan(\theta) \\ -1/[\jmath Z_0 \tan(\theta)] & 0 \end{bmatrix} \begin{bmatrix} 1 & 0 \\ -1/[\jmath Z_0 \tan(\theta)] & 1 \end{bmatrix} \\ &= \begin{bmatrix} 0 & \jmath Z_0 \tan(\theta) \\ \jmath/[Z_0 \tan(\theta)] & 0 \end{bmatrix}. \end{aligned} \tag{2.112}$$

Thus, equating Equations (2.111) and (2.112), the stub network is a good representation of the inverter if

$$K = Z_0 \tan(\theta), \tag{2.113}$$

and so the required characteristic impedance of each stub at frequency f_0 is

$$Z_0 = \frac{K}{\tan(\theta)} = \frac{K}{\tan\left(\frac{\pi}{2}\frac{f_0}{f_r}\right)}. \tag{2.114}$$

Special Case, $f_r = 2f_0$

In most designs the stub resonant frequency, f_r (also called the commensurate frequency), is chosen to be twice that of the center frequency of the design, f_0. So with $f_r = 2f_0$, then at f_0

$$Z_0 = \frac{K}{\tan\left(\frac{\pi}{2}\frac{f_0}{2f_0}\right)} = \frac{K}{\tan \pi/4} = K \tag{2.115}$$

and the input impedance of the stub is $\jmath K$. So the characteristic impedance of the transmission line stub is $Z_0 = K$.

2.9 Filter Transformations

So far the discussion has centered around lowpass filters. Filter design technology has developed so that the design of a corresponding lowpass filter is the essential first step, and this is used as a prototype to derive a filter with other characteristics. The three most important transformations are listed here:

1. Impedance scaling: A lowpass filter prototype is referenced to a standard impedance. Usually $1\ \Omega$ is used, so the reference source and load resistances are also $1\ \Omega$. To reference to a higher or lower impedance, scaling of the impedance of all elements of the filter is required.
2. Corner frequency scaling: The corner frequency of a lowpass filter prototype is normalized to 1 rad/s. To reference to another frequency, the values of the elements must be altered so that they have the same impedance at the scaled frequency.
3. Filter type transformation: These transformations enable the circuit of a lowpass filter to be converted to a circuit with a bandpass, bandstop, or highpass response. The concept is that the response at DC is to be replicated at infinite frequency for the highpass (so capacitors become inductors, etc.); to be replicated at the center of the passband for a bandpass filter (so capacitors become a shunt LC circuit); and to be inverted at the center of a bandstop filter (so capacitors become a series LC circuit).

The transformations can be performed in any order. The key point is that the complexity of the lowpass circuit design is minimal since the number of elements does not grow until the filter type transformation is performed, so this step is often done last.

2.9.1 Impedance Transformation

The lowpass prototypes discussed up to now have been referred to a $1\ \Omega$ system. The system impedance can be changed to any level by simply scaling the impedances of all the circuit elements in a filter by the same amount, as shown in Figure 2-23. The impedance transformation follows the same procedure for all filter types (the procedure is the same for lowpass, highpass, bandpass, and bandstop filters, for example). It should also be noted that impedance scaling of a transmission line is simply multiplication of the line's characteristic impedance by the scale factor.

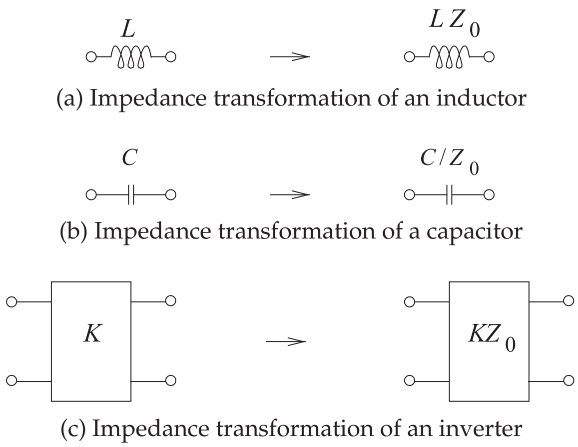

(a) Impedance transformation of an inductor

(b) Impedance transformation of a capacitor

(c) Impedance transformation of an inverter

Figure 2-23: Impedance transformations. The impedances of the elements are increased by a factor Z_0.

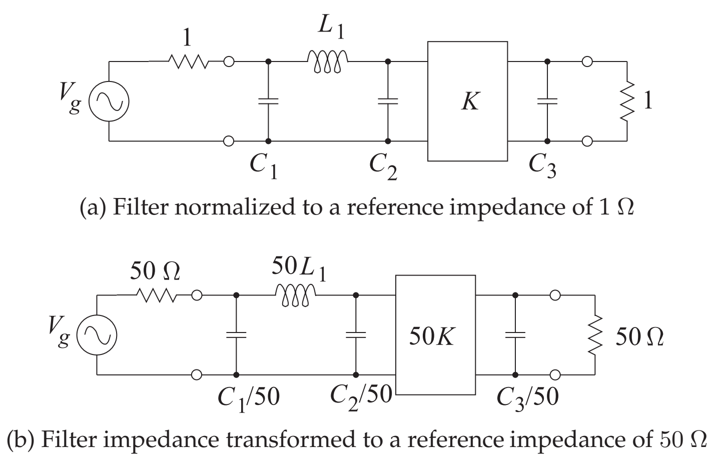

(a) Filter normalized to a reference impedance of 1 Ω

(b) Filter impedance transformed to a reference impedance of 50 Ω

Figure 2-24: Impedance transformation of an example filter.

EXAMPLE 2.7 Lowpass Filter Design

Consider the lowpass filter, with an inverter, shown in Figure 2-24(a). This filter is referenced to 1 Ω, as the source and load impedances are both 1 Ω. Redesign the filter so that the same frequency response is obtained with 50 Ω source and load impedances.

Solution:

It is necessary to impedance transform from 1 Ω to 50 Ω. The resulting filter is shown in Figure 2-24(b). Each element has an impedance (resistance or reactance) that is 50 times larger than it had in the 1 Ω prototype.

2.9.2 Frequency Transformation: Lowpass

Frequency transformations differ depending on the type of the filter. So it is normal to frequency transform the lowpass prototype before converting the prototype to another form (such as bandpass). The lowpass prototypes normally have a band-edge or cutoff frequency at an angular frequency of unity, that is, 1 rad/s. The band-edge frequency can be transformed from unity to an arbitrary angular frequency ω_c, as shown in Figure 2-25, by scaling the reactive elements, as shown in Figures 2-26 and 2-27(a), so that

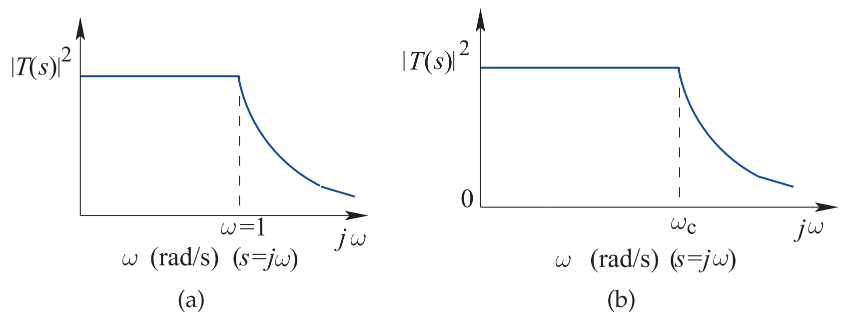

Figure 2-25: Frequency transformation of a lowpass filter response from (a) one normalized to a corner frequency of 1 rad/s, to (b) one with a radian corner frequency of ω_c.

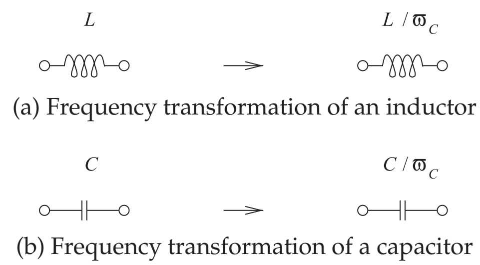

Figure 2-26: Frequency transformations. The impedance of the new (scaled) element at the new (scaled) frequency is the same as it was at the original frequency.

they have the same impedance at the transformed frequency as they did at the original frequency. The inverter is unchanged, as are the source and load resistances, since these are frequency independent.

2.9.3 Lowpass to Highpass Transformation

The transformation of a lowpass filter prototype to a highpass filter is shown diagrammatically in Figure 2-28. Mathematically ω in the transfer function of the lowpass prototype is replaced by $-1/\omega$, that is

$$T_{\text{highpass}}(\omega) = T_{\text{lowpass}}(-1/\omega). \tag{2.116}$$

In terms of a lumped element in the lowpass prototype circuit, if an element has an impedance $\jmath\omega L$ and L is frequency independent, then the corresponding element in the highpass prototype filter has an impedance $1/(\jmath\omega^2 L)$. Thus reactive elements are transformed as shown in Figure 2-27(b), where ω_0 is the corner frequency of both the lowpass and highpass prototype circuits. So inductors are transformed into capacitors and capacitors into inductors. For example, the odd-order lowpass filter prototypes shown in Figure 2-13 are transformed into the highpass filters shown in Figure 2-29.

2.9.4 Lowpass to Bandpass Transformation

Understanding the transformation of the lowpass filter into its corresponding bandpass form requires that the lowpass filter be considered with both its positive and negative frequency responses, as shown in Figure 2-30(a). This response is shifted in frequency to obtain the bandpass response shown in Figure 2-30(b). Mathematically the radian frequency, ω, in the response

Lowpass prototype		Reactance transformation
(a) LOWPASS PROTOTYPE TO LOWPASS TRANSFORMATION		
Lowpass prototype	Lowpass element	Reactance transformation ω_0 = corner frequency
C_0	C_1	$C_1 = C_0/\omega_0$
L_0	L_1	$L_1 = L_0/\omega_0$
(b) LOWPASS PROTOTYPE TO HIGHPASS TRANSFORMATION		
Lowpass prototype	Highpass element	Reactance transformation ω_0 = corner frequency
C_0	L_1	$L_1 = 1/(\omega_0 C_0)$
L_0	C_1	$C_1 = 1/(\omega_0 L_0)$
(c) LOWPASS PROTOTYPE TO BANDPASS TRANSFORMATION		
Lowpass prototype	Bandpass element	Reactance transformation ω_0 = center of passband
C_0	L_1 C_1 (parallel)	$C_1 = \alpha C_0/\omega_0 \quad L_1 = 1/(\alpha C_0 \omega_0)$
L_0	L_1 C_1 (series)	$L_1 = \alpha L_0/\omega_0 \quad C_1 = 1/(\alpha L_0 \omega_0)$
(d) LOWPASS PROTOTYPE TO BANDSTOP TRANSFORMATION		
Lowpass prototype	Bandstop element	Reactance transformation ω_0 = center of stopband
C_0	L_1 C_1 (series)	$L_1 = \alpha/(C_0 \omega_0) \quad C_1 = C_0/(\omega_0 \alpha)$
L_0	L_1 C_1 (parallel)	$L_1 = L_0/(\alpha \omega_0) \quad C_1 = \alpha/(L_0 \omega_0)$

Figure 2-27: Transformations of the elements of a prototype lowpass filter to obtain specific filter types. The corner frequency of the lowpass prototype is 1 rad/s. In the transformations to bandpass and bandstop filters, $\omega_0 = 1/\sqrt{L_1 C_1} = \sqrt{\omega_1 \omega_2}$; ω_1 and ω_2 are the band-edge frequencies, and α is the transformation constant, $\alpha = \omega_0/(\omega_2 - \omega_1)$.

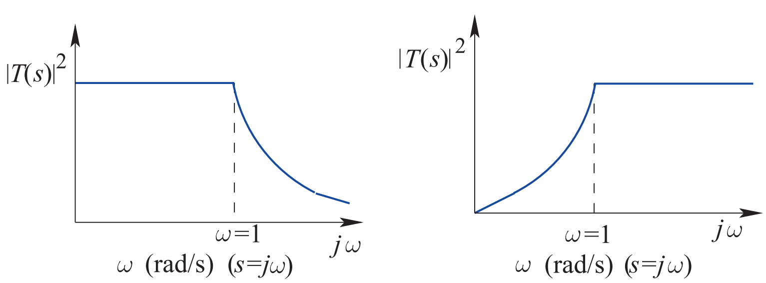

(a) Lowpass response (b) Highpass response

Figure 2-28: Lowpass to highpass transformation.

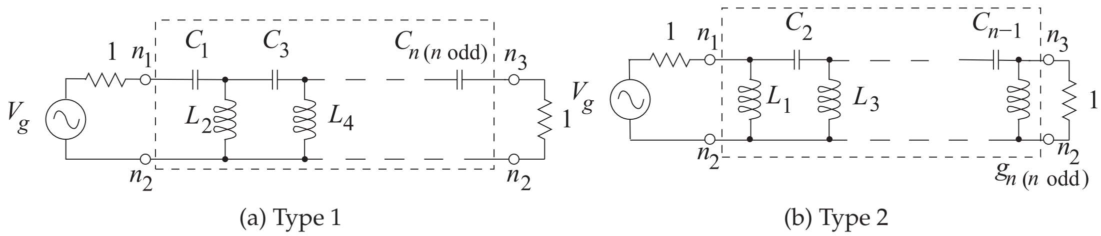

Figure 2-29: Odd-order Chebyshev highpass filter prototypes in the Cauer topology. Here n is the order of the filter.

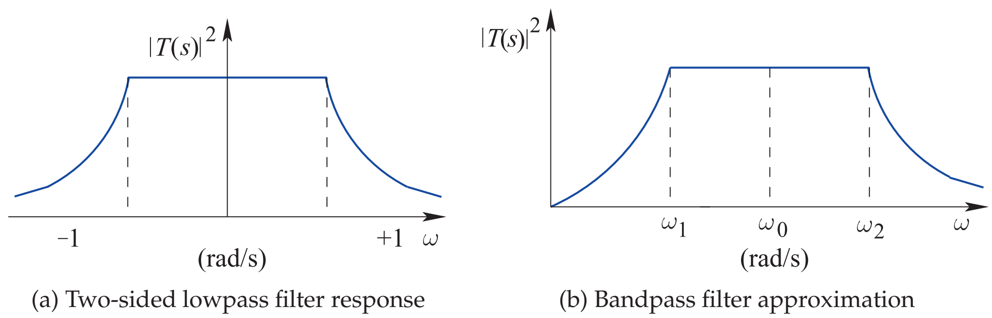

Figure 2-30: Frequency responses in lowpass to bandpass transformation ($s = \jmath\omega$).

function is replaced by its bandpass form,

$$\omega \to \left[\frac{\omega}{\omega_0} - \frac{\omega_0}{\omega}\right]. \tag{2.117}$$

That is, $$T_{\text{bandpass}}(\omega) = T_{\text{lowpass}}\left(\frac{\omega}{\omega_0} - \frac{\omega_0}{\omega}\right), \tag{2.118}$$

and so the transfer function of the bandpass filter is derived from the transfer function of the bandpass filter with ω replaced by $(\omega/\omega_0 - \omega_0/\omega)$. This separately maps the -1 and $+1$ band-edge radian frequencies of the lowpass response to the bandpass frequencies ω_1 and ω_2:

$$-1 \to \left[\frac{\omega_1}{\omega_o} - \frac{\omega_o}{\omega_1}\right] \quad \text{and} \quad +1 \to \left[\frac{\omega_2}{\omega_o} - \frac{\omega_o}{\omega_2}\right]. \tag{2.119}$$

Solving the above equations simultaneously yields the center frequency ω_0 and the band-edge frequencies ω_1 and ω_2 with

$$\omega_o = \sqrt{\omega_1 \omega_2} \tag{2.120}$$

and the so-called transformation constant

$$\alpha = \frac{\omega_o}{\omega_2 - \omega_1}. \tag{2.121}$$

The resulting element conversions are given in Figure 2-27(c).

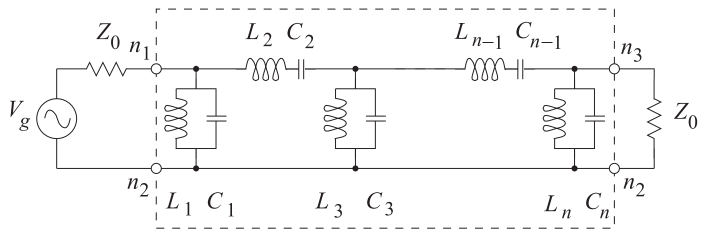

Figure 2-31: Lumped-element odd-order (nth-order) Chebyshev bandpass filter prototypes in the Type II Cauer topology.

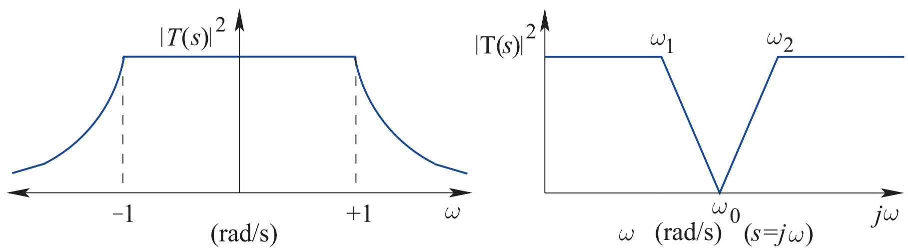

Figure 2-32: Frequency responses in lowpass to bandstop transformation.

As an example, a lumped-element Type 2 Cauer bandpass filter is shown in Figure 2-31. The shunt LC combination and the series LC combinations are resonators resonant at the center frequency of the filter. Here the filter is normalized to Z_0 source and load impedances. As these are the same, this filter topology only applies for an odd-order filter. Combining transformations, the element values of a lumped bandpass filter with center radian frequency $\omega_0 = 2\pi f_0$ and radian bandwidth $\omega_{\mathrm{BW}} = 2\pi(f_2 - f_1)$ are as follows (g_r is from the lowpass prototype):

$$C_r = \begin{cases} \dfrac{g_r}{\omega_{\mathrm{BW}} Z_0} & r = \mathrm{odd} \\[2ex] \dfrac{\omega_{\mathrm{BW}}}{\omega_0^2 g_r Z_0} & r = \mathrm{even} \end{cases} \quad \text{and} \quad L_r = \begin{cases} \dfrac{\omega_{\mathrm{BW}} Z_0}{\omega_0^2 g_r} & r = \mathrm{odd} \\[2ex] \dfrac{g_r Z_0}{\omega_{\mathrm{BW}}} & r = \mathrm{even} \end{cases}. \tag{2.122}$$

2.9.5 Lowpass to Bandstop Transformation

Again, consider both the positive and negative frequency responses of the lowpass filter prototype, as shown in Figure 2-32(a). This response is shifted in frequency to obtain the bandstop response shown in Figure 2-32(b). Mathematically the frequency, ω, in the response function is replaced by its bandstop form:

$$\omega \rightarrow \left[\alpha\left(\frac{\omega}{\omega_0} - \frac{\omega_0}{\omega}\right)\right]^{-1}. \tag{2.123}$$

That is, $$T_{\mathrm{bandstop}}(\omega) = T_{\mathrm{lowpass}}\left(\frac{1}{\alpha}\left[\frac{\omega}{\omega_0} - \frac{\omega_0}{\omega}\right]^{-1}\right). \tag{2.124}$$

The center frequency (corresponding to DC in the lowpass prototype response) is

$$\omega_o = \sqrt{\omega_1 \omega_2} \tag{2.125}$$

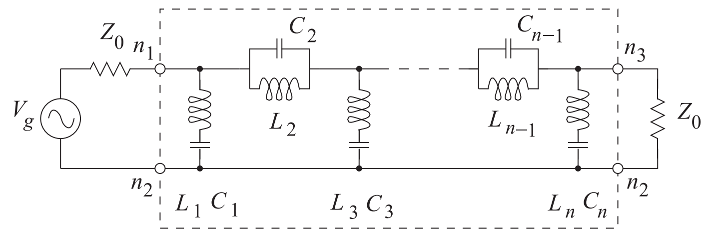

Figure 2-33: Lumped-element odd-order (nth-order) Chebyshev bandstop filter prototypes in the type II Cauer topology.

and the transformation constant is

$$\alpha = \frac{\omega_o}{\omega_2 - \omega_1}, \tag{2.126}$$

where ω_1 and ω_2 are the band-edge radian frequencies. The resulting element conversions are given in Figure 2-27(d).

Combining transformations, the element values of a lumped bandstop filter with center radian frequency $\omega_0 = 2\pi f_0$ and radian bandwidth $\omega_{\rm BW} = 2\pi(f_2 - f_1)$ are as follows:

$$C_r = \begin{cases} \dfrac{g_r \omega_{\rm BW}}{\omega_0^2 Z_0} & r = \text{odd} \\[2ex] \dfrac{1}{\omega_{\rm BW} g_r Z_0} & r = \text{even} \end{cases} \quad \text{and} \quad L_r = \begin{cases} \dfrac{Z_0}{\omega_{\rm BW} g_r} & r = \text{odd} \\[2ex] \dfrac{g_r \omega_{\rm BW} Z_0}{\omega_0^2} & r = \text{even} \end{cases}. \tag{2.127}$$

A lumped-element type II Cauer bandstop filter is shown in Figure 2-33. The parallel LC combination and the series LC combinations are resonators resonant at the center frequency of the filter. The parallel LC resonator is an open circuit at the center frequency of the stopband and the series LC resonators are short circuits. The LC resonators are implemented using resonators, usually transmission line segments and not lumped components.

2.9.6 Transformed Ladder Prototypes

Combining the filter type transformations, and with appropriate use of inverters, the original lowpass prototype ladder filter and its various filter type transforms are shown in Figure 2-34.

2.10 Cascaded Line Realization of Filters

In this section, filters are presented that use cascaded sections of transmission line, realizing series inductors and shunt capacitors. For example, a short (less than one-quarter wavelength long) length of relatively high-impedance line behaves predominantly as a series inductance. Also, a very short (much less than one-quarter wavelength long) length of relatively low-impedance line acts predominantly as a shunt capacitance. So a Pi network of lumped elements can be realized with alternate sections of low- and high-impedance microstrip lines. Such an inductive line is shown in Figure 2-35(a), which has the two equivalent circuits shown in Figure 2-35(b and c). Basic transmission line theory gives the input reactance of the line of length, ℓ (with a low-impedance load),

$$X_L = Z_0 \sin\left(2\pi\ell/\lambda_g\right), \tag{2.128}$$

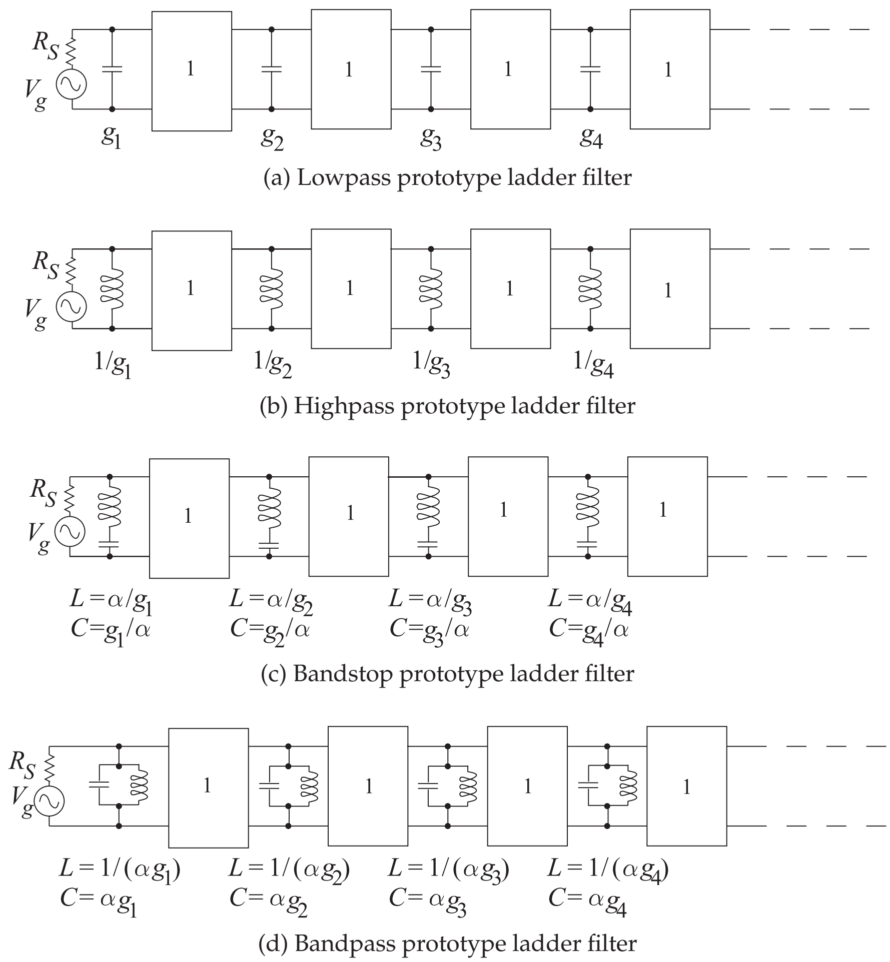

Figure 2-34: Ladder prototype filters.

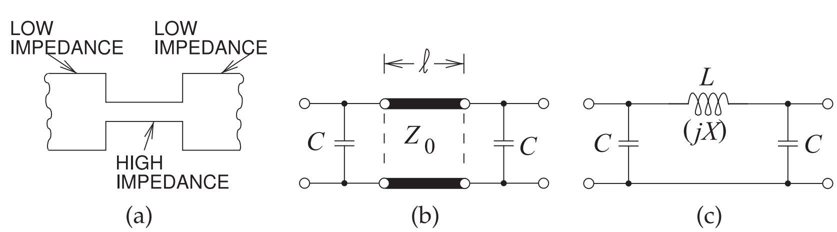

Figure 2-35: Inductive length of line with adjacent capacitive lines: (a) microstrip form; (b) lumped equivalent circuit; and (c) lumped-distributed equivalent circuit.

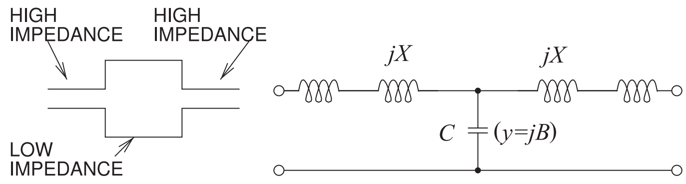

(a) (b)

Figure 2-36: Capacitive length of line with adjacent inductive lines: (a) microstrip; and (b) lumped equivalent (the left-most and right-most series inductors come from the high-impedance lines).

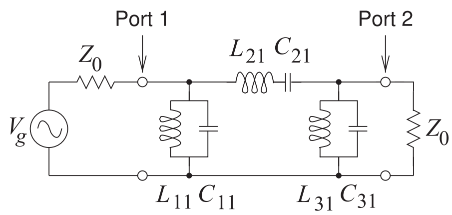

Butterworth
$C_{11} = C_{31} = 31.8310$ pF
$L_{11} = L_{31} = 795.775$ pH
$C_{21} = 159.155$ fF
$L_{21} = 159.155$ nH

Chebyshev
$C_{11} = C_{31} = 41.5369$ pF
$L_{11} = L_{31} = 609.824$ pH
$C_{21} = 188.299$ fF
$L_{21} = 134.522$ nH
ripple, ε = 0.1 = 0.043 dB

Figure 2-37: Lumped-element 3rd-order bandpass filters in a $Z_0 = 50\ \Omega$ system with center frequency $f_0 = 1$ GHz and a 3 dB bandwidth of 10%.

so that the length of this predominantly inductive line is

$$\ell = \frac{\lambda_g}{2\pi} \sin^{-1}\left(\frac{\omega L}{Z_0}\right). \tag{2.129}$$

Previously it was shown that a short length of line having a relatively low characteristic impedance yields a capacitive element and this is shown, together with its equivalent circuit, in Figure 2-36. The predominating shunt capacitance is determined by first considering the susceptance

$$B = \frac{1}{Z_0} \sin\left(\frac{2\pi\ell}{\lambda_g}\right) \tag{2.130}$$

so that

$$\ell = \frac{\lambda_g}{2\pi} \sin^{-1}(\omega C Z_0). \tag{2.131}$$

Thus a cascade of low-impedance and high-impedance lines can realize (approximately) an LC ladder network.

It is tempting to take filters synthesized in lumped-element form and realize them in the above manner with transmission lines. The series element realization concept presented in this section could be extended using shorted and open stubs to better realize shunt elements. The problem with this approach is that the resulting filters are narrowband and the response outside the desired operating range is unpredictable. It is far better to employ the Richards's transformation, considered in Section 2.12, which is a much broader bandwidth technique for realizing filters in distributed form.

2.11 Butterworth and Chebyshev Bandpass Filters

Designs of Butterworth and Chebyshev filters with center frequencies of 1 GHz and 3 dB bandwidths of 10% are shown in Figure 2-37. Their transmission, S_{21}, and reflection, S_{11}, responses are shown in Figure 2-38. The filter skirts, i.e. the transitions from the passband to the stopbands, is steeper for the Chebyshev filter than for the Butterworth filter as expected. The ripple of the Chebyshev filter is very small and not seen in this plot. In a real filter there will be loss and low-level ripples in the magnitude response

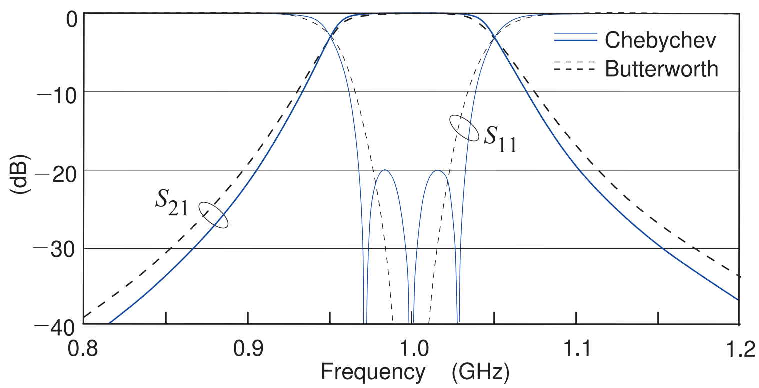

Figure 2-38: Insertion loss (S_{21}) and return loss (S_{11}) of the Butterworth and Chebychev lumped-element bandpass filters in a $50\ \Omega$ system.

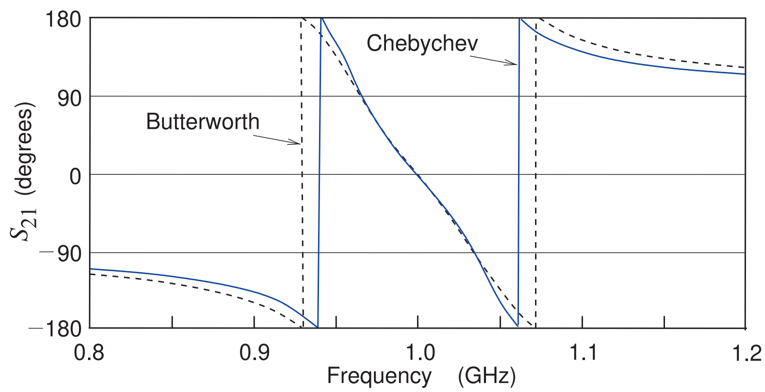

Figure 2-39: Phase of the transmission response (S_{21}) of the Butterworth and Chebyshev lumped-element filters. The discontinuities seen in the phase from $-180°$ to $+180°$ are artifacts and the phases of the filters reduce monotonically with increasing frequency. (For example, the phase at 0.8 GHz is $-110° + 360° = 250°$.)

disappear. However even with loss the steep skirts of the Chebyshev transmission response remain. Also, even with loss, the impact of the Chebyshev ripples is clearly seen in the reflection (S_{11}) response. In Figure 2-38 three distinct S_{11} zeros are seen and these correspond to the three poles of the Chebyshev filter's S_{21} response, but of course we cannot see these. (In the Laplace transfer function there are 3 complex poles each pair being transformed from one of the three poles of the lowpass prototype.) The Butterworth filter also has three (complex) S_{11} zeros and these are all at the center frequency of the bandpass filter, 1 GHz.

Another characteristic that differs between the Chebyshev and Butterworth responses is seen in their phase responses plotted in Figure 2-39. Each pole in the S_{21} characteristic causes a $90°$ phase change. The three complex poles (i.e. six actual poles) of S_{21} then result in six $90°$ phase changes in S_{21} for a total phase change of $450°$. Small ripples are seen in the Chebyshev phase responses in the pass band while the phase changes for the Butterworth filter are smooth. (The Chebyshev phase ripples remain even with low-level loss.)

The magnitude and phase responses, Figures 2-38 and 2-39, do not provide complete visualization of the filter characteristics. Additional insight is provided in the S_{11} loci on the Smith chart, see Figure 2-40. Figure 2-40 shows the S_{11} characteristics plotted on Smith charts. (In the passband the S_{21} locus would be very close to the unit circle and little of value is observed in the passband.) There is a wealth of information here. First consider the response for the Chebyshev filter, Figure 2-40(a). As frequency increases from 0.8 GHz, the locus of S_{11} is first close to the unit circle and then approaches the origin

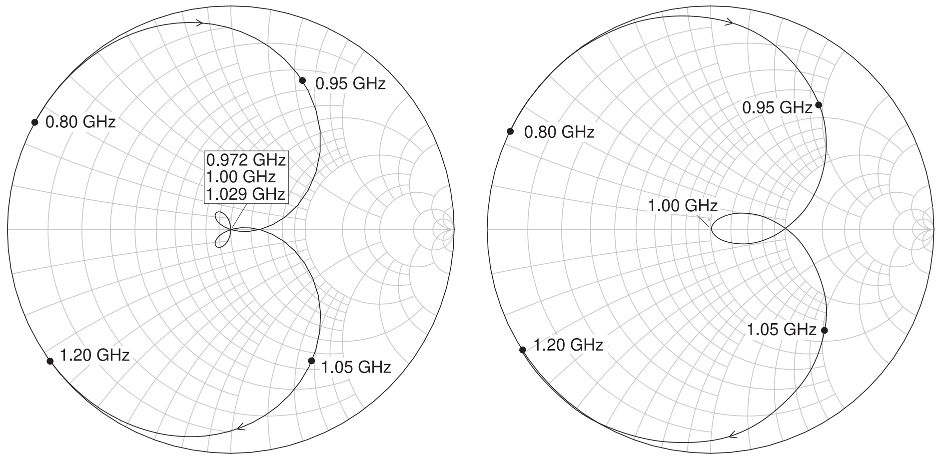

(a) Chebyshev (b) Butterworth

Figure 2-40: Smith chart plot of S_{11} of the Butterworth and Chebychev lumped-element filters.

of the polar plot as the frequency approaches the passband of the filter. A special characteristic of the Chebyshev response is the looping which here results in three passes of the locus through the origin. These are the three zeros. Eventually the locus of S_{11} increases as frequency increases above the passband. A loop is also seen in the Butterworth response, Figure 2-40(b). This loop goes through the origin and while it seems that there is just one zero there are actually three. What is happening is that as frequency increases and as the locus of the Butterworth S_{11} response approaches the origin, the movement of the locus with respect to frequency slows down. The best way to be convinced that there are three zeros of S_{11} is to look at the transmission phase ($\angle S_{21}$) response in Figure 2-38.

Comprehensive visualization of the filter response requires the rectangular plots of the magnitudes of S_{21} and S_{11}, Figure 2-38, of S_{21} phase, Figure 2-39, and the Smith chart plot of S_{11}, Figure 2-40. The phase plot convinces you of the number of zeros in your design which is important in interpreting the Butterworth results. A physical implementation of the design will not be exact and so tuning is required. Then the most important characterizations are the rectangular magnitude and Smith chart responses. Here the loops on the Smith chart, even if they do not go through the origin exactly, distinguish the Butterworth and Chebyshev responses. Matching may be required to shift the loops to the origin of the polar plot.

2.12 Richards's Transformation

Richards's transformation is a remarkable scheme that takes into account the actual properties of transmission lines, yielding broadband transmission line-based implementations of lumped-element filter prototypes [12–15].

2.12.1 Richards's Transformation and Transmission Lines

Consider a section of transmission line of electrical length θ with $ABCD$ parameters

$$T = \begin{bmatrix} \cos(\theta) & \jmath Z_0 \sin(\theta) \\ \jmath / Z_0 \sin(\theta) & \cos(\theta) \end{bmatrix}. \tag{2.132}$$

If this line is terminated in a load, Z_L, then its input impedance is

$$Z_{\text{in}}(\theta) = \frac{\cos(\theta) Z_L + \jmath Z_0 \sin(\theta)}{j/Z_0 \sin(\theta) Z_L + \cos(\theta)}. \tag{2.133}$$

Now examine two extreme conditions. As the load impedance increases, eventually becoming an open circuit, the input impedance of a line with electrical length θ is defined in terms of a cotangent of the electrical length:

$$Z_L \to \infty \quad \Rightarrow Z_{\text{in}}(\theta) = \frac{Z_0}{\jmath} \cot(\theta) \tag{2.134}$$

$$Y_{\text{in}}(\theta) = \jmath Y_0 \tan(\theta). \tag{2.135}$$

As the load impedance reduces to become a short circuit, the input impedance of a line with electrical length θ is defined in terms of a tangent of the electrical length:

$$Z_L \to 0 \quad \Rightarrow \quad Z_{\text{in}}(\theta) = \jmath Z_0 \tan(\theta). \tag{2.136}$$

These results lead to the Richards's transformation, which replaces the Laplace variable, s, by Richards's variable, S, where $S = \jmath\alpha \tan(\theta)$. This transformation is written

$$s \to S = \jmath\alpha \tan(\theta). \tag{2.137}$$

For now α and θ are constants that can be chosen as design variables. θ, of course, is the electrical length of the line. Also, α must have the units of impedance and it is the characteristic impedance of the transmission line.

Applying the Richards's transformation to a capacitor, the admittance of the element is transformed as follows:

$$y = sC \to Y = SC = \jmath\alpha C \tan(\theta), \tag{2.138}$$

so that the capacitor is transformed into an open-circuited stub with characteristic admittance

$$Y_0 = \alpha C\ . \tag{2.139}$$

If a lumped-element capacitor with admittance $y = sC$ is to be realized using a transmission line, the admittance $Y = SC = \jmath\alpha C \tan(\theta)$ is instead realized. There are two parameters to select to realize this admittance. The first, α, is the characteristic admittance of the transmission line (and for any given transmission line topology there is a minimum and maximum characteristic admittance or impedance that can be realized), and θ is the electrical length of the line.

Applying the transformation to an inductor, the impedance of the element is transformed as follows:

$$Z = sL \to Z = SL = \jmath\alpha L \tan(\theta), \tag{2.140}$$

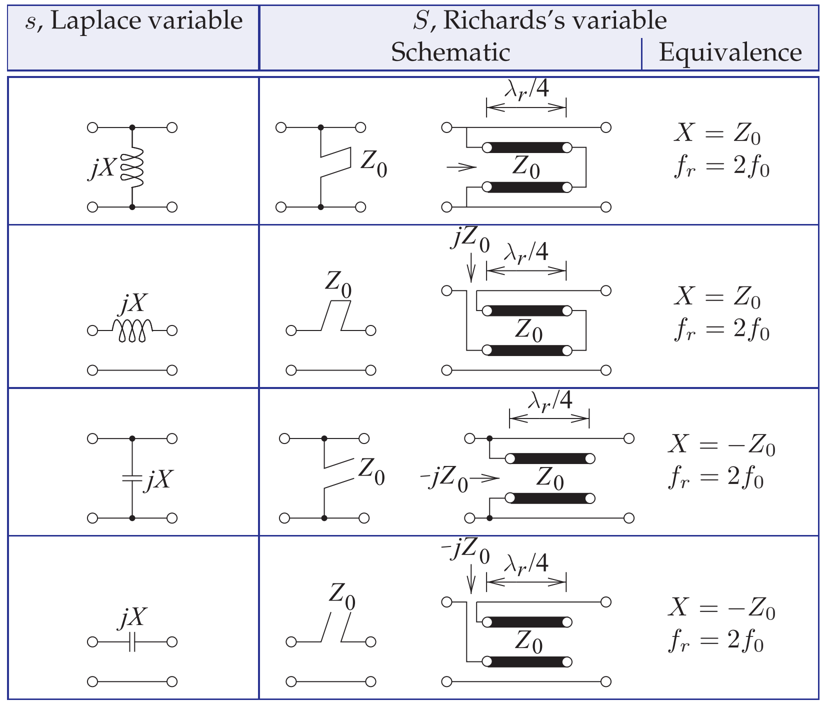

Figure 2-41: Equivalences resulting from Richards's transformation. With $f_r = 2f_0$ the transmission line stubs are one-eighth wavelength long at f_0.

so that the inductor is transformed into a short-circuited stub with characteristic impedance

$$Z_0 = \alpha L. \tag{2.141}$$

Thus the Richards's transform converts an inductor into a short-circuited stub and a capacitor into an open-circuited stub.

2.12.2 Richards's Transformation and Stubs

There is a duality between stubs and inductors and capacitors; they are coupled by Richards's transformation. One of the important quantities used in the transformation is the commensurate frequency, f_r, which most often is chosen as twice the operating frequency, f_0. Considering stubs that are one-quarter wavelength long at f_r, the duality is as shown in Figure 2-41.

2.12.3 Richards's Transformation Applied to a Lowpass Filter

In this section, Richards's transformation is used to realize a lumped-element filter in distributed form. The design example begins by considering a Chebyshev lowpass filter with the transmission characteristic

$$|T(s)|^2 = \frac{1}{1 + \varepsilon^2 |K(s)|^2}. \tag{2.142}$$

With the Richards's transformation ($s \to \jmath\omega \to \jmath\alpha \tan(\theta)$) this becomes

$$|T(\jmath\alpha \tan\theta)|^2 = \frac{1}{1 + \varepsilon^2 |K(\jmath\alpha \tan\theta)|^2}. \tag{2.143}$$

Thus the passband edge at $\omega = 1$ is mapped to $\omega = \theta_1$ as

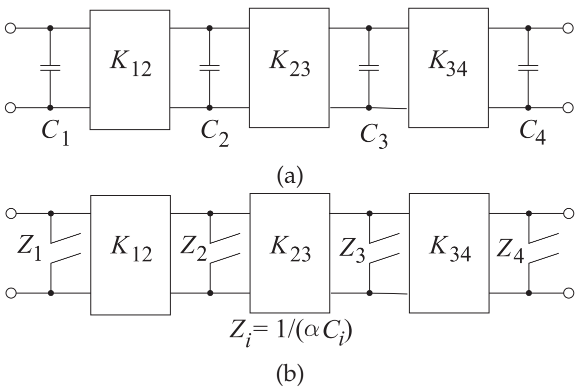

Figure 2-42: Lowpass prototypes: (a) lowpass prototype as a ladder filter with inverters; and (b) lowpass distributed prototype with open-circuited stubs (the impedance looking into the stub is indicated).

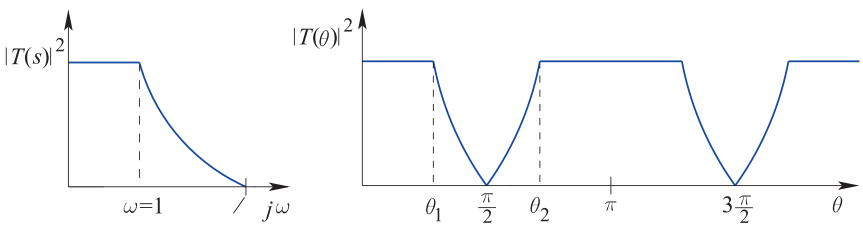

(a) Lowpass filter response

(b) Distributed lowpass filter response

Figure 2-43: Lowpass to distributed lowpass transformation. $s = \jmath\omega$.

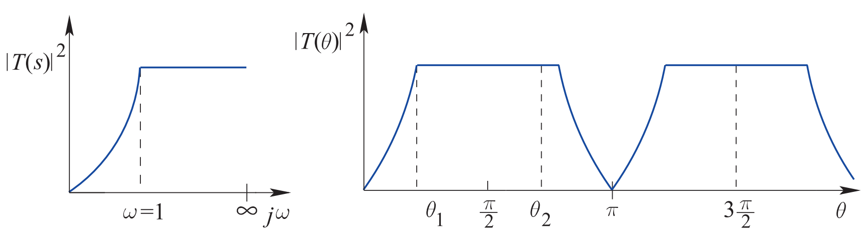

(a) Highpass filter response

(b) Distributed highpass filter response

Figure 2-44: Highpass to distributed highpass transformation. $s = \jmath\omega$.

$$\omega = 1 \rightarrow \alpha \tan(\theta_1) \qquad (2.144) \qquad \text{so that} \qquad \alpha = \frac{1}{\tan(\theta_1)}. \qquad (2.145)$$

Recalling that a capacitor is transformed into an open-circuited stub (see Equation (2.139)), Richards's transformation applied to the lowpass filter prototype results in a filter with transmission line elements only, as shown Figure 2-42, provided that the inverters are realized using transmission lines.

The implementation of a lowpass filter in distributed form results in passbands and stopbands that repeat in frequency, as shown in Figure 2-43. This occurs because transmission lines are used to realize lumped elements and the two-port parameters of a transmission line repeat every wavelength (or one-half wavelength in some cases). For example, the input impedance of a stub is the same whether it is one-half wavelength long or one wavelength long.

2.12.4 Richards's Transformation Applied to a Highpass Filter

With reference to Figure 2-44(a), the passband edge at $\omega = 1$ is mapped to θ_1, as shown in Figure 2-44(b). This means that the passband at $\omega = 1$ is mapped

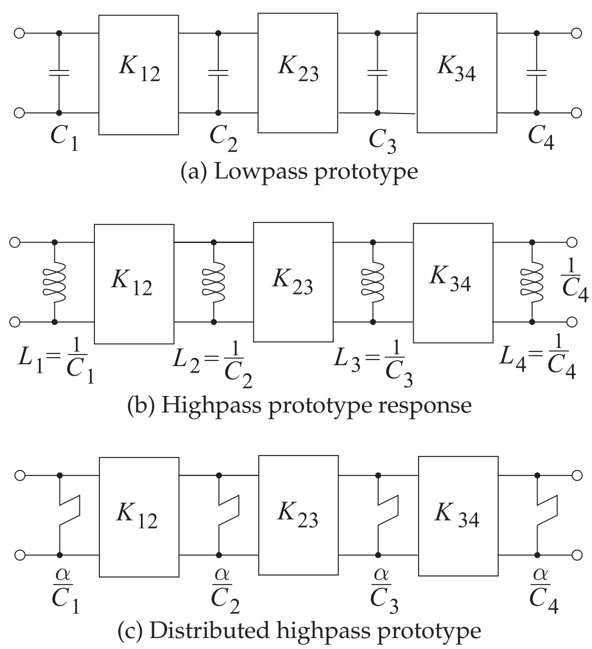

Figure 2-45: Ladder prototype transformation. (The input impedances of the stubs are indicated in (c).)

to θ_1 as (note that θ_1 is the electrical length at the band edge)

$$\omega = 1 \to \alpha \tan(\theta_1) \qquad (2.146) \qquad \text{so that} \qquad \alpha = \frac{1}{\tan(\theta_1)}. \qquad (2.147)$$

The sequence of steps transforming a lumped lowpass prototype to its distributed highpass prototype are shown in Figure 2-45. As previously discussed, all the inverters can be approximated by transmission lines of length $\pi/2$ at the corner frequency of the filter.

2.13 Kuroda's and Norton's Network Identities

Kuroda's and Norton's network identities are a number of pairs of equivalent networks that facilitate the transformation from one prototype to another, particularly transformations that enable realizable transmission line implementations.

2.13.1 Kuroda's Identities

Kuroda's identities embody a number of specific manipulations using impedance or admittance inverters. They are particularly useful in implementing Richards's transformations as they physically separate transmission line stubs, transform series stubs into shunt stubs, and can change characteristic impedances that are either too small or too high to practically realizable values. Kuroda's identities are a number of equivalent two-port networks, as shown in Figure 2-46. The proof is derived by obtaining the $ABCD$ parameters of the two ports similar to the technique used throughout this chapter. The identities shown in Figure 2-46 are narrowband. With stubs replacing the lumped elements, Kuroda's identities then have broader bandwidths. Kuroda's identities with stubs are shown in Figure 2-47. The major use of these identities is to transform designs with series stubs (in addition to possible shunt stubs) into designs with shunt

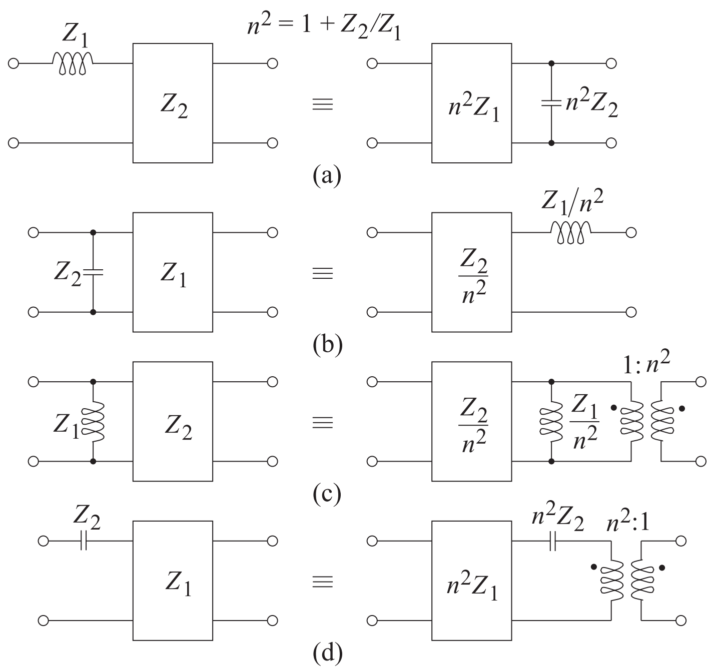

Figure 2-46: Kuroda's identities. Here the inverters are impedance inverters and the designation refers to the impedance of the inverter. Recall that an inverter of impedance Z_1 can be realized by a one-quarter wavelength long transmission line of characteristic impedance Z_1. (As usual, element impedances are indicated.)

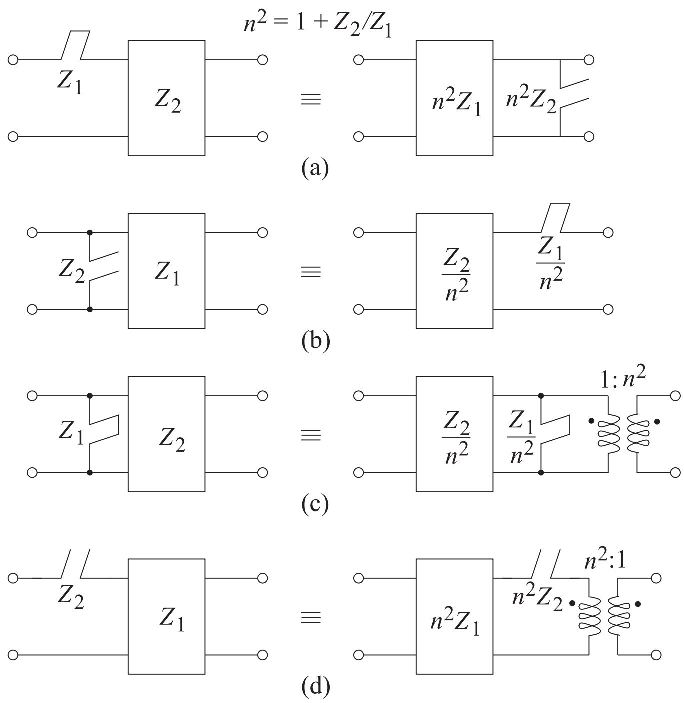

Figure 2-47: The stub form of Kuroda's identities with impedance inverters. The stub impedances shown are the input impedances of the stubs.

stubs only.

To see how these identities are used, consider the identity shown in Figure 2-46(a). The network on the left has a series inductor that, using transmission lines, is realized by a series stub. A series stub cannot be realized in most transmission line technologies, including microstrip. Using the identity shown on the right in Figure 2-46(a), the series stub is replaced by the shunt stub used to realize the shunt capacitor. At the same time, impedance scaling

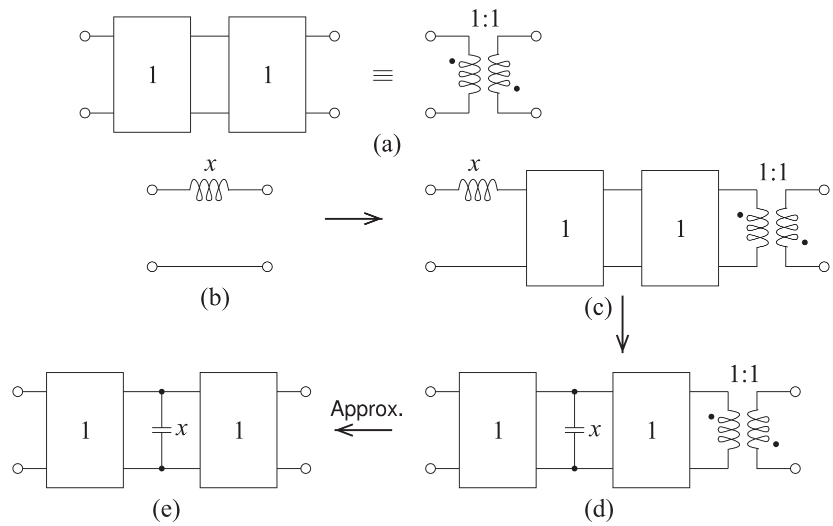

Figure 2-48: Transformation of a series inductor into a shunt capacitor between inverters.

can be used. If the impedance of the inverter in the network on the left is too low, then it can be scaled by a factor n^2, where $n^2 = 1 + Z_2/Z_1$.

One use of Kuroda's transforms is to convert a series inductor into a shunt capacitor. Consider the inductor transformation shown in Figure 2-48. Figure 2-48(a) shows that two inverters in cascade is electrically equivalent to an inverting transformer. Since each inverter is a unity inverter (either a 1 Ω impedance inverter or a 1 S admittance inverter), the equivalence is a unitary inverting transformer that corresponds to a 180° phase change. So the transformation of a series inductor begins with the transformation of the inductor (with value x) in Figure 2-48(b) into the network of Figure 2-48(c) in which the inverter cascade and the inverting transformer cancel each other out. Using the Kuroda identity in Figure 2-47(a), the network in Figure 2-48(c) converts to the electrically identical network in Figure 2-48(d). Since the 180° rotation usually does not matter in circuits, the final transformation shown in Figure 2-48(e) is usually acceptable. (The rotation would only matter if there was another path between the input and output as then phasing would affect the way signals on multiple paths combined.) Now the capacitor in Figure 2-48(e) has the numerical value x, the same as the numerical value of the original inductor. This is a result of using unitary inverters. The key result here is that a series inductor is equivalent to a shunt capacitor flanked by two inverters.

2.13.2 Norton's Identities

Norton's transformations enable the magnitude of lumped element values to be scaled [16, 17]. Norton's transformations are shown in Figure 2-49 where K is the scaling factor. Additional elements are introduced in these transformations including possibly negatively valued elements. Generally these elements can be combined with other elements so that the elements to be realized are positive (e.g. positive capacitor) and the transformer can also be replaced through subsequent transformations using, for example, Kuroda's identities.

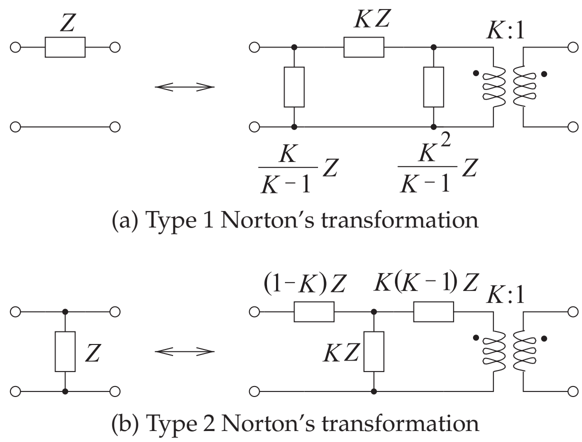

(a) Type 1 Norton's transformation

(b) Type 2 Norton's transformation

Figure 2-49: Norton's transformations.

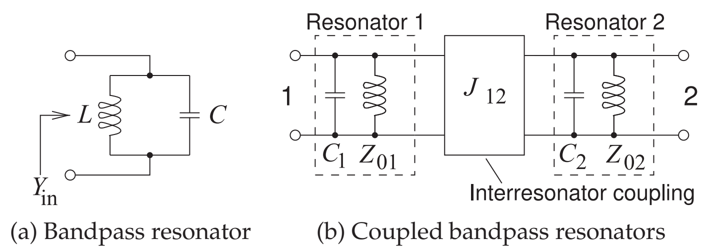

(a) Bandpass resonator (b) Coupled bandpass resonators

Figure 2-50: Bandpass resonators.

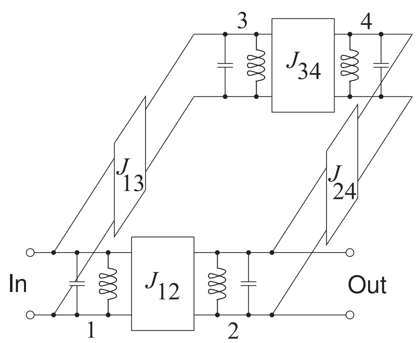

Figure 2-51: The electrical design of a cross-coupled filter. There are four resonators labeled 1, 2, 3, and 4. Thebandpass resonators are coupled by admittance inverters.

2.14 Inter-resonator Coupled Bandpass Filters

The synthesis method that has been described so far leads to bandpass filters that are a cascade of coupled bandpass resonators. A bandpass filter then comprises pairs of resonators of the type shown in Figure 2-50(a) that are coupled using what is called inter-resonator coupling (see Figure 2-50(b)). A generalization of this architecture is that a bandpass filter comprises coupled resonators that do not need to be in a linear cascade. Coupling the output of one resonator latter in a cascade to the input of an earlier resonator is called cross coupling, and a filter that uses this arrangement is said to be a cross-coupled resonator filter or a cross-coupled filter. By reusing resonators in this way, fewer resonators are required to achieve a specified bandpass response and the filter can have higher performance or be smaller. An example of the electrical design of a cross-coupled filter is shown in Figure 2-51.

Design of a cross-coupled bandpass filter is not as systematic as the design of a ladder filter. The design concept is based on using a number of resonators where each resonator on its own has the same resonant

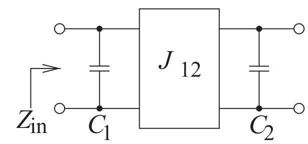

Figure 2-52: Lowpass filter approximation with capacitors separated by an admittance inverter.

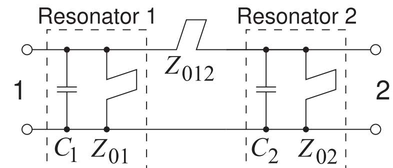

Figure 2-53: Segment of a filter with two resonators. $C_1 = C_2 = 2.7171$ pF, $Z_{01} = Z_{02} = 67.7535\ \Omega$, and $Z_{012} = 442.3836\,\Omega$. The stubs are resonant at $f_r = 2f_0$ where the filter center frequency $f_0 = 1$ GHz. Thus the stubs are $\lambda/8$ long at f_0.

frequency f_0, where f_0 is the center frequency of the filter. The desired filter characteristics are obtained by adjusting the inter-resonator coupling, that is, the coupling between pairs of resonators. Design is not a synthesis process based on a series of mathematical transformations, but instead is based on the understanding of the impact of changing the coupling. The design process will now be described for a pair of resonators.

Coupling of a Pair of Resonators

A segment of a bandpass filter fundamentally comprises a pair of coupled bandpass resonators. This is based on the lowpass prototype with a pair of capacitors separated by an admittance inverter (see Figure 2-52). In transforming this to a bandpass filter with a center frequency of f_0, each capacitor is replaced by a resonator such as that shown in Figure 2-50(a). This leads to a pair of resonators, each resonant at f_0, that are coupled by an inverter (see Figure 2-50(b)). The value of the inverter determines the level of coupling of the resonators.

Consider the circuit in Figure 2-53, which consists of a pair of coupled resonators, with each resonator resonant at $f_0 = 1$ GHz, and the resonators are coupled by the series stub with characteristic impedance Z_{012} (i.e., the Z_{012} stub). The circuit of Figure 2-53 is a segment of a Chebyshev 1 GHz bandpass filter with a fractional bandwidth of 10%. This is an interim stage of a bandpass filter design[3] and the system impedance of this circuit segment is $139.4\ \Omega$. The magnitude and phase of the 139.4-Ω S_{21} and S_{11} parameters of this circuit are shown in Figure 2-54(a), and the phase of S_{21} is shown in Figure 2-54(b). Specific features to identify here are the two peaks in the phase response at f_1 and f_2. These are also the frequencies of peak transmission response where $|S_{21}|$ = 1. The bandwidth defined by f_1 and f_2 is called the coupling bandwidth ($= f_2 - f_1$) or the bandwidth of the filter (note that this is not the 3-dB bandwidth of the filter). The level of coupling determines the coupling bandwidth. That is, changing the level of coupling provided by the Z_{012} stub changes the position of f_1 and f_2. An interpretation of what is happening is that by coupling the two resonators, the resonate frequency of the resonators on their own, f_0, has been split by the coupling, resulting in two peaks at f_1 and f_2. The higher the coupling, the larger the coupling bandwidth, and the lower the coupling, the smaller the coupling bandwidth. For example, a narrowband bandpass filter comprises

[3] Specifically these resonators are the left-most resonators in a design developed in Chapter 3 (see Figure 3-31).

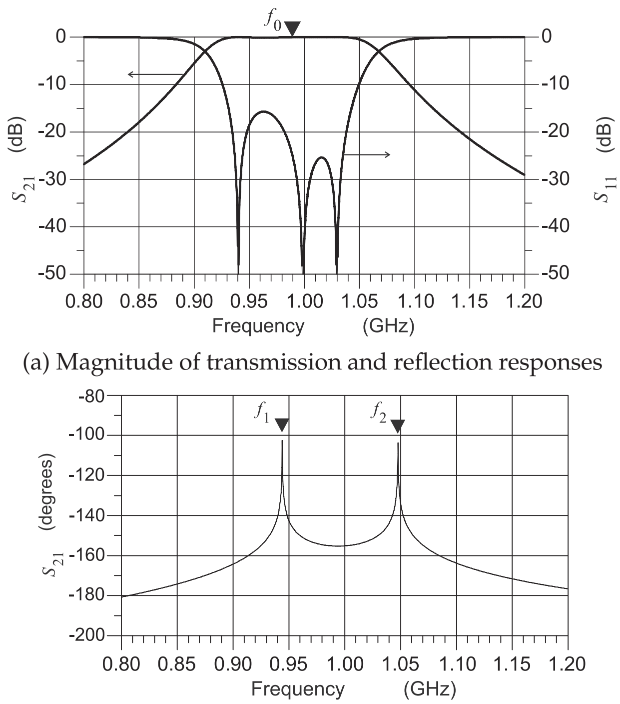

(a) Magnitude of transmission and reflection responses

(b) Phase of transmission response

Figure 2-54: Response of the coupled resonator network in Figure 2-53.

resonators that have low-level coupling.

So following the choice of an appropriate architecture, that is, the number of resonators and the coupling arrangement, design and manual optimization becomes one of changing the level of coupling between pairs of resonators. Design is not as clean as for ladder filters, but the advantages of a design with fewer resonators is a compelling justification. Invariably, extensive (perhaps a day's worth) manual adjustment of the coupling of the final fabricated filter is required. Overall this is an approach worth adopting for high-value filters such as those used in a basestation, where the high unit costs resulting from manual tuning of individual filters can be justified. This type of filter design is considered further in [3, 18–21].

Relationship of Ladder Synthesis and Inter-resonator Coupling

The relationship of design focused on interresonator coupling and design based on the ladder synthesis approach can be demonstrated for a pair of resonators as follows. Consider the lowpass prototype circuit of Figure 2-52. The input impedance of this circuit is

$$Z_{\rm in}(s) = \left[sC_1 + J_{12}^2/(sC_2)\right]^{-1}. \tag{2.148}$$

With $s = \jmath\omega$, the poles of $Z_{\rm in}$ occur when

$$J_{12}^2 - \omega^2 C_1 C_2 = 0, \tag{2.149}$$

thus the radian frequencies of the poles are

$$\omega = \pm\frac{J_{12}}{\sqrt{C_1 C_2}}. \tag{2.150}$$

Applying the bandpass transformation (so that the capacitors are replaced by the resonators of Figure 2-50(a)) results in the bandpass circuit of Figure 2-50(b). With this transformation the frequency is transformed as

$$\omega \to \alpha\left(\frac{\omega}{\omega_0} - \frac{\omega_0}{\omega}\right). \tag{2.151}$$

That is, the transmission coefficient of the bandpass filter is

$$T_{\mathrm{BPF}}(\omega) = T_{\mathrm{LPF}}\left(\alpha\left[\frac{\omega}{\omega_0} - \frac{\omega_0}{\omega}\right]\right), \tag{2.152}$$

where $T_{\mathrm{LPF}}(\omega)$ is the transmission coefficient of the lowpass filter at the radian frequency ω. The poles of the bandpass filter are at ω_1, where

$$\alpha\left(\frac{\omega_1}{\omega_0} - \frac{\omega_0}{\omega_1}\right) = +\frac{J_{12}}{\sqrt{C_1 C_2}}, \tag{2.153}$$

and ω_2, where

$$\alpha\left(\frac{\omega_2}{\omega_o} - \frac{\omega_0}{\omega_2}\right) = -\frac{J_{12}}{\sqrt{C_1 C_2}}. \tag{2.154}$$

Then the coupling bandwidth of the filter is

$$f_1 - f_2 = \frac{\omega_1 - \omega_2}{2\pi} = \frac{J_{12}\omega_0}{2\pi\alpha\sqrt{C_1 C_2}}. \tag{2.155}$$

Thus the coupling bandwidth can be directly related to the steps in the ladder-based synthesis of a bandpass ladder filter.

Group Delay

Group delay of a network, and in particular of a filter, is the delay to send information through a network. It is the time required for a modulated carrier signal to appear at the output of a filter after being applied to the input of the filter. Phase delay is a similar measure of delay but does not describe the time it takes to send information. It describes the delay to send a particular phase of a single sinewave. Group delay is a steady-sate concept and so only approximately captures the transient response of a filter.

If a two-port has the transmission coefficient

$$T(s) = S_{21} = a + \jmath b = t\angle\varphi, \tag{2.156}$$

where a and b are its real and imaginary parts, t is its magnitude, and φ is its phase. With $s = \jmath\omega$, the phase of T is

$$\varphi(\omega) = \tan^{-1}\left(\frac{b}{a}\right). \tag{2.157}$$

The group delay, τ_D, is the negative of the derivative of this phase as follows:

$$\text{Group delay} = \tau_g(\omega) = -\frac{d\varphi}{d\omega} = -\frac{d}{d\omega}\left[\tan^{-1}\left(\frac{b}{a}\right)\right]. \tag{2.158}$$

This compares to the phase delay:

$$\text{Phase delay} = \tau_\varphi(\omega) = -\frac{\varphi}{\omega} = -\tan^{-1}\left(\frac{b}{a}\right). \tag{2.159}$$

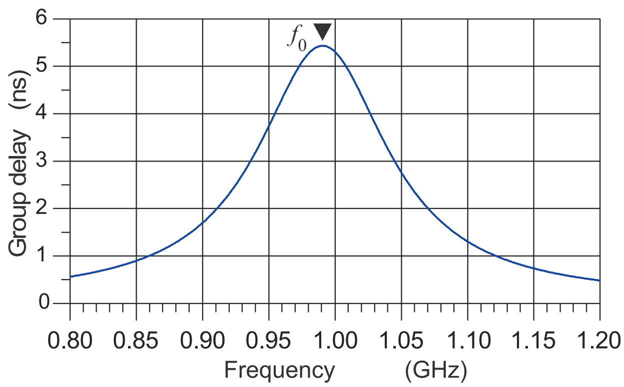

Figure 2-55: Group delay of a resonator.

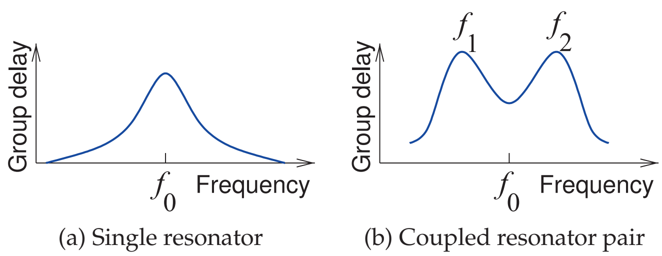

Figure 2-56: Group delay of resonators in a filter. Additional delay is introduced by the coupling inverter.

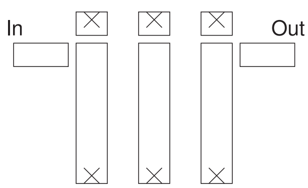

Figure 2-57: Microstrip layout of a third-order combline filter based on coupled lines. Each of the vertical microstrip line forms a resonator with the top gap capacitors. The input and output gap capacitors provide impedance matching.

Figure 2-55(c) shows the group delay response of one of the resonators in Figure 2-53, where the group delay peaks at the resonant frequency of the resonator f_0. The peak of the group delay occurs at the resonant frequency of the resonator without loading. From examination of the phase of S_{21} (see Figure 2-54(b)), it is clear that the group delay peaks very close to f_1 and f_2. So the coupled resonator pair has two peaks in the group delay. This can be seen in Figure 2-56, which plots the group delay of a single resonator and a coupled pair of resonators.

2.15 Bandpass Filter Topologies

The essential structure of a bandpass filter comprises resonators that are coupled to each other. A large number of filter architectures based on this concept have been deployed. A parallel coupled line (PCL) filter called a combline filter is shown in Figure 2-57. Here the microstrip lines form the resonator and the coupling of parallel lines provides the interresonator coupling. A variation on a filter with PCL resonators is shown in Figure 2-58 [22]. This filter uses edge-coupled microstrip resonators that are $\lambda/2$ long (at the center frequency). Figure 2-59 shows another distributed bandpass filter topology utilizing end-coupled microstrip resonators. That is, the gaps provide the interresonator coupling. All transmission line bandpass filters have spurious passbands [23–25]. The root cause of the spurious responses derives from the transformation of the parallel LC resonators into their

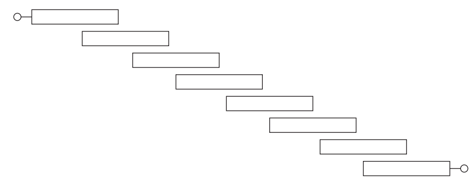

Figure 2-58: Microstrip layout of a parallel coupled bandpass filter.

Figure 2-59: General microstrip layout for an end-coupled bandpass filter (series coupling gaps between cascaded straight resonator elements).

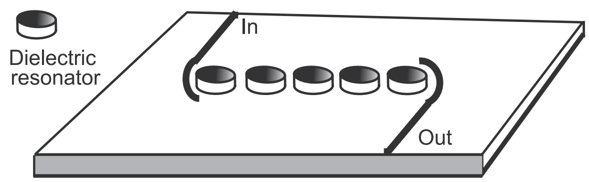

Figure 2-60: A microstrip coupled dielectric resonator bandpass filter configuration.

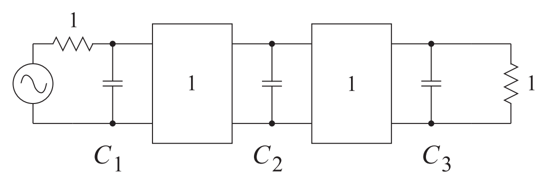

$C_1 = 0.85239$ F $= C_3$ $\quad C_2 = 1.10422$ F

Figure 2-61: Bandpass filter approximation.

transmission line form.

A **dielectric-resonator**-based bandpass filter is shown in Figure 2-60 [26]. Here the pucks are the bandpass resonators and they are coupled and the evanescent fields outside the pucks provide the interresonator coupling. The pucks shown are cylinders of high-permittivity material (typically having a relative permittivity of 500–85 000) with an approximate magnetic wall at the cylindrical surface of the puck. Thus the puck resonates when its diameter is approximately $\lambda/2$.[4]

With all these filters the interresonator coupling functions as an inverter. Thus the basic functional unit of the bandpass filters is the coupled resonator structure shown in Figure 2-50(b).

2.16 Case Study: Design of a Bandstop Filter

The design of a bandstop filter begins with the lowpass filter prototype shown in Figure 2-61. To the lowpass prototype, the highpass transformation is applied to obtain the highpass prototype of Figure 2-62. Picking a center frequency of approximately 1 GHz and corner frequencies of $f_1 = 950$ MHz and $f_2 = 1050$ MHz, corresponding to a bandwidth of approximately 10%, the bandstop transformation is now applied. This results in the prototype of Figure 2-63. Finally, scaling the system impedance to 50 Ω leads to the prototype of Figure 2-64. The impedance inverters must remain set at 50 Ω in order to obtain a broad match. In the passband, energy will pass at all

[4] A better estimate is developed from the zeros of Bessel functions, as the fields inside the pucks have a Bessel function dependence (this is the form of the solution of the wave equation in cylindrical coordinates).

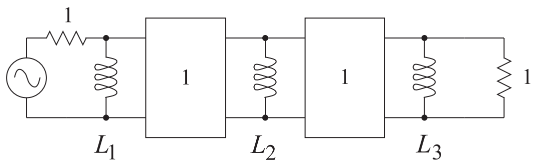

$L_1 = L_3 = \frac{1}{C_1} = \frac{1}{C_3} = 1.1743\ \text{H}$ $\quad L_2 = \frac{1}{C_2} = 0.9064\ \text{H}$

Figure 2-62: Bandstop filter prototype.

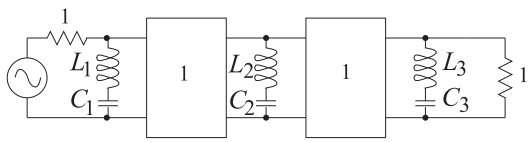

$L_1 = L_3 = 1.868\ \text{nH}$ $\quad C_1 = C_3 = 13.587\ \text{pF}$
$L_2 = 1.442\ \text{nH}$ $\quad C_2 = 17.601\ \text{pF}$

Figure 2-63: Bandstop filter following transformation from the lowpass prototype.

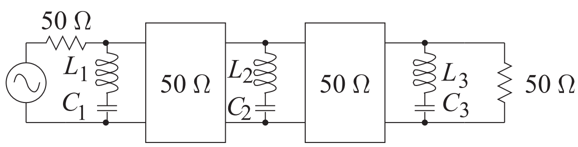

$L_1^{'} = L_3^{'} = 1.868 \times 50 = 93.448\ \text{nH}$
$C_1^{'} = C_3^{'} = 13.587/50 = 0.2717\ \text{pF}$
$L_2^{'} = 1.442 \times 50 = 72.1362\ \text{nH}$
$C_2^{'} = 17.601/50 = 0.352\ \text{pF}$

Figure 2-64: Bandstop filter after impedance transformation.

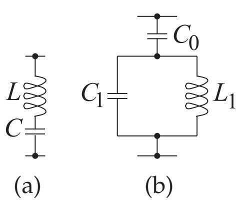

Figure 2-65: Transformations of the resonators in the bandstop filter to obtain realizable values. The series LC resonator in (a) is transformed to the form in (b).

frequencies.

In Figure 2-64, the inductor values are relatively large and the capacitor values are relatively small so that it will be difficult to realize the filter in either lumped or distributed forms. These values must be scaled to obtain realizable values. One possible transformation is shown in Figure 2-65. To establish that the left-hand and right-hand networks are equivalent, at least near one frequency, the impedances and derivatives must be matched. For the circuit in Figure 2-65(a),

$$Z_1 = \jmath \frac{\omega^2 LC - 1}{\omega C} \qquad (2.160) \quad \text{and} \quad \frac{dZ_1}{d\omega} = \jmath \frac{\omega^2 LC + 1}{\omega^2 C}, \qquad (2.161)$$

and for the circuit in Figure 2-65(b),

$$Z_2 = \jmath \frac{\omega^2 L_1 C_1 - 1 + \omega^2 L_1 C_0}{\omega C_0 \left(1 - \omega^2 L_1 C_1\right)} \qquad (2.162)$$

and
$$\frac{dZ_2}{d\omega} = \jmath \frac{\omega^4 L_1^2 C_1^2 - 2\omega^2 L_1 C_1 + \omega^4 L_1^2 C_0 C_1 + \omega^2 L_1 C_0 + 1}{\omega^2 C_0 \left(\omega^2 L_1 C_1 - 1\right)^2}. \qquad (2.163)$$

Equating the above enables C_0 and C_1 to be found for a chosen value of L_1. Thus the series LC resonators in Figure 2-66(a and c) are replaced by the

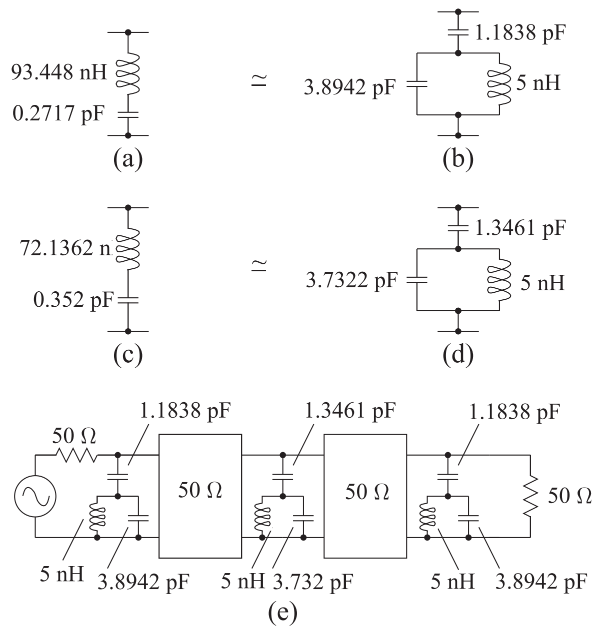

Figure 2-66: Intermediate bandstop filter prototype.

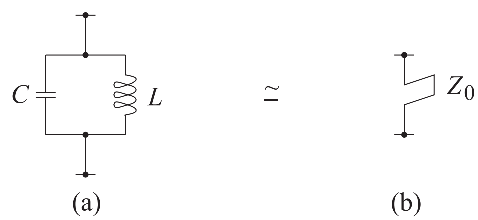

Figure 2-67: Equivalence of shunt bandpass resonator to shunt short-circuited stub.

networks in Figure 2-66(b and d). This results in the filter of Figure 2-66(e).

At this stage the bandpass resonators are then equated to short-circuited stubs by equating the admittance, Y_1, of the lumped circuit in Figure 2-67(a) with the admittance, Y_2, of the stub in Figure 2-67(b). That is, by equating

$$Y_1 = \jmath \frac{\left(\omega^2 CL - 1\right)}{\omega L} \quad \text{and} \quad Y_2 = \frac{1}{\jmath Z_0 \tan\left(\frac{\pi}{2}\frac{\omega}{\omega_r}\right)}. \tag{2.164}$$

The characteristic impedance of the stub, Z_0, is selected so that the frequency, ω_r, is not too far above the upper band-edge frequency of the filter, in this case 1.05 GHz. Choosing $Z_0 = 20\ \Omega$ results in the stub transformations shown in Figure 2-68(a–d). The bandstop filter prototype with stubs is shown in Figure 2-68(e). The final physical layout of the bandstop filter is shown in Figure 2-69. The response of the final bandstop filter design is shown in Figure 2-70.

2.17 Active Filters

With active circuits, losses in lumped-element components can be compensated for by the gain of active devices resulting in filters with high Q. Inverters can also be realized efficiently. The net result is that active filters provide a performance per unit area advantage over passive element realizations. Of course, active filters are limited to low-level signals (such as in the receive circuitry, and prior to the power amplifier stages) as the full power of the

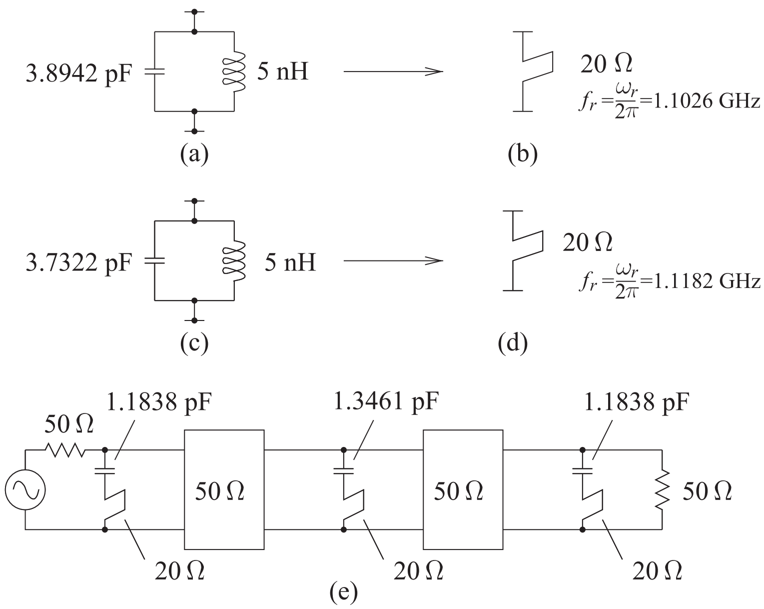

Figure 2-68: Bandstop filter prototype using stub approximations. The stub in (b) is the transmission line approximation of the parallel resonant circuit in (a). The stub in (d) approximates the circuit in (c).

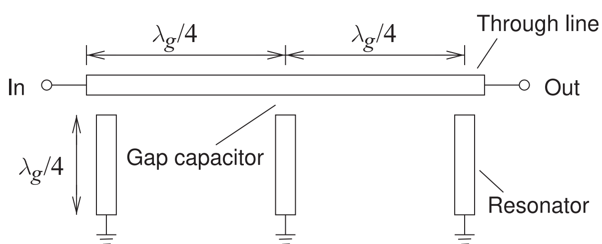

Figure 2-69: Physical layout of a bandstop filter in microstrip.

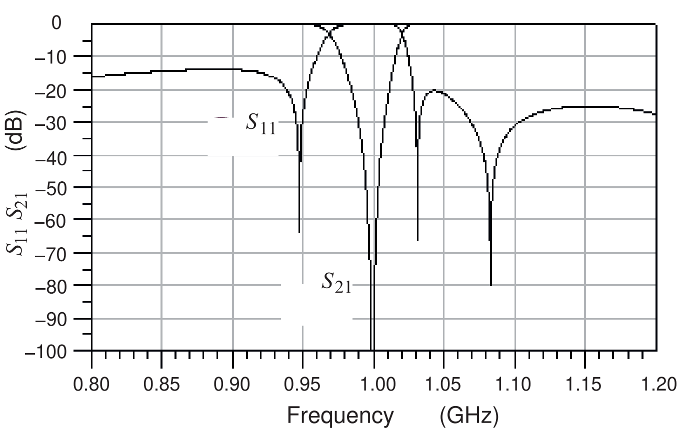

Figure 2-70: Response of the bandstop filter shown in Figure 2-69.

signal must be handled by the active devices in the active filter. With active devices, additional noise is introduced and so the noise figure of an active filter must be considered at RF where bandwidths are significant.

At microwave frequencies active filters based on traditional low-frequency concepts have relatively low Q. Higher Q and narrower-band applications require active inductors or distributed techniques. The smallest active filters are the ones that use active inductors and the largest use distributed transmission line elements.

Sometimes the main role of a filter is to limit the dynamic range of signals presented to active circuits, thereby limiting distortion. Clearly active filters are not suitable when large out-of-band signals are a concern.

2.17.1 Radio Frequency Active Filters

There are several problems with lumped-element filters. High-order filters require many poles and zeros that must be precisely placed, requiring small tolerances. With active filters it is possible, to some degree, to achieve higher-order filters with fewer reactive elements and so the tolerancing problem is considerably reduced. Also, there are a few designs that can be tuned electronically. Lumped-element bandpass filters and highpass filters require inductors. Inductors are a major problem, as RF inductors are lossy and also only relatively small values can be obtained. On-chip inductors take considerable area and can thereby dominate the cost of RFICs. With active filters, feedback and capacitors can be used to realize inductor-like characteristics, defined as a positive imaginary impedance increasing with frequency at least over a small frequency range. Many times, and especially at lower radio frequencies, lumped inductors are no longer required. The size of capacitors in filters is another issue, and using feedback and gain, the effective value of capacitors can be magnified. All this comes with limits. The principle limit is that the cutoff frequency of the transistors must be much higher than the operating frequency of the filters. This is a cost incurred whenever feedback is used. A rough rule of thumb is that the transistor cutoff frequency should be about 10 times the operating frequency. So for a 5 GHz bandpass filter, a 50 GHz transistor process is required. The other significant cost is that active filters are only suitable for small signals. The efficiency, a measure of the amount of DC power used in producing the RF output signal, is then not a consideration. Active filters cannot be used where signal levels are likely to be large (such as at the output of a power amplifier or at the receiver input, due to likely out-of-band signals).

The essential aspect of low-RF active filters is the use of feedback, with reactive feedback elements, to realize a frequency-domain transfer function with poles and zeros. The aim is not to synthesize effective capacitors and inductors, but to focus on the overall response. Active filters are generally developed as stages, with each stage realizing a second- or higher-order transfer function. Design is simulation driven, as this is the only way to account for the active device parasitics.

In operational amplifier design, feedback is used to achieve gain stability, but at the cost of reduced bandwidth. If reactive feedback elements are used, high-order transfer functions can be obtained with just a few reactive elements. In Figure 2-71, a twin-T notch network is connected in the operational amplifier feedback path to obtain a bandpass filter [27]. Away from the notch frequency the feedback path has a high impedance and the overall amplifier gain falls off. As the signal frequency approaches the notch frequency, the feedback path becomes effective and the amplifier gain increases. The notch frequency, f_n, is proportional to the RC product of the feedback components and the Q is proportional to the amplifier gain. The governing equations for this filter are

$$f_n = 1/(2\pi RC) \qquad \text{and} \qquad Q = (1+G)/4. \tag{2.165}$$

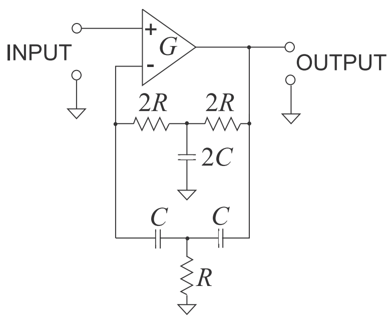

Figure 2-71: Active twin-T bandpass filter: center frequency $f_0 = \pi RC/4$ and $Q = (G+1)/4$.

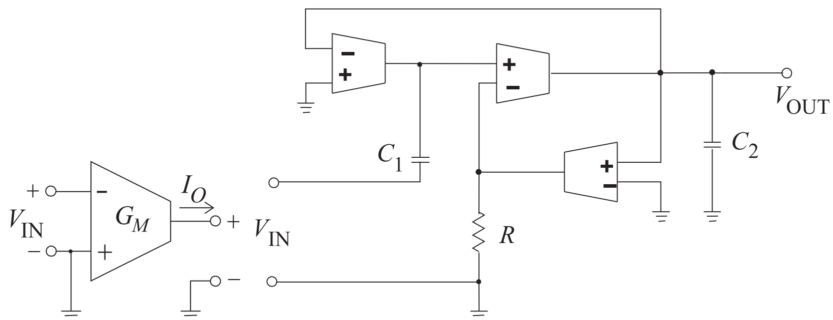

(a) Schematic (b) RF biquad bandpass filter

Figure 2-72: Operational transconductance amplifier with transconductance G_M. In (a) $I_O = G_M V_{\rm IN}$.

2.17.2 Biquadratic Filters

Biquadratic filters are an important class of filters and are the basic building block used in analog and RF active filters. Biquad filters commonly use operational **transconductance amplifiers** (**OTAs**), the schematic of which is shown in Figure 2-72(a). Here $I_O = G_M V_{\rm IN}$, which is also the basic characteristic of an individual transistor. These circuits have characteristics typical of operational amplifiers, including gain stability and resistance to component tolerance variations. OTA-based filters have the advantage of easy tunability, with pole and zero frequencies electronically adjustable. An RF bandpass **biquad** filter is shown in Figure 2-72(b). Stages such as this are cascaded to realize high-order filters.

Biquadratic filters implement the transfer function

$$H(s) = \frac{V_{\rm OUT}}{V_{\rm IN}} = \frac{N(s)}{D(s)} = \frac{a_2 s^2 + a_1 s + a_0}{s^2 + b_1 s + b_0} = \frac{a_2(s+z_1)(s+z_2)}{(s+p_1)(s+p_2)}. \tag{2.166}$$

This is referred to as a biquadratic function and filters that implement this function are called biquadratic filters or simply biquad filters. There are several special types of biquad filters.

The form of the biquadratic function for a second-order lowpass filter is

$$H_{\rm LP}(s) = \frac{a_0}{s^2 + b_1 s + b_0} = \frac{K\omega_p^2}{s^2 + (\omega_p/Q_p)s + \omega_p^2}. \tag{2.167}$$

$H_{\rm LP}(s)$ has a double zero at $s = \infty$ and thus negligible response at very high frequencies.

The highpass form of the biquadratic filter is described by

$$H_{\rm HP}(s) = \frac{a_2 s^2}{s^2 + b_1 s + b_0} = \frac{Ks^2}{s^2 + (\omega_p/Q_p)s + \omega_p^2}. \tag{2.168}$$

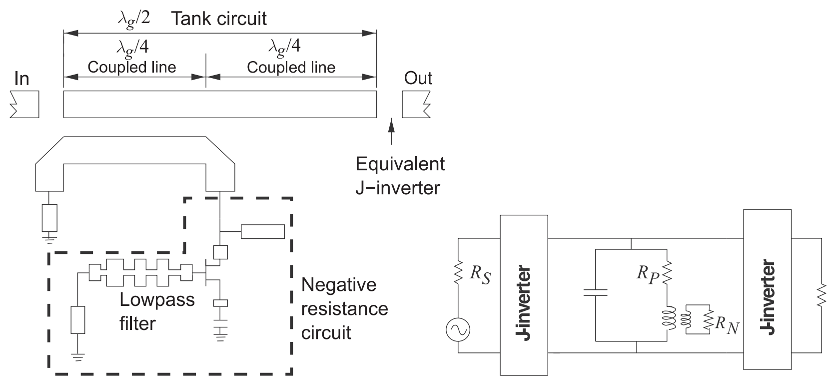

(a) Layout (b) Equivalent circuit model

Figure 2-73: Active coupled distributed filter. After [30].

The response of $H_{\rm HP}(s)$ at high frequencies is K and the response at very low frequencies goes to zero.

The bandpass form of the biquadratic filter is described by

$$H_{\rm BP}(s) = \frac{a_1 s}{s^2 + b_1 s + b_0} = \frac{K(\omega_p/Q_p)s}{s^2 + (\omega_p/Q_p)s + \omega_p^2}. \tag{2.169}$$

The response of $H_{\rm BP}(s)$ at high and low frequencies goes to zero, and only at and near the center frequency, $\omega = \omega_p$, is there a reasonable response.

The band-reject or notch form of the biquadratic filter is described by

$$H_{\rm BR}(s) = \frac{a_2 s^2 + a_0}{s^2 + b_1 s + b_0} = \frac{K(s^2 + \omega_z^2)}{s^2 + (\omega_p/Q_p)s + \omega_p^2}. \tag{2.170}$$

The response of $H_{\rm BR}(s)$ at high and low frequencies is high, but there is a double zero at the notch frequency, $\omega = \omega_z$, where the response is very low.

With all of the biquadratic filters, the sharpness of the response is determined by Q_p. The edge frequency or center frequency is ω_p for the bandpass, lowpass, and highpass filters, and the notch frequency is ω_z for the bandstop filter.

2.17.3 Distributed Active Filters

At high microwave frequencies, good results can be obtained by combining distributed elements with a gain stage. Commonly the active devices are used as coupling devices. A negative resistance can be produced using the active devices that can compensate for the losses associated with the transmission line elements or lumped passive elements in the filter. The concept uses a resonant tank circuit formed by a transmission line or lumped-element resonator with a negative resistance coupled into the tank circuit by the active devices [28–30]. This concept is illustrated in Figure 2-73. Here a one-half wavelength long resonator forms a resonant circuit (commonly called a tank circuit in this context). A negative resistance is coupled into the tank circuit to compensate for losses in the resonator and the result is effectively a lossless tank circuit.

An active resonator circuit is shown in Figure 2-74. The design of the lossless resonator is based on the negative resistance obtained when the capacitor is connected at the source of the MESFET. This element in the

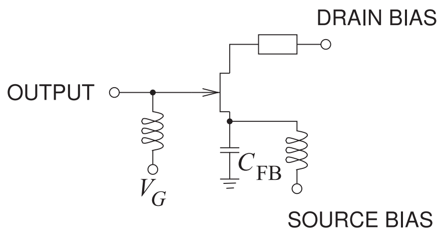

Figure 2-74: An active resonator circuit. After [31].

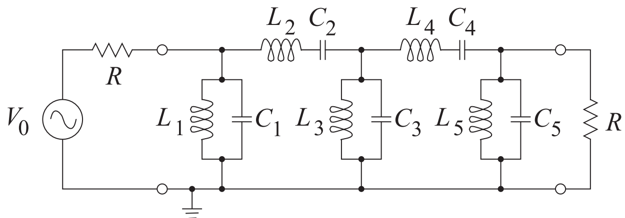

Figure 2-75: Lumped-element 5th-order Chebyshev filter.

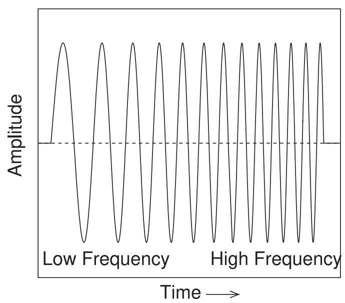

Figure 2-76: A linear chirp.

source provides a feedback path between the output of the circuit, the drain-to-ground voltage, and the input gate-to-source voltage. An increase in the drain-source current leads to a voltage at the source that changes the gate-source voltage. This induces a negative resistance that is adjusted through the feedback capacitance, C_{FB}, to compensate for inductor losses. An additional inductor, L_P, is added at the gate. The inductor resonates with the series combination of C_{FB} and C_{GS}. C_{FB} can be implemented using a varactor diode to enable electronic tuning.

2.18 Transient Response of a Bandpass Filter

A bandpass filter is normally characterized by its center frequency and bandwidth, and sinusoidal signals that are within the bandwidth are transmitted by the filter and those outside the passband are reflected by the filter. However, if the signal changes frequency quickly, the transient response of the filter can be unexpected [32, 33].

Figure 2-75 is a fifth-order filter with each pair of shunt resonators coupled by a series resonator. In response to an RF pulse (a pulse of sinusoidally varying RF), the filter passes energy in-band when all of the resonators have reached steady state. When the RF pulse is removed, the resonators will loose energy and eventually the RF signals on the resonators disappear. There will be a finite time to “charge” and “discharge” the filter’s resonators.

A classic test of the RF response over frequency is to use a linear RF chirp, as shown in Figure 2-76. With a linear **chirp**, the frequency of the signal in the pulse changes linearly and smoothly over time from one frequency to another. Figure 2-77(a) presents the transient response at the output of

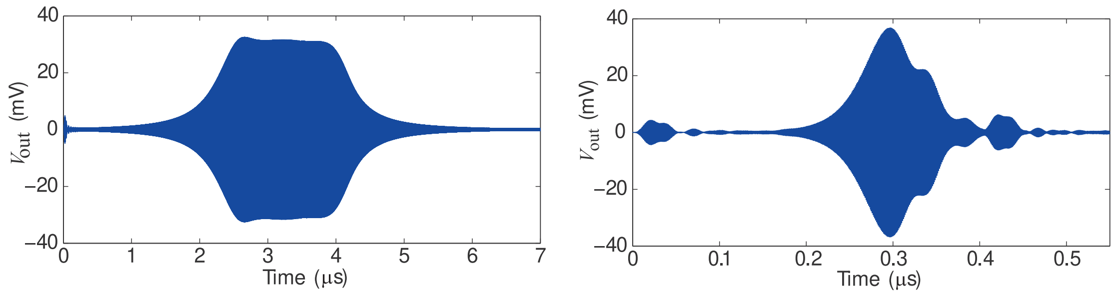

(a) Slow chirp response (b) Fast chirp response

Figure 2-77: Output transient response of a 3rd-order Chebyshev filter with a center frequency of 1 GHz and a 30 MHz bandwidth excited by a -20 dBm linear chirp from 950 MHz to 1050 MHz: (a) chirp rate = 20 MHz/μs, (b) chirp rate = 400 MHz/μs. At the slower chirp rate, the filter response is approximately a superposition of steady-state responses as the frequency changes (i.e., the response is quasi-stationary). At the higher chirp rate, the filter response can no longer be approximated as a sum of steady-state responses (i.e., it is no longer quasi-stationary). After [34].

a 30 MHz-bandwidth 1 GHz filter excited by a 1 μs-long linear chirp from 950 MHz to 1050 MHz with a chirp rate of 20 MHz/μs. This is a relatively slow chirp. The chirp starts at 0 μs and stops at 5 μs. Thus the frequency of the chirp is in-band at 1.75 μs and is out-of-band at 3.25 μs. The chirp is sufficiently slow that the transient transmission response corresponds to the frequency response of the filter. However, if the chirp is fast, the resonators may not reach steady state, and then the transient response of the filter cannot be simply extrapolated from its frequency-domain response. This is seen in Figure 2-77(b), which is the response of the filter to a fast chirp with a chirp rate of 400 MHz/μs and a chirp duration of 250 ns, and beginning at 950 MHz and ending at 1050 MHz. The RF chirp begins out of band at 0 ns, becomes in-band at 0.0875 μs, and goes out-of-band again at 0.1625 μs before turning off at 0.25 μs. Interestingly, there is an almost immediate output response, around 0.03 μs when the RF chirp is out of band. Overall the chirped-filter response does not follow the frequency response of the filter.

Another view of the same phenomenon is examined for a 7th-order Chebyshev filter with a center frequency of 900 GHz and 34 MHz bandwidth from 883 MHz to 917 MHz. The frequency-domain transmission response of the filter is shown in Figure 2-78. The transmission responses to 0.25 μs-long RF pulses of different frequencies are shown in Figure 2-79. The frequency of the RF pulse is shown in each subplot. The top-left plot is the response when the RF pulse is in-band. Here the RF pulse is applied at 0 μs and removed at 0.25 μs. An initial delay in the transmission response and what is referred to as a **long-tail response** is seen when the RF pulse is removed. The other plots in Figure 2-79 show the filter response as the RF is backed off from the passband. So, even when the RF is out of band, there can be an appreciable output from the filter at the beginning and end of the RF pulse.

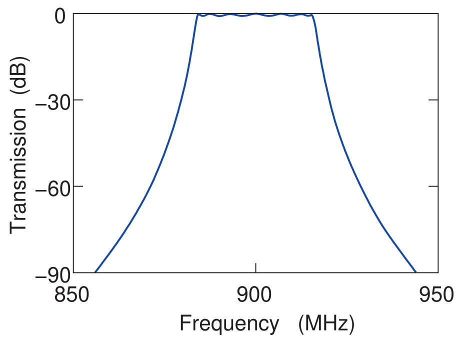

Figure 2-78: Frequency-domain transmission response of a 7th-order Chebyshev filter with a center frequency of 900 GHz and 34 MHz bandwidth from 883 MHz to 917 MHz.

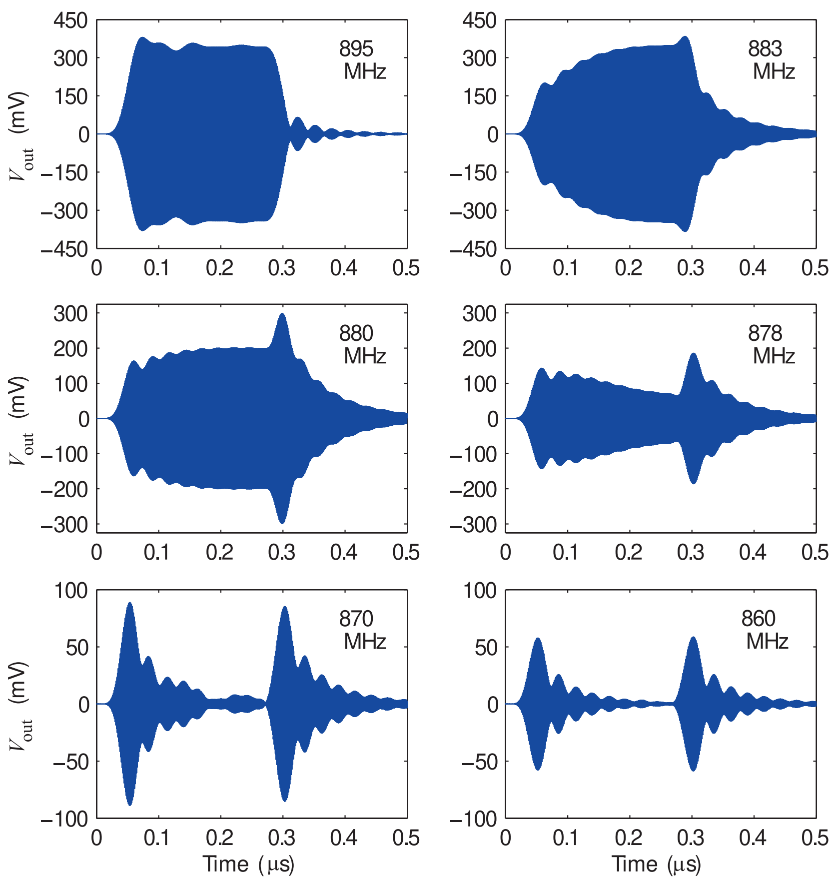

Figure 2-79: Transient response at the output of the 900 MHz 7th-order Chebyshev bandpass filter with a passband from 883 MHz to 917 MHz. The frequency response is shown in Figure 2-78. After [34].

2.19 Summary

Radio frequency and microwave filter design combines the mathematical synthesis of a circuit with the required performance and the intuitive realization that particular structures inherently have a desired frequency selectivity. The art of filter design is to direct the mathematical synthesis and companion circuit so that the circuit structures in the synthesized filter prototype match the functionality of physical microwave structures. A very important step in this process is the development of circuit equivalent models of physical structures. Once a microwave filter with appropriate topology has been designed and the close-to-final physical filter is designed, the physical layout is optimized in a circuit simulator to account for parasitics and higher-order EM effects.

A similar design procedure applies to active filter designs where particular circuit topologies, for example, the biquad network blocks, are identified and exploited. The synthesis approach provides design insight and exploitation of all parameters of a transfer function, leading to optimum network topologies. Synthesis can be time consuming and specialized, but it is the only way to develop filters with optimum performance. Insight gained during design identifies yield issues and provides the basis for inventing new filter topologies.

Further Reading

The design of microwave filters has a rich tradition. Many excellent books and articles have been written about microwave filter design techniques. Books and articles with extensive treatments are references [1, 3, 4, 14, 16–19, 35–46]. However the most important systematic approaches to microwave filter design were presented in this chapter. Many journal and conference papers present topologies in various technologies that can be used to implement filters. The best way to locate these papers is to search using the specifics of the technology of interest. For example "wideband microstrip bandstop filters on glass substrates" will yield a list of papers on the topic. There are many small companies that specialize in different types of filter design. For very high performance filters, for example in basestation applications, the number of designers and vendors is quite small and filter designers follow the literature and patents closely. For designers building microwave systems with small to medium volumes the best approach is to use microstrip design. For bandpass microstrip design the most common choice is to use filter design based on coupled microstrip design which is considered in the next chapter.

2.20 References

[1] G. Matthaei, L. Young, and E. Jones, *Microwave Filters, Impedance-Matching Networks and Coupling Structures*. McGraw-Hill, 1965, reprinted in 1980, Artech House.

[2] D. M. Pozar, *Microwave engineering*, 4th ed. John Wiley & Sons, 2012.

[3] I. Hunter, *Theory and Design of Microwave Filters*. IEE Press, 2001.

[4] J. Scanlan and R. Levy, *Circuit Theory*. Oliver & Boyd, 1973, vol. 2.

[5] ——, *Circuit Theory*. Oliver & Boyd, 1973, vol. 1.

[6] V. Belevitch, "Techbyshev filters and amplifier networks," *Wireless Engineer*, pp. 106–110, Apr. 1952.

[7] H. Orchard, "Formulae for ladder filters," *Wireless Engineer*, pp. 3–5, Jan. 1953.

[8] R. Daniels, *Approximation Methods for Electronic Filter Design*. McGraw-Hill, 1974.

[9] M. Lutovac, D. Miroslav, D. Tosic, V. Dejan, and B. Evans, *Filter Design for Signal Processing using MATLAB and Mathematica*. Prentice Hall, 2001.

[10] M. Steer, *Microwave and RF Design, Transmission Lines*, 3rd ed. North Carolina State University, 2019.

[11] ——, *Microwave and RF Design, Networks*, 3rd ed. North Carolina State University, 2019.

[12] P. Richards, "Resistor-transmission-line circuits," *Proc. of the IRE*, vol. 36, no. 2, pp. 217–220, Feb. 1948.

[13] ——, "General impedance-function theory," *Quarterly Applied Mathematics*, vol. 6, no. 6, pp. 21–29, 1948.

[14] J. Rhodes, *Theory of Electrical Filters*. John Wiley & Sons, 1976.

[15] H. Baher, *Synthesis of Electrical Networks*. John Wiley & Sons, 1984.

[16] M. E. Van Valkenburg, *Introduction to modern network synthesis*. John Wiley & Sons, 1960.

[17] A. I. Zverev *et al.*, *Handbook of filter synthesis*. John Wiley & Sons, 1967.

[18] R. Cameron, R. Mansour, and C. Kudsia,

Microwave Filters for Communication Systems: Fundamentals, Design and Applications. John Wiley and Sons, 2007.
[19] R. Cameron, "Advanced coupling matrix synthesis techniques for microwave filters," *IEEE Trans. on Microwave Theory and Techniques*, vol. 51, no. 1, pp. 1–10, Jan. 2003.
[20] I. Hunter, J. Rhodes, and V. Dassonville, "Dual-mode filters with conductor-loaded dielectric resonators," *IEEE Trans. on Microwave Theory and Techniques*, vol. 47, no. 12, pp. 2304–2311, Dec. 1999.
[21] W. Fathelbab and M. Steer, "A reconfigurable bandpass filter for RF/microwave multifunctional systems," *IEEE Trans. on Microwave Theory and Techniques*, vol. 53, no. 3, pp. 1111–1116, Mar. 2005.
[22] A. Nakamura, K. Hibino, F. Yamamoto, and S. Kamihashi, "Expert system for microwave filter design," in *1990 IEEE MTT-S Int. Microwave Symp. Dig.*, May 1990, pp. 1183–1186.
[23] W. Fathelbab and M. Steer, "Broadband network design," in *Multifunctional Adaptive Microwave Circuits and Systems*, M. Steer and W. Palmer, Eds., 2008, ch. 8.
[24] ——, "Parallel-coupled line filters with enhanced stopband performance," *IEEE Trans. on Microwave Theory and Techniques*, vol. 53, no. 12, pp. 3774–3781, Dec. 2005.
[25] P. Cheong, S.-W. Fok, and K.-W. Tam, "Miniaturized parallel coupled-line bandpass filter with spurious-response suppression," *IEEE Trans. on Microwave Theory and Techniques*, vol. 53, no. 5, pp. 1810–1816, May 2005.
[26] I. Bahl and P. Bhartia, *Microwave Solid State Circuit Design*. John Wiley & Sons, 1988.
[27] F. Rosenbaum, R. Gregory, W. Richard, W. Ou, F. Kuhns, and T. Trimble, "An MMIC twin-tee active bandpass filter," in *1993 IEEE MTT-S Int. Microwave Symp. Dig.*, 1993, pp. 361–364.
[28] B. Kapilevich, "Active microwave filters," *Telecommunication Radio Engineering*, vol. 4, no. 2, pp. 51–58, Feb. 1985.
[29] C. Chang and T. Itoh, "Narrowband planar microwave active filter," *Electronics Letters*, vol. 25, no. 18, pp. 1228–1229, Aug. 1989.
[30] C.-Y. Chang and T. Itoh, "A varactor-tuned, active microwave band-pass filter," in *1990 IEEE MTT-S Int. Microwave Symp. Dig.*, May 1990, pp. 499–502.
[31] U. Karacaoglu and I. Robertson, "High selectivity varactor-tuned MMIC bandpass filter using lossless active resonators," in *IEEE 1994 Microwave and Millimeter-Wave Monolithic Circuits Symp. Dig. of Papers*, May 1994, pp. 237–240.
[32] G. Mazzaro, M. Steer, and K. Gard, "Intermodulation distortion in narrowband amplifier circuits," *IET Microwaves, Antennas Propagation*, vol. 4, no. 9, pp. 1149–1156, Sep. 2010.
[33] G. Mazzaro, M. Steer, K. Gard, and A. Walker, "Response of RF networks to transient waveforms: Interference in frequency-hopped communications," *IEEE Trans. on Microwave Theory and Techniques*, vol. 56, no. 12, pp. 2808–2814, Dec. 2008.
[34] G. Mazzaro, "Time-frequency effects in wireless communication systems," Ph.D. dissertation, North Carolina State University, 2009.
[35] J. Malherbe, *Microwave Transmission Line Filters*. Artech House, 1979.
[36] J.-S. Hong and M. Lancaster, *Microstrip Filters for RF/Microwave Applications*. John Wiley & Sons, 2001.
[37] H. Howe, *Stripline Circuit Design*. Artech House, 1974.
[38] R. E. Collin, *Foundations for Microwave Engineering*. John Wiley & Sons, 2007.
[39] D. G. Swanson and W. J. Hoefer, *Microwave circuit modeling using electromagnetic field simulation*. Artech House, 2003.
[40] W.-K. Chen, *Theory and design of broadband matching networks*. Pergamon Press, 1976.
[41] ——, *Passive and Active Filters: Theory and Implementations*. John Wiley & Sons, 1986.
[42] H. J. Blinchikoff and A. I. Zverev, *Filtering in the time and frequency domains*. Krieger Publishing Co., 1986.
[43] L. Zhu, S. Sun, and R. Li, *Microwave Bandpass Filters for Wideband Communications*. John Wiley & Sons, 2011.
[44] J.-S. Hong, *Microstrip Filters for RF/Microwave Applications*, 2nd ed. John Wiley & Sons, 2011.
[45] N. Kinayman and M. Aksun, *Modern microwave circuits*. Artech House, 2005.
[46] R. M. Foster, "Academic and theoretical aspects of circuit theory," *Proc. IRE*, vol. 50, no. 5, pp. 866–871, May 1962.

2.21 Exercises

1. The characteristic function of a doubly terminated network is $K(s) = s^2$.
   (a) What is the magnitude-squared transmission coefficient ($|T(s)|^2$)?
   (b) What is the magnitude-squared reflection coefficient ($|\Gamma(s)|^2$)?
   (c) What is transmission coefficient $T(s)$ for a circuit that can be realized using positive R, L, and C elements)?
2. The characteristic function of a doubly terminated network is $K(s) = s^4$. What is the magnitude-squared transmission coefficient ($|\Gamma(s)|^2$)?
3. Consider the design of a fourth-order lowpass Butterworth filter. [This problem follows the development in Section 2.4.]
   (a) What is the magnitude-squared characteristic polynomial, $|K(s)|^2$, of the Butterworth filter?
   (b) What is the magnitude-squared transmission coefficient (or transfer function)?
   (c) What is the magnitude-squared reflection coefficient function?
   (d) Derive the reflection coefficient function (i.e., $\Gamma(s)$). Write down the reflection coefficient in factorized form using up to second-order factors.
   (e) What are the roots of the numerator polynomial of the reflection coefficient function?
   (f) What are the roots of the denominator polynomial of the reflection coefficient function?
   (g) Identify the conjugate pole pairs in the factorized reflection coefficient.
   (h) Plot the poles and zeros of the reflection coefficient on the complex s plane.
4. Derive the reflection coefficient poles of a second-order Butterworth filter and write out the reflection coefficient with nominator and denominator polynomials, that is not in factorized form. [Parallels Example 2.1]
5. Derive the reflection coefficient poles and zeros of a fourth-order Chebyshev filter with a ripple factor, ε, of 0.1.
6. Synthesize the impedance function
$$Z_x = \frac{s^3 + s^2 + 2s + 1}{s^2 + s + 1}.$$
   That is, develop the RLC circuit that realizes Z_x. [Parallels Example 2.2]
7. Synthesize the impedance function
$$Z_w = \frac{4s^2 + 2s + 1}{8s^3 + 8s^2 + 2s + 1}.$$
   That is, develop the RLC circuit that realizes Z_w. [Parallels Example 2.3]
8. Synthesize the impedance function
$$Z_x = \frac{4s^2 + 2s + 1}{4s^2 + 1}.$$
   That is, develop the RLC circuit that realizes Z_x. [Parallels Example 2.2. You may also want to consult Figure 2-9.]
9. Synthesize the impedance function
$$Z_x = \frac{4s^4 + 2s^3 + 5s^2 + 2s + 1}{4s^4 + 4s^3 + 7s^2 + s + 1}.$$
   That is, develop the RLC circuit that realizes Z_x. [Parallels Example 2.2. You may also want to consult Figure 2-9.]
10. Develop the lowpass prototype of a fifth-order Butterworth lowpass filter. There may be more than one solution. That is, draw the circuit of the lowpass filter prototype with element values.
11. Develop the lowpass prototype of a fifth-order Chebyshev lowpass filter with 1 dB ripple and 1 rad/s corner frequency.
12. Develop the lowpass prototype of a ninth-order Chebyshev lowpass filter with 0.01 dB ripple and 1 rad/s corner frequency.
13. A 0.04 S admittance inverter is to be implemented in microstrip using a single length of transmission line. The effective permittivity of the line is 9 and the design center frequency is 10 GHz.
   (a) What is the characteristic impedance of the transmission line?
   (b) What is the wavelength in millimeters at the design center frequency in free space?
   (c) What is the wavelength in millimeters at the design center frequency in microstrip?
   (d) What is electrical length of the microstrip transmission line in degrees at the design center frequency?
   (e) What is the length of the microstrip transmission line in millimeters?
14. In Section 2.8.2 it was seen that a series inductor can be replaced by a shunt capacitor with inverters and a negative unity transformer. If the inverter is realized with a one-quarter wavelength long transmission line of characteristic impedance 50 Ω:
   (a) Derive the $ABCD$ parameters of the cascade of Figure 2-16(c) with 50 Ω inverters.

(b) What is the value of the shunt capacitance in the cascade required to realize a 1 nH inductor?

15. A series inductor of 10 pH must be realized by an equivalent circuit using shunt capacitors and sections of one-quarter wavelength long 1 Ω transmission line. Design the equivalent circuit. [Hint: The one-quarter wavelength long lines are impedance inverters.]

16. A series inductor of 10 nH must be realized by an equivalent circuit using shunt capacitors and sections of one-quarter wavelength long 50 Ω transmission line. [Hint: The one-quarter wavelength long lines are impedance inverters.] Design the equivalent circuit.

17. At 5 GHz, a series 5 nH inductor is to be realized using one or more 75 Ω impedance inverters, a unity transformer, and a capacitor. What is the value of the capacitor?

18. In Section 2.8.3 it was seen that a series capacitor can be replaced by a shunt inductor with inverters and a negative unity transformer. Consider that the inverters are realized with a one-quarter wavelength long transmission line of characteristic impedance 100 Ω.

    (a) Derive the $ABCD$ parameters of the cascade of Figure 2-17 with the 100 Ω inverters.
    (b) What is the value of the shunt inductance in the cascade required to realize a 1 pH capacitor?

19. A 50 Ω impedance inverter is to be realized using three resonant stubs. The center frequency of the design is f_0. The first resonant frequency of the stubs is $f_r = 2f_0$.

    (a) Draw the circuit using stubs. On your diagram indicate the input impedance and characteristic impedance of each of the stubs if $f_r = 2f_0$.
    (b) What is the input impedance of a shorted one-eighth wavelength long transmission line if the characteristic impedance of the line is Z_{01}?
    (c) What is the input impedance of an open-ended one-eighth wavelength long transmission
    (d) What is the input impedance of a shorted one-eighth wavelength long transmission if the characteristic impedance of the line is Z_{02}?
    (e) What is the length of each of the stubs in the inverter in terms of the wavelength at the frequency f_0?

20. Design a third-order Type 1 Chebyshev highpass filter with a corner frequency of 1 GHz, a system impedance of 50 Ω, and 0.2 dB ripple. There are a number of steps in the design, and to demonstrate that you understand them you are asked to complete the partial designs indicated below. A Cauer 1 lowpass filter prototype is shown below with ω_c being the corner radian frequency, $f_c = \omega_c/(2\pi)$ being the corner frequency, and Z_0 being the system impedance.

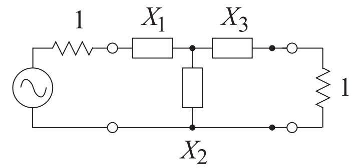

    (a) Design an LPF with $\omega_c = 1$ rad/s, $Z_0 = 1$ Ω.
    (b) Design a HPF with $\omega_c = 1$ rad/s, $Z_0 = 1$ Ω.
    (c) Design a HPF with $f_c = 1$ GHz, $Z_0 = 1$ Ω.
    (d) Design a HPF with $f_c = 1$ GHz, $Z_0 = 50$ Ω.

21. This problem considers the design of a Butterworth bandpass filter at 900 MHz.

    (a) Design an LC second-order Butterworth lowpass filter with a corner frequency of 1 rad/s in a 1 Ω system.
    (b) Using the above filter prototype, design a lowpass filter with a corner frequency of 900 MHz.
    (c) Design a second-order Butterworth bandpass filter at 900 MHz using the lowpass filter prototype in (a). Use a fractional bandwidth of 0.1 and a system impedance of 50 Ω.
    (d) What is the 3 dB bandwidth of the filter in (c)?

22. Design a third-order maximally flat bandpass filter prototype in a 50 Ω system centered at 1 GHz with a 10% bandwidth. The lowpass prototype of a third-order maximally flat filter is shown in Figure 2-10.

    (a) Convert the prototype lowpass filter to a lowpass filter with inverters and capacitors only; that is, remove the series inductors.
    (b) Scale the filter to take the corner frequency from 1 rad/s to 1 GHz.
    (c) Transform the lowpass filter into a bandpass filter. That is, replace each shunt capacitor by a parallel LC network. This step will establish the bandwidth of the filter.
    (d) Transform the system impedance of the filter from 1 to 50 Ω.

23. The lowpass prototype of a fourth-order lowpass Butterworth filter is shown below. The corner frequency is 1 rad/s.

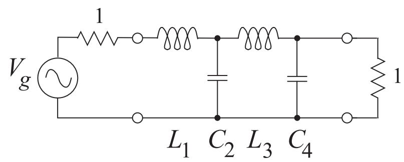

$L_1 = 0.765369$ H $\quad C_2 = 1.847759$ F
$L_3 = 1.847759$ H $\quad C_4 = 0.765369$ F

Based on this, develop a fourth-order Butterworth bandpass filter prototype centered at 10^9 rad/s with a fractional bandwidth of 5%.

(a) Scale the lowpass prototype to have a corner frequency of 10^9 rad/s. Draw the prototype with element values.

(b) Draw the schematic of the lumped-element fourth-order Butterworth bandpass prototype based on the original lowpass filter prototype.

(c) Derive the element values of the lumped-element bandpass filter prototype in a 75 Ω system.

24. Design a third-order Type 2 Chebyshev highpass filter with a corner frequency of 1 GHz, a system impedance of 50 Ω, and 0.2 dB ripple. There are a number of steps in the design, and to demonstrate that you understand them you are asked to complete the table below. For each stage of the filter synthesis you must indicate whether the element is an inductance or a capacitance by writing L or C in the appropriate cell. Other cells require a numeric value and you must include units. The X element is identified in the prototype below. A Cauer 2 lowpass filter prototype is shown with ω_c being the corner radian frequency, $f_c = \omega_c/(2\pi)$ being the corner frequency, and Z_0 being the system impedance.

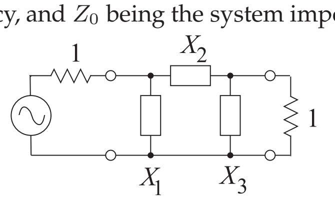

(a) Complete the LPF (lowpass filter) column of the table with $\omega_c = 1$ rad/s, $Z_0 = 1$ Ω.

(b) Complete the HPF (highpass filter) column of the table with $\omega_c = 1$ rad/s, $Z_0 = 1$ Ω.

(c) Complete the second HPF column of the table with $f_c = 1$ GHz, $Z_0 = 1$ Ω.

(d) Complete the third HPF column of the table with $f_c = 1$ GHz, $Z_0 = 50$ Ω.

ELEMENT	LPF $\omega_c = 1$ rad/s, $Z_0 = 1$ Ω	
	L or C	Value (units)
X_1		
X_2		
X_3		

ELEMENT	HPF $\omega_c = 1$ rad/s, $Z_0 = 1$ Ω	
	L or C	Value (units)
X_1		
X_2		
X_3		

ELEMENT	HPF $f_c = 1$ GHz, $Z_0 = 1$ Ω	
	L or C	Value (units)
X_1		
X_2		
X_3		

ELEMENT	HPF $f_c = 1$ GHz, $Z_0 = 50$ Ω	
	L or C	Value (units)
X_1		
X_2		
X_3		

25. What is the input impedance of a shorted $\lambda/8$ long transmission line with a characteristic impedance of Z_0?

26. What is the input impedance of an open-circuited $\lambda/8$ long transmission line with a characteristic impedance of Z_0?

27. Apply Richards's transformation to a shunt inductor with a reactance of 50 Ω. What is the electrical length of the shorted stub if the stub has a characteristic impedance of 50 Ω?

28. Apply Richards's transformation to a shunt capacitor with a reactance of −50 Ω. What is the characteristic impedance of the open-circuited stub if the electrical length of the stub is one-quarter wavelength long?

2.21.1 Exercises by Section

†challenging, ‡very challenging

§2.2 $1^\dagger, 2$
§2.4 $3^\dagger, 4^\dagger$
§2.5 $5^\dagger$
§2.6 $6^\dagger, 7^\dagger, 8^\dagger, 9^\dagger$
§2.7 $10, 11^\dagger, 12^\dagger$
§2.8 $13, 14^\dagger, 15^\dagger, 16^\dagger, 17^\dagger, 18^\dagger, 19^\dagger$
§2.9 $20^\dagger, 21^\dagger, 2^\dagger 2, 23^\dagger, 24^\dagger$
§2.12 $25, 26, 27^\dagger, 28^\dagger$

2.21.2 Answers to Selected Exercises

1(c) $\Gamma(s) = \dfrac{s^2}{s^2 + \sqrt{2}s + 1}$

2 $|T(\omega)|^2 = 1/(1 + \omega^8)$

3(f) $-0.38 + \jmath 0.92$
$-0.38 - \jmath 0.92$
$-0.92 + \jmath 0.38$
$-0.38 - \jmath 0.92$

7

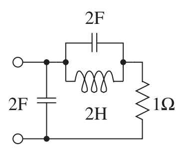

14(a) $\begin{bmatrix} 1 & sC(50)^2 \\ 0 & 1 \end{bmatrix}$

13(c) 9

17 889 fF

18 10 nH

19(c) $-Z_2 = -\jmath 50\ \Omega$

24 1 GHz, 50 Ω,
HPF: $X_3 = 6.5$ nH

CHAPTER 3

Parallel Coupled-Line Filters

3.1 Introduction

Central to microwave filter design is the identification of a particular distributed structure that inherently has the desired frequency-shaping attributes. Then this structure is adjusted to match an ideal mathematical, or perhaps lumped-element, representation of a filter. Filter design is both science and art, matching synthesis with instinctive knowledge of appropriate physical and circuit structures.

A large number of microwave filters are realized using coupled transmission lines and the most important of these are parallel coupled line (PCL) filters. These are derived from prototypes, with the development following a strategy that enables the filter to be realized using one of several coupled-line configurations. So the strategy is to first examine coupled-line configurations and determine the types of circuit structures that can be realized. Then the steps in synthesis are designed to go from an LC filter prototype to a prototype that has the structures that can be realized by a coupled-line configuration.

Since the beginnings of microwave circuit synthesis, it has become common to present circuit concepts using examples, very often because the steps in realizing a filter may be too difficult to specify algorithmically and there are many steps that require intuition. This procedure is followed here.

This introduction concludes with an example that illustrates the art and science of microwave engineering. It is seen that a simple pair of coupled lines with appropriate matching has a bandpass filter response. The intrinsic bandpass response is supported by coupled lines, so the synthesis procedure is adapting the intrinsic response to specifications.

EXAMPLE 3.1 Coupled Lines as a Basic Element of a Bandpass Filter

AWR Design Environment Project File: RFDesign_Coupled_Shorted_Microstrip_Lines_C.emp

A coupled pair of microstrip lines terminated in short circuits is shown in Figure 3-1. This circuit has a bandpass response centered at 7.5 GHz, as shown in Figure 3-2. So while the insertion loss reduces to about 3.5 dB at 7.5 GHz, the return loss is not very high. This is a good indication that matching could be used to reduce the insertion loss. So the problem is then one of determining the appropriate matching network and to do this an understanding of the circuit response needs to be gained. Figure 3-3 plots the S_{11} and S_{21} responses on a Smith chart. By looking at S_{11} it is seen that between 7 and 8 GHz the input impedance is primarily inductive. This indicates that a series capacitance could be used in matching. Another view is shown in Figure 3-4, which plots the magnitude and phase of the input impedance at Port 1 of the coupled microstrip lines (this will be the same as the input impedance at Port 2). So around 7 GHz, the input impedance is inductive since the phase of the impedance is close to 90° and the magnitude of the impedance is increasing with frequency. At 7 GHz the impedance is approximately $\jmath 50\ \Omega$, which would be resonated out by a series capacitor of 0.45 pF. However it will not be as simple as this, as the tuning capacitor will need to be placed at both Ports 1 and 2. However, this does serve to provide an initial design point.

The schematic required to implement the design above is shown in Figure 3-5. In this circuit schematic, the coupled line shown in Figure 3-1(b) is captured as a subcircuit called ”CoupledLine.” The series capacitors at Ports 1 and 2 are ”C1” and ”C2,” that is, C_1 and C_2, respectively. C_1 and C_2 are established as tunable elements with the governing variable being ”CC.” This capacitor is tuned to obtain the optimum bandpass response. With $C_1 = C_2 = 44.8$ fF, the bandpass response shown in Figure 3-6 is obtained. This is an almost ideal maximally flat bandpass filter response. The main passband is at 7 GHz and there is a parasitic bandpass response at the third harmonic. This spurious passband at an odd harmonic occurs often in transmission line designs. A small alteration of the tuning capacitor can change the response to have ripples in the passband and sharper filter skirts (see Figure 3-7), where the tuning capacitors are each 37.6 fF. (To convince yourself of the sharper skirt consider the insertion loss at 100 MHz away from the passband. The insertion loss of the filter with the maximally flat response is 23 dB there, and that of the filter with the ripple response is 27 dB.) This filter has two passband poles and is simple enough to design as done here. Higher-order filters (with more than two passband resonators) require a more sophisticated design approach. Still this example demonstrates that the coupled-line structure has a good passband response on its own provided that appropriate matching is used.

The bandpass characteristic is a result of the phase velocities of the even and odd modes being different. If they were the same, the transmission coefficient would be zero at 7 GHz.

3.2 Parallel Coupled Lines

Several of the key advantages of coupled-line filters over other distributed filters is that the coupling between resonators can be strong if the pair of coupled-line resonators are close to each other, or low if they are widely separated. This enables filters to be realized with high (30–70%), medium (10–30%), or low (2–10%) bandwidths. The low-bandwidth filters require low coupling of the resonators, while the high bandwidth filters require high coupling. Coupled-line filters are also compact and can be implemented in microstrip configurations or most of the other transmission line technologies. The different transmission line forms have different Qs. Planar transmission lines have moderate Qs especially at high frequencies, due principally to

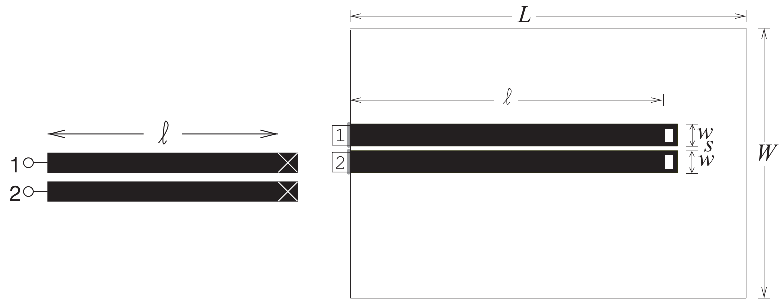

(a) (b)

Figure 3-1: Coupled microstrip line layout: (a) schematic; and (b) layout in an EM simulator. Dimensions of the coupled lines are w = 500 μm, s = 100 μm, ℓ = 1 cm, W = 6 mm, and L = 12 mm. The metal is 6 μm thick gold (conductivity $\sigma = 42.6 \times 10^6$ S/m) and the alumina substrate height is 600 μm with relative permittivity ε_r = 9.8 and loss tangent of 0.001.

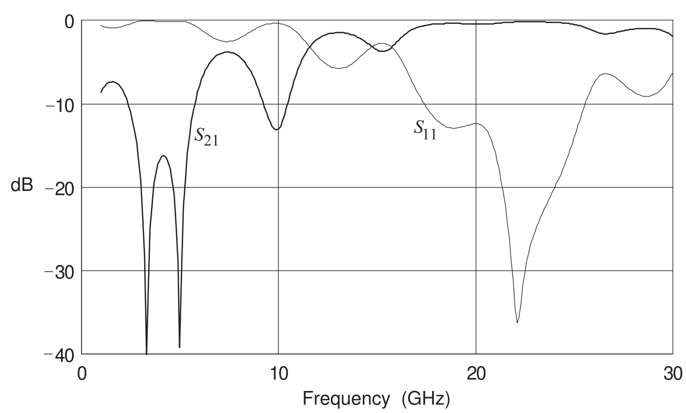

Figure 3-2: Insertion loss (S_{21}) and return loss (S_{11}) of the coupled line of Figure 3-1 with an $s = 100$ μm gap.

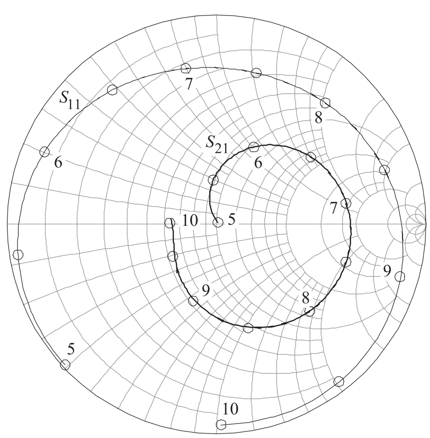

Figure 3-3: Insertion loss and return loss over a narrow frequency range plotted on a Smith chart. The annotation at the markers is the frequency in GHz.

radiated fields. Low Q means that the insertion loss of filters will be high and the filter skirts will not be as steep as they would be if a high-Q transmission line structure was used. For example, up to the early 2000s the RF filters in the front end of cellular phones were mostly seventh-order Chebyshev filters using coupled slablines as shown in Figure 3-8 (although here only

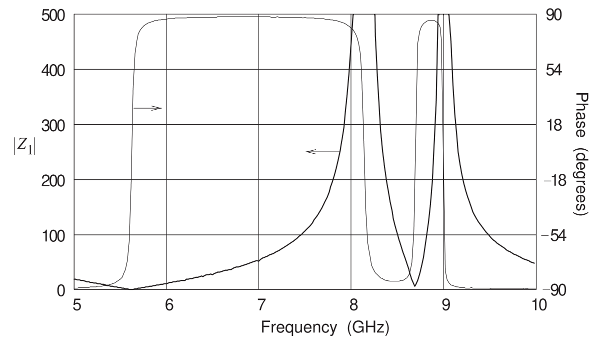

Figure 3-4: Input impedance at Port 1 of the coupled microstrip lines in Figure 3-1. Port 2 is terminated in 50 Ω.

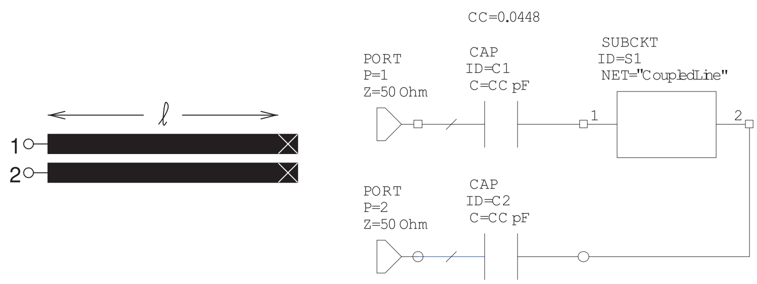

(a) (b)

Figure 3-5: Capacitively coupled microstrip lines: (a) schematic; and (b) representation in a microwave CAD tool with a subcircuit representing the coupled lines. The layout of the subcircuit is shown in Figure 3-1.

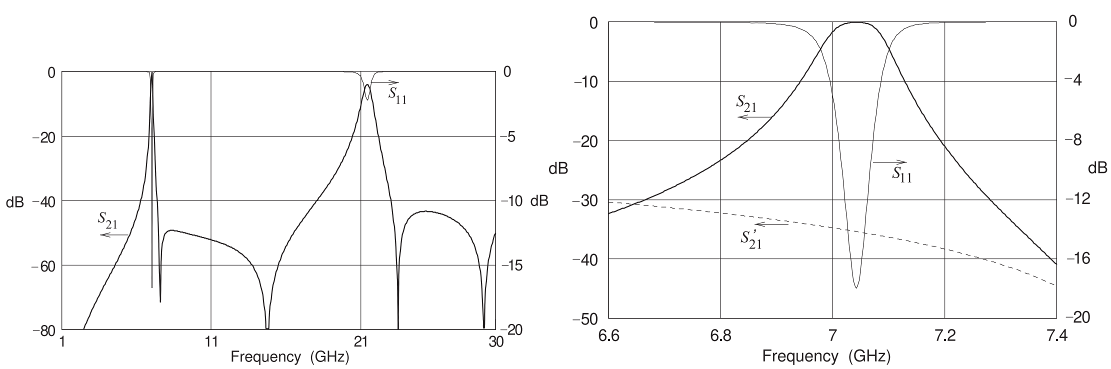

(a) Wide frequency view (b) Detail

Figure 3-6: Return loss and insertion loss when the coupling capacitors are 44.8 fF. This results in a Butterworth-like response. S'_{21} is the response without C_1 and C_2.

four resonators are shown for clarity). Typically the top and bottom plates of the resonators were 2–3 mm apart and the area of the slabline filter was 1 cm×1 cm. This is too large for today's thin smart phones. However, they are very good filters and cheap to produce. The electrical design procedure for parallel coupled slabline filters and for using other transmission line structures is the same as for parallel coupled microstrip filters. The difference is only in the final physical implementation.

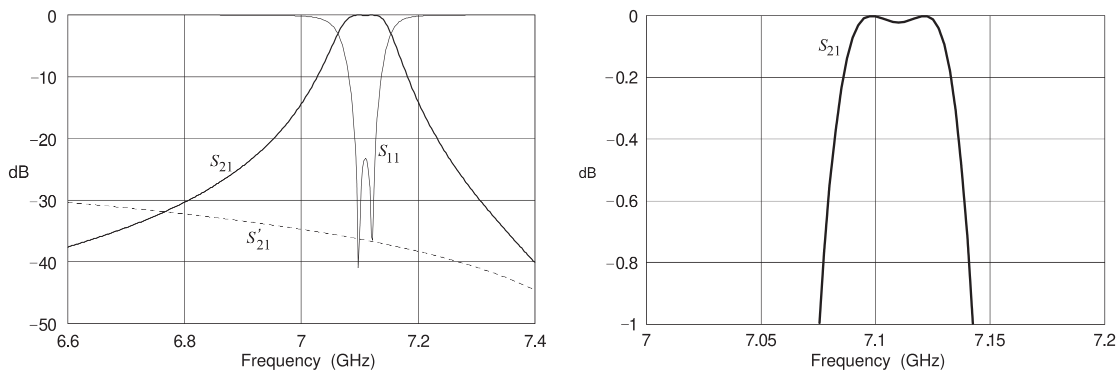

(a) Narrowband response (b) Detail showing ripples

Figure 3-7: Return loss and insertion loss when the coupling capacitors are 37.6 fF. This results in a Chebyshev-like response. S'_{21} is the response without C_1 and C_2.

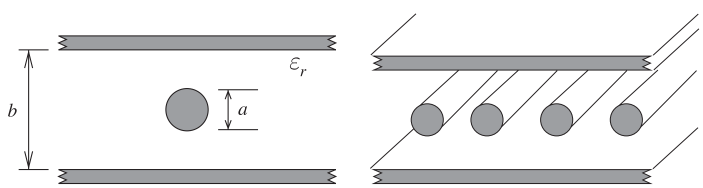

(a) (b)

Figure 3-8: Slabline: (a) cross section of a single slabline; and (b) parallel coupled-line configuration with four coupled slablines.

3.2.1 Coupled-Line Configurations

The coupled-line configuration considered in Example 3.1 is called a combline section. This is one of many that have desirable frequency-selective responses. The characteristics of many parallel coupled-line configurations having bandpass, all-pass, or all-stop characteristics are shown in Table 3-1. The most important configurations are starred ($\star$).

The PCL section of Filter (a) in Table 3-1 is called an interdigital section and is a bandpass filter. The dual filter is Filter (b), with what is called a parallel coupled section, and both can be used to realize narrow (2–3%) to wide (up to 30%) bandwidth filters with close to symmetrical responses around the center frequency f_0. For a wide bandwidth filter the lines are close and for a narrow bandwidth filter the parallel lines are widely separated so that there is low-level coupling. Filter (c) is also a bandpass filter, however, the frequency selectivity is not as good as with Filters (a) and (b). Filters (d), (e), and (f) are all-pass filters. These filters are used to adjust the phase of a transmitted signal, usually to accommodate phase dispersion (e.g., phase variation with respect to frequency) that was introduced somewhere else. While this analog function was once important, it is less so now as DSP techniques can usually equalize the phase sufficiently. Filter (g) is an all-stop filter, meaning that negligible signal is transmitted. This filter has no practical use. Filters (h) and (i) are inherently all-stop filters. An example of the response of the combline section of Filter (h) was seen in Figure 3-2 of Example 3.1, where the all-stop response is centered at 4 GHz. The response is too broad to be useful as a bandstop filter (in any practical application).

Table 3-1: Responses of the nine coupled-line configurations with narrow (2–3%), moderate (3–10%), and wide (10%–30%) bandwidth. The most important configurations are starred ($\star$).

Attributes	Circuit	Response
$\star$ (a) Interdigital section. Bandpass. Narrow to wide bandwidth. $\ell = \lambda/4$ at f_0. Symmetrical passband.	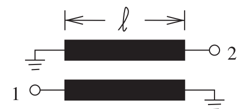	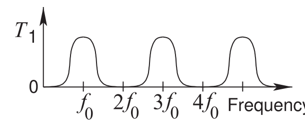
$\star$ (b) Parallel coupled section. Bandpass. Narrow to wide bandwidth. $\ell = \lambda/4$ at f_0. Symmetrical passband.		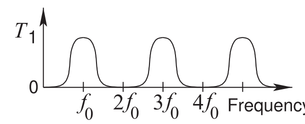
(c) Bandpass. Moderate to wide bandwidth. $\ell = \lambda/4$ at f_0.		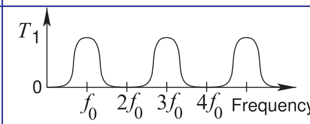
(d) All-pass. $0 < \ell \leq \lambda/2$ at f_0.		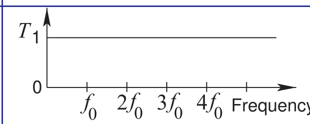
(e) All-pass. $0 < \ell \leq \lambda/2$ at f_0.		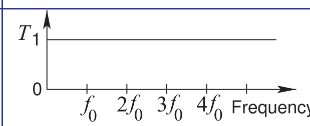
(f) All-pass. $0 < \ell \leq \lambda/2$ at f_0.		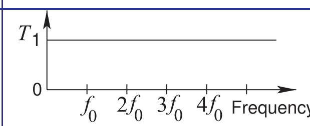
(g) All-stop (no practical use).	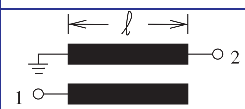	
$\star$ (h) Combline section. All-stop without matching. Bandpass with matching. Moderate to wide bandwidth. $\ell = \lambda/4$ at f_0. Compact. Asymmetrical response.		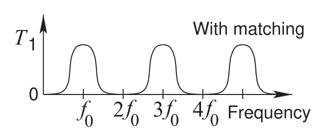
(i) All-stop without matching. Bandpass with matching. Moderate to wide bandwidth. $\ell = \lambda/4$. Compact. Asymmetrical response.	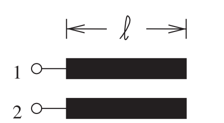	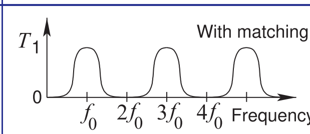

However, with minimal matching, such as a series capacitor at each of ports (see Figure 3-5), the combline section becomes a very good bandpass filter (see Figures 3-6 and 3-7). The combline bandpass filter, Filter (h), is more compact than Filters (a) and (b). However, it has an asymmetrical bandpass response (which can be seen in Figure 3-7(a)), whereas Filters (a) and (b) have a symmetrical frequency response. Which type of response is preferred depends on the application. Filter (i) is the dual of Filter (h), but in practice

Table 3-2: Responses of coupled-line configurations having lowpass and bandstop responses.

Attributes	Circuit	Response
⋆ (j) Lowpass. Narrow to moderate bandwidth. $\ell = \lambda/2$ at f_0	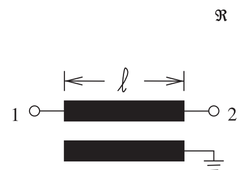	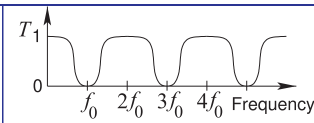
⋆ (k) Lowpass. Narrow to moderate bandwidth. $\ell = \lambda/4$ at f_0	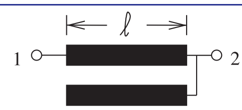	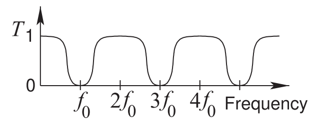
⋆ (l) Lowpass. Narrow bandwidth. $\ell = \lambda/4$ at f_0.	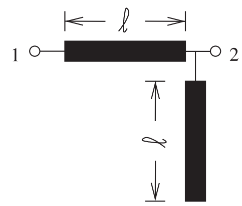	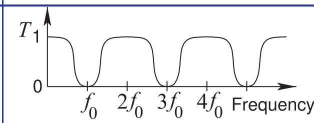
⋆ (m) Bandstop. Narrow bandwidth. $\ell = \lambda/4$ at f_0.	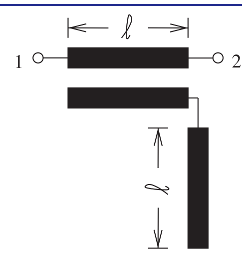	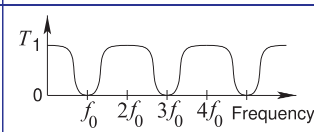

the combline configuration of Filter (h) is preferred.

Table 3-2 presents coupled-line sections having lowpass and bandstop responses. All of these filters have desirable characteristics and so all are starred (⋆). Filter (l) is not a PCL filter but it is used in trade-off among the three lowpass filters (i.e., Filters (j), (l) and (m)). The usual application of a bandstop filter is to notch out an undesired signal (e.g. to prevent an LO from appearing where it is not desired). As such, the desired frequency response is narrowband and Filter (m) is a good choice for a bandstop filter.

Filter design using PCL sections begins with the choice of a PCL configuration having the essential desired frequency response. Each of the PCL sections in Tables 3-1 and 3-2 have two resonators and can implement bandpass, bandstop, and lowpass filters having second-order responses.[1] To meet specifications it is generally necessary to replicate the basic section. So treating the two resonator configurations as unit cells, a multi-cell filter can be realized. The multi-cell forms of the main bandpass configurations are shown in Table 3-3. The multi-cell implementation of the interdigital, parallel

[1] Recall that the order designation comes from the lowpass prototype so that here a second-order bandpass filter actually has two resonators, each having an LC-like response.

Table 3-3: Multi-cell forms of bandpass parallel coupled-line configurations. The wavelength, λ, is at the center frequency of the filter.

Name	Unit cell	Multi-cell form
(a) Interdigital bandpass filter. $\ell = \lambda/4$.		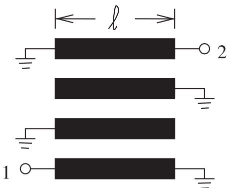
(b) Parallel edge-coupled bandpass filter. $\ell = \lambda/4$.		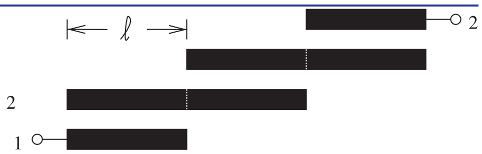
(c) Parallel edge-coupled hairpin bandpass filter. $\ell > \lambda/4$.		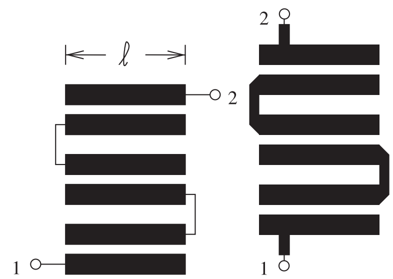
(d) Combline bandpass filter. $\ell = \lambda/4$. Matching required. 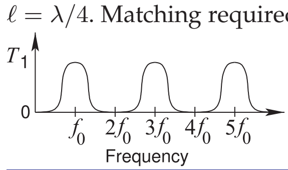	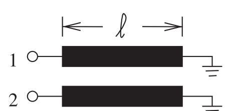	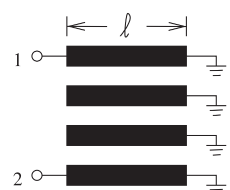
(e) Combline bandpass filter with extended stopband. $\ell = \lambda/4$. $\ell_2 \approx \lambda/8$ (typically). Matching required. 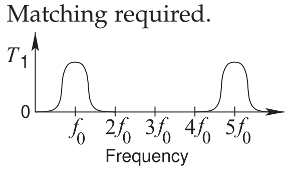		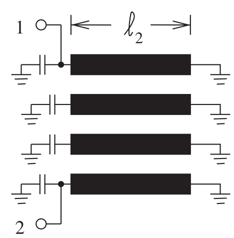

edge-coupled bandpass filters, (a) and (b) in Tables 3-3, is straightforward. A variation is shown in Filter (c), which folds the parallel edge-coupled sections to realize a compact multi-cell form called a hairpin filter [1–3]. One of the consequences of using transmission line segments to realize a filter is that there are spurious passbands. This results because a $\lambda/4$ section of line looks the same electrically as a $3\lambda/4$ section. Consequently there are normally spurious passbands at the odd-harmonic frequencies. If the basic resonator is $\lambda/2$ long, then the spurious passbands would be at all of the harmonic frequencies. A solution is to incorporate capacitors in the

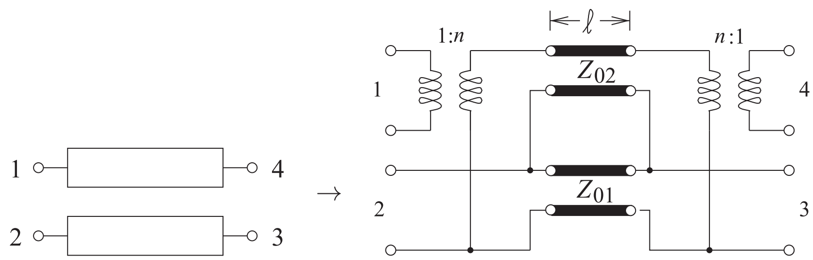

Figure 3-9: Network model of a pair of coupled lines.

resonators as shown in Filter (e) in Table 3-3 [2, 4, 5]. Thus each of the original transmission line resonators now becomes a combination of a capacitor and a shorter transmission line segment. If the new transmission line segment is $\lambda/8$ long, the first spurious passband will now be at $5f_0$ rather than $3f_0$. The spurious passbands can be pushed further up in frequency by using even shorter transmission line lengths, but the performance of the filter at the passband frequency, f_0, will be compromised.

There are many variations on the PCL filter and several different design techniques have been developed [6–28]. Refer to these citations to explore alternative PCL configurations and alternative methods of design to that presented here. This chapter presents one of the common approaches to synthesizing PCL filters and the scheme accommodates the use of capacitive loading used to extend the stopband of a passband filter.

Before launching into the synthesis procedure for a PCL filter, a comment on synthesis versus optimization is warranted. With a simple topology such as the second-order filter topologies shown in Table 3-1, an optimization procedure could be used to design the widths and lengths of the lines and the two or four variables describing the required external matching networks that are not shown. A global optimization is certainly feasible. However, it is not feasible to use global optimization of, for example, a seventh-order filter required to meet typical cell phone specifications. An exception is if a design for a very similar specification is available and the changes required are small. Competitive filter design requires synthesis. This will lead to optimum performance, and the insight gained can be used in topology modifications.

3.2.2 Coupled-Line Circuit Models

An approximate coupled-line model of a pair of coupled lines was presented in Section 5.9.5 of [29]. This model is repeated in Figure 3-9. The parameters of the network model are related to the model impedances as follows:

$$n = \frac{1}{K} = \frac{Z_{0e} + Z_{0o}}{Z_{0e} - Z_{0o}} \qquad (3.1)$$

$$Z_{0S} = \sqrt{(Z_{0e} Z_{0o})}, \qquad (3.2)$$

$$Z_{01} = \frac{Z_{0S}}{\sqrt{1 - K^2}}, \qquad (3.3)$$

$$Z_{02} = Z_{0S}\frac{\sqrt{1 - K^2}}{K^2}. \qquad (3.4)$$

Various terminating arrangements of the coupled lines result in several useful filter elements. One arrangement is shown in Figure 3-10. Also shown in this figure is the development of the network model based on the model in Figure 3-9. The final network model is a transmission line of characteristic impedance Z_{01} in cascade with an open-circuited stub. Consider what happens at the resonant frequency, f_r (the frequency at which the lines are one-quarter wavelength long). At lower frequencies, $f \ll f_r$, the Z_{02} line

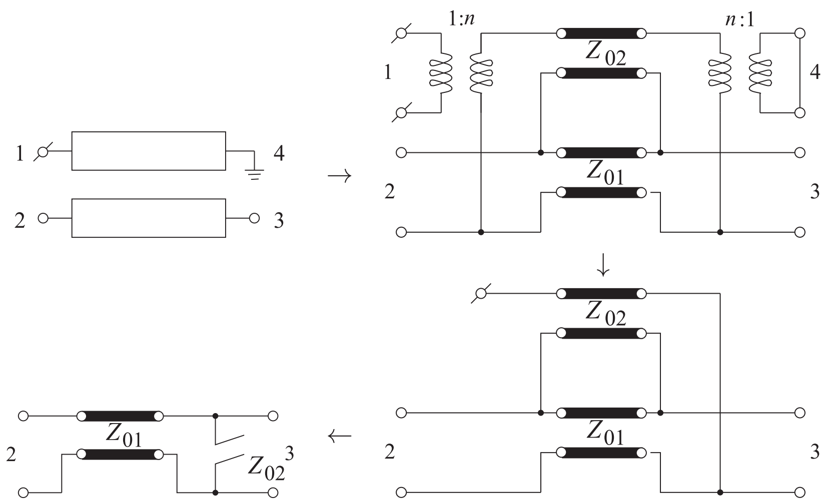

Figure 3-10: Lowpass distributed network section derived from a pair of coupled lines with Port 1 open-circuited. The open circuit is indicated by a node (open circle) with a line through it. The final network model is a transmission line of characteristic impedance Z_{01} and an open-circuited stub of characteristic impedance Z_{02}. The lines and stubs are one-quarter wavelength long at the corner frequency. (Thus with the stub $f_r = f_0$, and the characteristic impedance of the stub is as shown.)

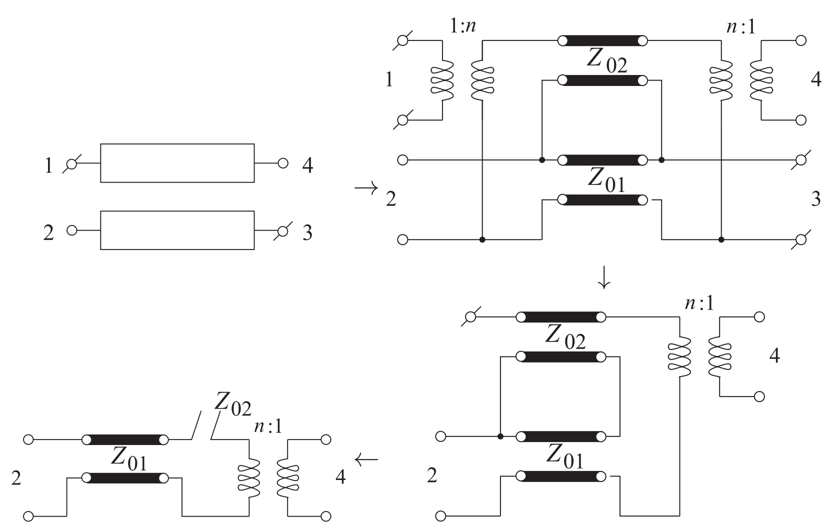

Figure 3-11: Parallel coupled-line section with Ports 1 and 3 open-circuited and network models. (For the stub, the characteristic impedance of the stub is shown and $f_r = f_0$.)

is an open circuit and signals travel along Z_{01}. At resonance the Z_{02} stub becomes a short circuit and signals do not pass. This is a crude verification that this is a lowpass structure. The process is visual and is expected to be self-explanatory. Other examples are shown in Figures 3-11 to 3-13.

The model of a combline section is shown in Figure 3-13. The final network reduction is repeated in Figure 3-14, and it will be shown that the model in Figure 3-14(b) is equivalent to the model in Figure 3-14(a). In the synthesis of a combline filter, the network of Figure 3-14(b) is obtained and this can be

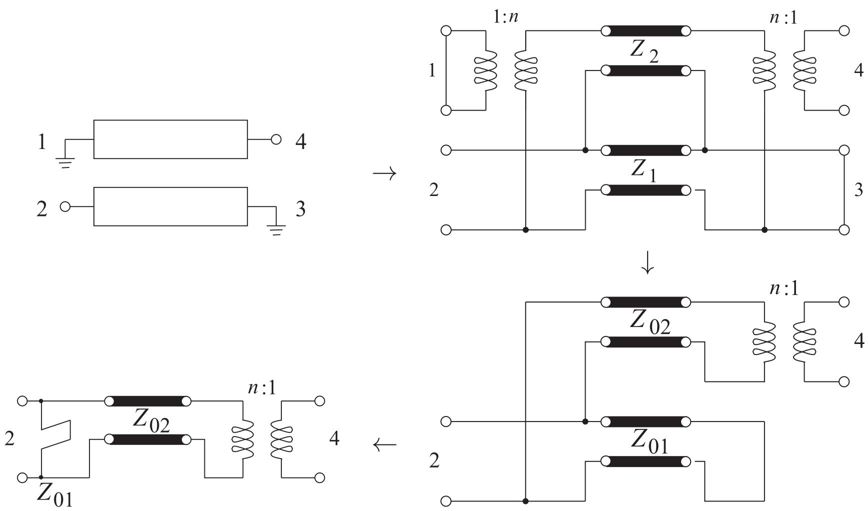

Figure 3-12: Interdigital section and network models. (For the stub, the characteristic impedance of the stub is shown and $f_r = f_0$.)

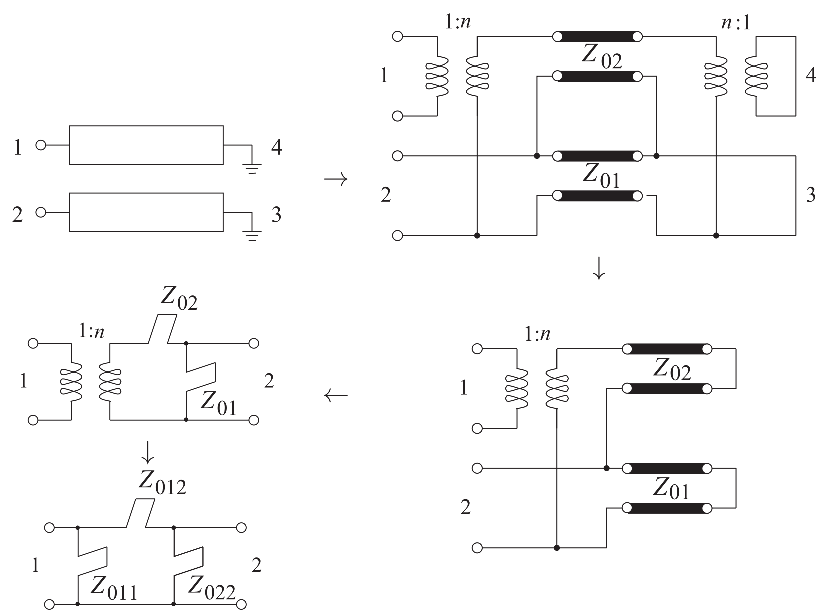

Figure 3-13: Combline section and network models. (For the stubs, the characteristic impedances of the stubs are shown and $f_r = f_0$.)

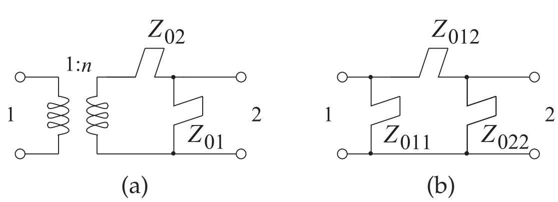

Figure 3-14: Equivalent models of a section of combline. (For the stubs, the characteristic impedances of the stubs are shown and $f_r = f_0$.)

related back to the dimensions of the coupled line. The equivalence is done using $ABCD$ parameters and, as will be seen, the equivalence will not be at just one frequency but will be broadband. The $ABCD$ parameters of the network in Figure 3-14(a) are obtained by cascading the $ABCD$ parameters of three two-ports (the $ABCD$ parameters of which are given in Table 2-1 of [30]). The $ABCD$ parameters of the network in Figure 3-14(a) are (from the multiplication of three $ABCD$ parameter matrices)

$$T_A = T_{\text{TRANSFORMER}} T_{\text{SERIES STUB}} T_{\text{SHUNT STUB}} \tag{3.5}$$

$$= \begin{bmatrix} 1/n & 0 \\ 0 & n \end{bmatrix} \begin{bmatrix} 1 & \jmath Z_{02}\tan\theta \\ 0 & 1 \end{bmatrix} \begin{bmatrix} 1 & 0 \\ -\jmath/(Z_{01}\tan\theta) & 1 \end{bmatrix} \tag{3.6}$$

$$= \begin{bmatrix} 1/n & \jmath Z_{02}\tan\theta/n \\ 0 & n \end{bmatrix} \begin{bmatrix} 1 & 0 \\ -\jmath/(Z_{01}\tan\theta) & 1 \end{bmatrix} \tag{3.7}$$

$$= \begin{bmatrix} \frac{1}{n}\left(1+\frac{Z_{02}}{Z_{01}}\right) & \jmath Z_{02}\tan\theta/n \\ -\jmath n/(Z_{01}\tan\theta) & n \end{bmatrix}. \tag{3.8}$$

The $ABCD$ parameters of the network in Figure 3-14(b) are

$$T_B = T_{\text{SHUNT STUB}} T_{\text{SERIES STUB}} T_{\text{SHUNT STUB}} \tag{3.9}$$

$$= \begin{bmatrix} 1 & 0 \\ -\jmath/(Z_{011}\tan\theta) & 1 \end{bmatrix} \begin{bmatrix} 1 & \jmath Z_{012}\tan\theta \\ 0 & 1 \end{bmatrix} \begin{bmatrix} 1 & 0 \\ -\jmath/(Z_{022}\tan\theta) & 1 \end{bmatrix} \tag{3.10}$$

$$= \begin{bmatrix} 1 & \jmath Z_{012}\tan\theta \\ -\jmath/(Z_{011}\tan\theta) & 1+Z_{012}/Z_{011} \end{bmatrix} \begin{bmatrix} 1 & 0 \\ -\jmath/(Z_{022}\tan\theta) & 1 \end{bmatrix} \tag{3.11}$$

$$= \begin{bmatrix} 1+\frac{Z_{012}}{Z_{022}} & \jmath Z_{012}\tan\theta \\ \frac{-\jmath}{\tan\theta}\left(\frac{1}{Z_{011}}+\frac{1}{Z_{022}}+\frac{Z_{012}}{Z_{011}Z_{022}}\right) & 1+\frac{Z_{012}}{Z_{011}} \end{bmatrix}. \tag{3.12}$$

Equating Equations (3.8) and (3.12) yields

$$1+\frac{Z_{012}}{Z_{022}} = \frac{1}{n}\left(1+\frac{Z_{02}}{Z_{01}}\right) \tag{3.13}$$

$$Z_{012} = Z_{02}/n \tag{3.14}$$

$$\left(\frac{Z_{011}+Z_{022}+Z_{012}}{Z_{011}Z_{022}}\right) = \frac{n}{Z_{01}} \tag{3.15}$$

$$1+\frac{Z_{012}}{Z_{011}} = n, \tag{3.16}$$

which have the solution

$$Z_{012} = \frac{Z_{02}}{n} \tag{3.18}$$

$$Z_{011} = \frac{Z_{012}}{n-1} = \frac{Z_{02}}{n(n-1)} \tag{3.17}$$

$$Z_{022} = \frac{Z_{01}Z_{02}}{Z_{02}-(n-1)Z_{01}}. \tag{3.19}$$

Rearranging these, expressions for Z_{01}, Z_{02}, and n can be obtained:

$$n = 1+\frac{Z_{012}}{Z_{011}},\quad Z_{01} = \left(\frac{nZ_{011}Z_{022}}{Z_{011}+Z_{022}+Z_{012}}\right), \text{ and } Z_{02} = nZ_{02}Z_{012}. \tag{3.20}$$

Using these, Equations (3.1)–(3.4), and the coupled-line analysis of Section 5.6 of [29], the geometric parameters of the combline coupled-line section can be obtained corresponding to the stub circuit of Figure 3-14(b).

Thus the equivalent circuit of the combline section, the top left figure in Figure 3-13, has the equivalent circuit shown in Figure 3-14. Filter synthesis can be directed at developing circuit structures like that in Figure 3-14(b) and from this electrical design, the physical design consisting of combline sections can be developed.

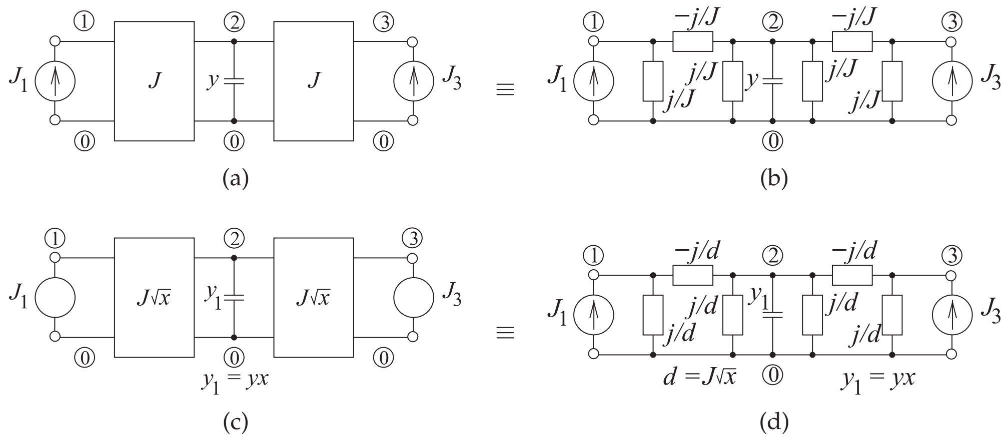

Figure 3-15: Inverter network: (a) network with two identical admittance inverters with an inserted shunt element of admittance, y; (b) equivalent network using equivalence shown in Figure 2-19; (c) scaled original network; and (d) scaled equivalent network. Element values are impedances except for J, y and y_1, which are admittances. The use of the equivalent networks in filter synthesis is illustrated in the case study in Section 3.4.

3.3 Inverter Network Scaling

A filter that uses transmission lines is nearly always synthesized from a filter prototype that contains inverters. The synthesis of a filter begins with a normalized prototype that is transformed to the desired frequency, impedance, and type. It is the purpose of this section to show how to use such scaling when there are inverters in the prototype. In particular, it is shown that scaling the admittance of the network of Figure 3-15(a), a common inverter subnetwork, by a factor x results in the network in Figure 3-15(c).

The nodal admittance matrix of the network in Figure 3-15(a) is

$$Y = \begin{bmatrix} 0 & -\jmath J & 0 \\ -\jmath J & y & -\jmath J \\ 0 & -\jmath J & 0 \end{bmatrix}. \tag{3.21}$$

Assigning nodal voltages to Terminals 1, 2, and 3, the nodal admittance matrix equation is

$$\begin{bmatrix} 0 & -\jmath J & 0 \\ -\jmath J & y & -\jmath J \\ 0 & -\jmath J & 0 \end{bmatrix} \begin{bmatrix} v_1 \\ v_2 \\ v_3 \end{bmatrix} = \begin{bmatrix} J_1 \\ 0 \\ J_3 \end{bmatrix}, \tag{3.22}$$

and by eliminating Node 2 using network condensation (see Section 1.A.16) of [31], this reduces to

$$\begin{bmatrix} J^2/y & J^2/y \\ J^2/y & J^2/y \end{bmatrix} \begin{bmatrix} v_1 \\ v_3 \end{bmatrix} = \begin{bmatrix} J_1 \\ J_3 \end{bmatrix}, \tag{3.23}$$

and this describes the external characteristics of the subnetwork in Figure 3-15(a).

The nodal admittance matrix of the scaled network in Figure 3-15(c) is

$$Y' = \begin{bmatrix} 0 & -\jmath J\sqrt{x} & 0 \\ -\jmath J\sqrt{x} & yx & -\jmath J\sqrt{x} \\ 0 & -\jmath J\sqrt{x} & 0 \end{bmatrix}. \tag{3.24}$$

That is,

$$\begin{bmatrix} 0 & -\jmath J\sqrt{x} & 0 \\ -\jmath J\sqrt{x} & yx & -\jmath J\sqrt{x} \\ 0 & -\jmath J\sqrt{x} & 0 \end{bmatrix} \begin{bmatrix} v_1 \\ v_2 \\ v_3 \end{bmatrix} = \begin{bmatrix} J_1 \\ 0 \\ J_3 \end{bmatrix}, \tag{3.25}$$

and by eliminating Node 2 this reduces to

$$\begin{bmatrix} (J^2x)/(yx) & (J^2x)/(yx) \\ (J^2x)/(yx) & (J^2x)/(yx) \end{bmatrix} \begin{bmatrix} v_1 \\ v_3 \end{bmatrix} = \begin{bmatrix} J^2/y & J^2/y \\ J^2/y & J^2/y \end{bmatrix} \begin{bmatrix} v_1 \\ v_3 \end{bmatrix} = \begin{bmatrix} J_1 \\ J_3 \end{bmatrix}. \tag{3.26}$$

Thus the original network shown in Figure 3-15(a) has the same external electrical characteristics as the scaled network of Figure 3-15(c), with the characteristic admittance of the inverters scaled by $\sqrt{x}$ and the shunt admittance scaled by x.

A generalization of this result (which is useful when there are additional connections between Nodes 1 and 3) is that multiplying a row and a column of the nodal admittance matrix by the same factor results in identical external characteristics. Note that the element sharing a row and column is multiplied twice.

EXAMPLE 3.2 Inductor Synthesis

Lumped inductors have low Q. Fortunately, in microwave design they can be realized using inverters and a shunt capacitor that have a high Q. Realize the series inductor in Figure 3-16(a) with a shunt capacitor and 10 Ω impedance inverters.

Solution:

The series inductor in a 1 Ω system is transformed into a network with inverters and a shunt capacitor using the transformation shown in Figure 2-48. Thus here the series inductor can be realized by the circuit of Figure 3-16(b), where the shunt capacitor C has the same numeric value as the series inductor. The inverters here can be either impedance inverters or admittance inverters, as their value is equal to one. The design requires that these be realized as 10 Ω inverters, but scaling is performed on admittance inverters, as shown in Figure 3-16(c), where the value of the admittance inverters is 0.1 S = $\sqrt{x}$. Thus $x = 0.01$ and the admittance of the capacitor is scaled by 0.01, so $C_1 = C/100$ = 10 pF. The final design is shown in Figure 3-16(d).

3.4 Case Study: Third-Order Chebyshev Combline Filter Design

This section presents the design of a 1 GHz third-order Chebyshev combline bandpass filter with 10% bandwidth. The combline filter is one of the most commonly used transmission line-based filters and uses the combline section shown in Figure 3-13. The synthesis that will be presented here combines many of the concepts discussed previously in this chapter. There are also design decisions that must be made in response to particular situations encountered during synthesis. An example of a design decision is deciding what to do if the characteristic impedance of a transmission line is too low.

Step 1: Choice of Lowpass Filter Prototype

Design begins with the choice of a prototype that is expected to achieve the required specifications. If the choice is eventually found to be not suitable, then another topology must be chosen and the synthesis restarted. Consider a third-order Chebyshev lowpass filter prototype, shown in Figure 3-17, with a passband ripple factor of $\varepsilon = 0.1$ (or 0.043 dB). The element values were calculated using Equations (2.83)–(2.90). Note that at the corner frequency that defines the bandwidth of the lowpass filter, the square of the transmission coefficient is the ripple level (see Figure 2-7). That is, at frequency $\omega_0 = 1$ rad/s, the squared transmission coefficient is $1/(1+\varepsilon^2)$ (or in decibels the ripple is $R_{\text{dB}} = 10\log(1+\varepsilon^2)$).

Step 2: Replace Series Elements

The next step in the transformation of the lowpass prototype in Figure 3-17 is replacing the series inductor by a shunt capacitor in cascade with admittance inverters, as shown in Figure 3-18. This step uses the series inductor transformation shown in Figure 2-16.

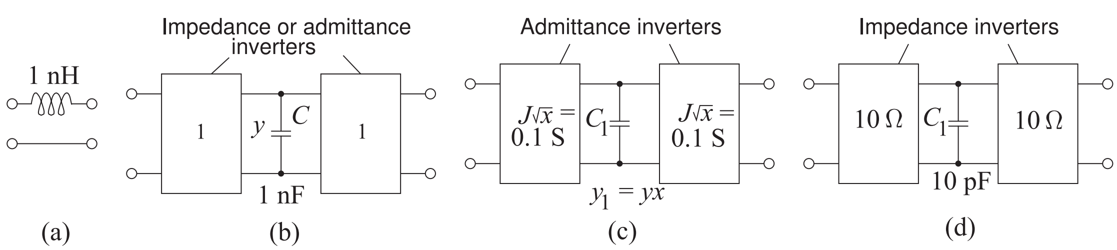

Figure 3-16: Realization of a series inductor as a shunt capacitor with inverters.

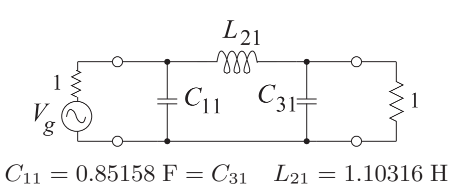

Figure 3-17: Step 1. A third-order Chebyshev lowpass filter prototype.
$g_1 = g_3 = 0.85158$, $g_2 = 1.10316$.

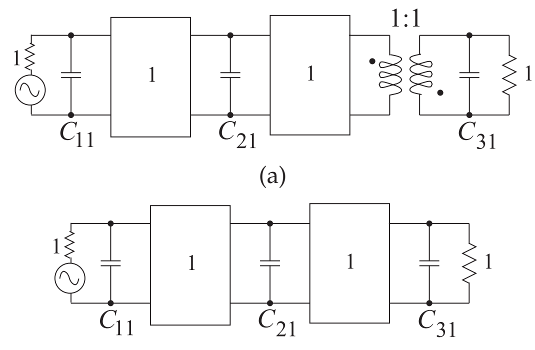

$C_{11} = 0.85158$ F $= C_{31}$ $C_{21} = 1.10316$ F

Figure 3-18: Step 2. Prototype filter with inductor replaced by a capacitor and admittance inverter combination: (a) with a unity inverting transformer; and (b) with the transformer eliminated as it shifts the transmission phase by $180°$ and so has no effect on the filter response. Note that $|C_{21}| = |L_{21}|$.

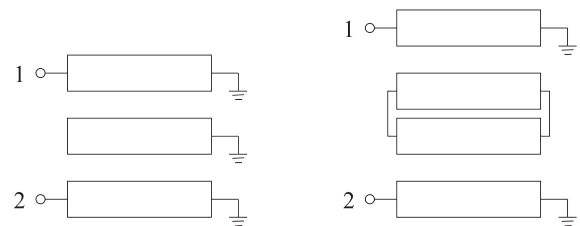

(a) Three-resonator combline filter   (b) Model

Figure 3-19: Target combline filter physical layout.

Step 3: Bandpass Filter Transformation

In synthesizing the bandpass filter the final physical topology must be considered. The essential element of a third-order combline filter comprises three coupled lines as shown in Figure 3-19(a). The three resonators can be modeled as two pairs of coupled lines, as shown in Figure 3-19(b), with one line shared by each pair. Each pair of coupled lines can be modeled by a Pi network of stubs as shown in Figure 3-14(b). Thus the lowpass prototype of Figure 3-18(b) needs to be converted to a bandpass filter and eventually this needs to be transformed into two cascaded Pi networks of stubs.

In this step the prototype is converted to a bandpass circuit. The filter has 10% bandwidth with approximate corner frequencies at $f_1 = 950$ MHz and $f_2 = 1050$ MHz. Using the filter type transformations in Figure 2-27, $\omega_0 = 2\pi 10^9$, and $\alpha = \omega_0/(\omega_2 - \omega_1)$ = 1/(fractional bandwidth) = 10, the first capacitor in Figure 3-18, C_{11}, is transformed to

$$C_1' = \frac{\alpha C_{11}}{\omega_0} = 1355.33\,\text{pF} \;\; \text{in parallel with} \;\; L_1' = \frac{1}{\alpha C_{11}\omega_0} = 0.0186894\,\text{nH}. \tag{3.27}$$

The other capacitors are transformed similarly and the bandpass prototype becomes that shown in Figure 3-20.

The lumped-element version of the bandpass filter is shown in Figure 3-21 along with its simulated response. This response is the ideal electrical response and provides a reference in design. Note that the ripples in the transmission response, i.e. S_{21}, are not evident on this scale. Losses in the implemented filter will smooth the ripples even further although the poles in the S_{21} response are not evident, these correspond to the zeros in the S_{11} response and these are clearly visible. Figure 3-21 shows three zeros in the S_{11} response, as expected for a third-order filter.

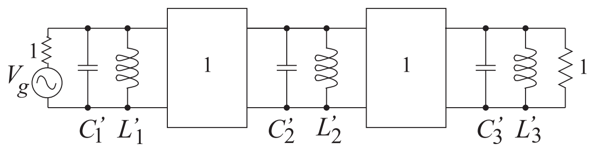

$C_1' = 1355.33\,\text{pF} = C_3' \quad L_1' = 0.0186894\,\text{nH} = L_3'$
$C_2' = 1755.73\,\text{pF} \quad L_2' = 0.0144271\,\text{nH}$

Figure 3-20: Step 3. Bandpass filter prototype with inverters derived from the lowpass filter prototype of Figure 3-18.

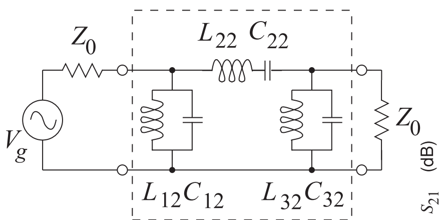

$Z_0 = 1\,\Omega$
$C_{12} = 1.35533\,\text{nF} = C_{32}$
$L_{12} = 18.6894\,\text{pH} = L_{32}$
$C_{22} = 14.4271\,\text{pF}$
$L_{22} = 1.75573\,\text{nH}$

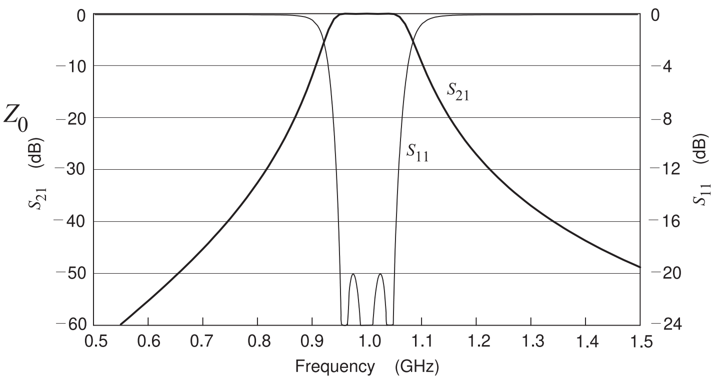

Figure 3-21: A third-order lumped-element Chebyshev bandpass filter with 10% bandwidth, ripple factor of $\varepsilon = 0.1$, and center frequency of 1 GHz. The S parameters are referenced to 1 Ω.

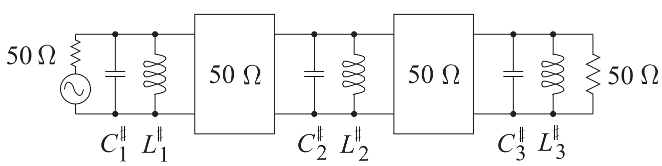

$C_1^\sharp = 27.1066\,\text{pF} = C_3^\sharp \quad L_1^\sharp = 0.934468\,\text{nH} = L_3^\sharp$
$C_2^\sharp = 35.1147\,\text{pF} \quad L_2^\sharp = 0.721359\,\text{nH}$

Figure 3-22: Step 4. Bandpass filter approximation where the inverters are now impedance inverters.

Step 4: Impedance Scaling

The system impedance is now scaled from 1 to 50 Ω, leading to the prototype in Figure 3-22 (derived from Figure 3-20).

Step 5: Conversion of Lumped-Element Resonators

Each lumped-element resonator in Figure 3-22 comprises a capacitor and an inductor. The inductors are particularly difficult to realize efficiently and have high loss. The idea is to replace each lumped resonator (e.g., $C_1^\sharp$ and $L_1^\sharp$ in Figure 3-22) with a network comprising a lumped capacitor and a transmission line stub.

Equivalence of a Capacitively-Loaded Stub and an LC Resonator

Here it will be shown that a capacitively-loaded stub is a broadband approximation of a lumped LC resonator. The resonator equivalence is shown in Figure 3-23. The equivalence is first developed at frequency $f_0 = \omega_0/(2\pi)$ by making sure that the circuits have the same admittance at the

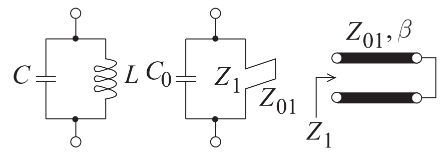

Figure 3-23: Resonator equivalence: (a) lumped resonator resonant at radian frequency ω_0; (b) mixed lumped-distributed resonator containing a short-circuited stub of characteristic impedance Z_0 and resonant at radian frequency ω_r; and (c) short-circuited transmission line stub resonant at radian frequency ω_r. In (b) and (c) Z_{01} is the characteristic impedance of the transmission line and Z_1 is the input impedance of the shorted transmission line.

filter center frequency. The broadband approximation is obtained by also equating the derivatives of the admittances at ω_0.

The input admittance of the parallel LC lumped-element resonator is

$$Y_{\text{in}} = \frac{\jmath\left(\omega^2 LC - 1\right)}{\omega L}, \tag{3.28}$$

and has a radian frequency derivative of

$$\frac{dY_{\text{in}}}{d\omega} = \frac{\jmath\left(\omega^2 LC + 1\right)}{\omega^2 L}. \tag{3.29}$$

Now consider a short-circuited stub that is resonant at radian frequency ω_r; that is, the short-circuited stub is one-quarter wavelength long at ω_r. From Equation (2.100) of [29], the input impedance at ω is

$$Z_1 = \jmath Z_{01} \tan\left(\frac{\pi}{2}\frac{\omega}{\omega_r}\right). \tag{3.30}$$

Thus for the lumped-distributed network in Figure 3-23(b), the input admittance is

$$Y'_{\text{in}} = \frac{\jmath\left[\omega C_o Z_{01} \tan\left(\frac{\pi}{2}\frac{\omega}{\omega_r}\right) - 1\right]}{Z_{01}\tan\left(\frac{\pi}{2}\frac{\omega}{\omega_r}\right)}, \tag{3.31}$$

and its radian frequency derivative is

$$\frac{dY'_{\text{in}}}{d\omega} = \jmath\frac{1}{2}\left(\frac{\left\{2C_o Z_{01}\left[\tan\left(\frac{\pi}{2}\frac{\omega}{\omega_r}\right)\right]^2 \omega\omega_r + \pi + \pi\left[\tan\left(\frac{\pi}{2}\frac{\omega}{\omega_r}\right)\right]^2\right\}}{Z_{01}\left[\tan\left(\frac{\pi}{2}\frac{\omega}{\omega_r}\right)\right]^2 \omega_r}\right). \tag{3.32}$$

For the lumped-element and lumped-distributed resonators to be identical at ω_0 and approximating each other at nearby frequencies, Equations (3.28) and (3.31) are equated,

$$Y_{\text{in}}(\omega_0) = Y'_{\text{in}}(\omega_0), \tag{3.33}$$

and Equations (3.29) and (3.32) are also equated,

$$\left.\frac{dY_{\text{in}}}{d\omega}\right|_{\omega=\omega_0} = \left.\frac{dY'_{\text{in}}}{d\omega}\right|_{\omega=\omega_0}. \tag{3.34}$$

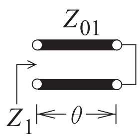

At ω_r,
$\theta = 90°, Z_1 = \infty$
At $\omega = \omega_r/2$,
$\theta = 45°, Z_1 = \jmath Z_{01}$

Figure 3-24: Short-circuited transmission line used as a stub resonator in a bandpass filter. The line is resonant at the radian frequency ω_r and so the electrical length of the line is $\theta = 90°$. Using the design choice here, the filter center passband frequency $\omega = \omega_r/2$, and so $\theta = 45°$ and so the input impedance of the shorted stub is $Z_1 = \jmath Z_{01}$.

Specific Design Choice, $\omega_r = 2\omega_0$

At this stage a design choice must be made regarding the relationship of ω_0 and ω_r; that is, the resonant frequency of the stub in relation to the resonant frequency of the resonator (which is also the center frequency of the filter passband). Here a shorted stub is considered that is resonant when it is $\lambda/4$ long. The specific design choice made here is that the resonant frequency of the stub, f_r, is twice the center frequency of the filter passband, i.e. $\omega_r = 2\omega_0$. This is a common design choice. The consequence of this choice is illustrated in Figure 3-24. The frequency f_r is called the **commensurate frequency** to avoid confusion resulting from the resonant frequency of the filter resonators being different from the resonant frequency of stub[2]. The stub design proceeds as follows.

The equivalence expressed by Equations (3.33) and (3.34) is established at the center of the passband (i.e., at ω_0). Now $\omega = \omega_0 = \frac{1}{2}\omega_r$, so Equations (3.28), (3.31), and (3.33) become

$$\frac{\jmath\left[\left(\frac{\omega_r}{2}\right)^2 LC - 1\right]}{\frac{\omega_r}{2}L} = \frac{\jmath\left[\frac{\omega_r}{2}C_0 Z_{01}\tan\left(\frac{\pi}{2}\frac{\omega_r/2}{\omega_r}\right) - 1\right]}{Z_{01}\tan\left(\frac{\pi}{2}\frac{\omega_r/2}{\omega_r}\right)}. \tag{3.35}$$

That is,
$$\frac{\left(\omega_r^2 LC - 4\right)}{2\omega_r L} = \frac{\left[\frac{\omega_r}{2}C_0 Z_0 \tan(\pi/4) - 1\right]}{Z_{01}\tan(\pi/4)}. \tag{3.36}$$

Since $\tan\frac{\pi}{4} = 1$,
$$\frac{\left(\omega_r^2 LC - 4\right)}{2\omega_r L} = \frac{\left(\frac{1}{2}\omega_r C_0 Z_{01} - 1\right)}{Z_{01}}, \tag{3.37}$$

and rearranging,
$$C_0 = C - \frac{4}{\omega_r^2 L} + \frac{2}{\omega_r Z_{01}}. \tag{3.38}$$

Another relationship comes from equating derivatives. From Equations (3.29), (3.32), and (3.34), and with $\omega = \frac{1}{2}\omega_r$ and $\tan(\frac{\pi}{2}\frac{\omega}{\omega_r}) = \tan\frac{\pi}{4} = 1$,

$$\frac{\left(\omega_r^2 LC + 4\right)}{\omega_r^2 L} = \frac{1}{2}\frac{\left(2C_0 Z_{01}\frac{1}{2}\omega_r^2 + \pi + \pi\right)}{Z_{01}\frac{1}{2}\omega_r} = \frac{\left(C_0 Z_{01}\omega_r^2 + 2\pi\right)}{Z_{01}\omega_r}. \tag{3.39}$$

Substituting for C_0 from Equation (3.38) and rearranging, the characteristic impedance of the stub is

$$Z_{01} = \frac{\omega_r L}{4}\left(1 + \frac{\pi}{2}\right). \tag{3.40}$$

---

[2] Of course there are resonant frequencies at every multiple of one-quarter wavelength. The first resonance occurs at f_r, as then the input impedance of the short-circuited stub is an open circuit. The characteristic that establishes resonance is that the input is either an open- or short-circuit and energy is stored.

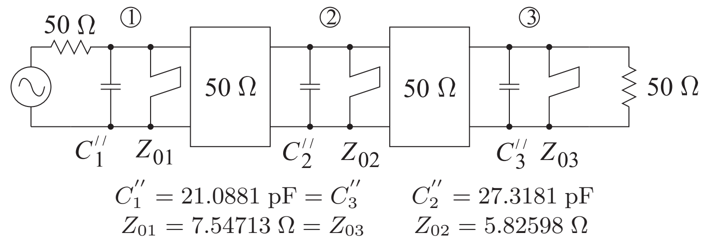

Figure 3-25: Step 5. Bandpass combline filter with impedance inverters. The transmission line stubs present impedances $Z_1 = \jmath Z_{01}$, $Z_2 = \jmath Z_{02}$, and $Z_3 = \jmath Z_{03}$ since the resonant frequencies of the stubs are twice that of the design center frequency, i.e. $f_r = 2f_0$.

In the passband the input impedance of the stub is

$$Z_1 = \jmath Z_{01} \tan(\beta\ell) = \jmath Z_{01} \tan(\pi/4) = \jmath Z_{01}. \tag{3.41}$$

Thus the broadband (≈30%) approximation of the parallel LC resonant circuit is a capacitively-loaded stub, see Figure 3-23(b), of length $\lambda/8$ at the resonant frequency of the LC resonator. The resonant frequency of each stub, i.e. the frequency f_r at which they are $\lambda/4$ long, is twice the design center frequency f_0, i.e. $f_r = 2f_0$. So the concept used here is that the resonant frequency of a stub does not need to be the same as the design center frequency. It is common for all the stubs in a design to have the same resonant frequency f_r and this is specified in the design documentation. In general f_r can have any relationship to f_0 but the most common situation is $f_r = 2f_0$ as used here.

Returning to Step 5

For this filter, the center of the passband is 1 GHz, and so $\omega_0 = 2\pi 10^9$ and $\omega_r = 2\omega_0 = 2\pi(2 \cdot 10^9)$ defines the stub resonant frequency as 2 GHz. The first resonator in Figure 3-22 with $L = 0.934468$ nH and $C = 27.1066$ pF can be replaced by the capacitively-loaded stub in Figure 3-23(b). where, from Equation (3.40),

$$Z_{01} = 7.54713\,\Omega, \quad \text{and from Equation (3.38)}, \quad C_0 = 21.0881\,\text{pF}. \tag{3.42}$$

This process is repeated for each lumped-element resonator in Figure 3-22, leading to the prototype shown in Figure 3-25.

Steps 6 and 7: Equating Characteristic Impedances of Stubs

The stubs in Figure 3-25 can be physically realized using transmission line segments. It would be ideal if the impedances of the stubs (i.e., the impedances looking into the stubs) are identical. To achieve this, the method of nodal admittance matrix scaling described in Section 3.3 is used with the impedance inverters multiplied by $\sqrt{Z_{01}/Z_{02}}$ and the admittance, $C_2''//Z_2$, divided by Z_{01}/Z_{02} (C_2'' is divided by Z_{01}/Z_{02}, and Z_2 is multiplied by Z_{01}/Z_{02}). This step scales each inverter impedance to 56.9084 Ω and also sets the characteristic impedance of all the shunt stubs to 7.54713 Ω. The combline filter is now as shown in Figure 3-26.

In Section 2.8.6 it was shown that a good narrowband model of an inverter is a Pi network of stubs. So the inverter in the current filter design, shown in Figure 3-27(a), is modeled by the lumped-element circuit in Figure 3-27(b) and the stub circuit shown in Figure 3-27(c).

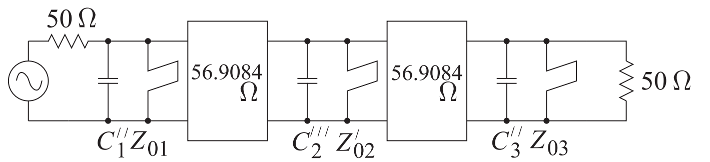

$C_1'' = C_3'' = C_2''' = 21.0881$ pF and $Z_{02}' = 7.54713\ \Omega = Z_{01} = Z_{03}$

Figure 3-26: Step 6. Bandpass combline filter with impedance inverters with $f_r = 2f_0$.

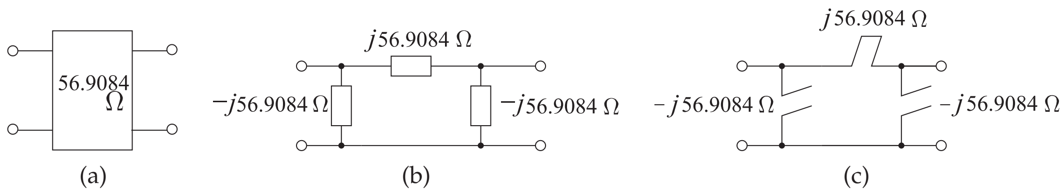

Figure 3-27: Inverter translation used with the combline filter design: (a) impedance inverter; (b) realization as a lumped-element circuit; and (c) realization using stubs resonant at twice the passband center frequency.

Stub Impedance When $f_r = 2f_0$

The most common design choice is to select the resonant (i.e., the commensurate) frequency of the stubs to be twice the center frequency of the design. With $f_r = 2f_0$, Equation (2.114) becomes

$$Z_0 = \frac{1}{J\tan\left(\dfrac{\pi}{2}\dfrac{\omega_0}{2\omega_0}\right)} = \frac{1}{J\tan\left(\dfrac{\pi}{4}\right)} = \frac{1}{J} = K. \tag{3.43}$$

Equation (3.43) defines the characteristic impedance of the transmission line stubs realizing an inverter. Then the elements of the subnetwork in Figure 3-27(b) all have the admittance magnitude

$$J = 1/K = 1/(56.9084\ \Omega) = 17.5721\ \text{mS} \tag{3.44}$$

and the stubs in Figure 3-27(c) have the characteristic impedance

$$Z_0 = \frac{1}{J\tan(\theta)} = \frac{K}{\tan(\theta)} = \left.\frac{K}{\tan\left(\dfrac{\pi}{2}\dfrac{\omega}{\omega_r}\right)}\right|_{\omega=\omega_0} = 56.9084\ \Omega. \tag{3.45}$$

At this stage there are several pairs of stubs in parallel. Figure 3-28 illustrates how a pair of parallel stubs can be replaced by a single stub. Now the prototype is as shown in Figure 3-29.

Step 8: Scaling Characteristic Impedances of Stubs

The filter will be realized using coupled microstrip lines and a general statement can be made about how the stubs in the prototype in Figure 3-29 correspond to the physical structure of the coupled lines. The stubs with characteristic impedances Z_{01}', Z_{02}'', and Z_{03}' are largely realized by the properties of the individual microstrip lines. A low Z_{01}', for example, would

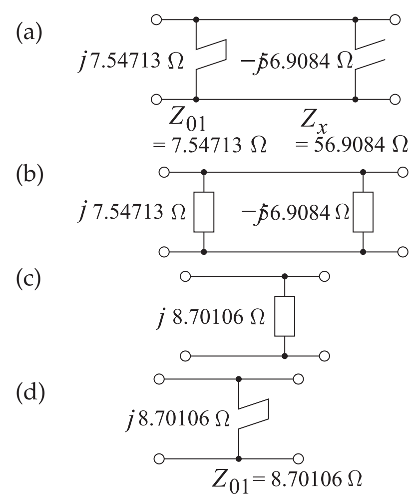

Figure 3-28: Step 6b. Procedure combining two parallel stubs to obtain one stub: (a) two parallel stubs; (b) represented as parallel impedances; (c) as one impedance; and (d) final representation as one stub. Note that the stubs must have the same commensurate frequency, i.e. they must have the same electrical length.

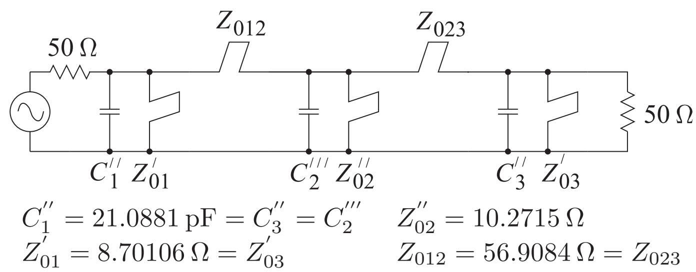

Figure 3-29: Step 7: Bandpass filter approximation where $Z_{01}^{'}$, $Z_{02}^{''}$, $Z_{03}^{'}$, Z_{012}, and Z_{023} are the characteristic impedances of the stubs with commensurate frequency $f_r = 2f_0$.

require a wide microstrip line. The stubs with characteristic impedances Z_{012} and Z_{023} each correspond to coupling between pairs of microstrip lines with high impedances corresponding to low-level coupling and widely spaced microstrip lines.

In Figure 3-29 the short-circuited shunt stubs have characteristic impedances of $8.7\ \Omega$ and $10.3\ \Omega$, which are too low, and will result in wide microstrip lines.[3] These need to be scaled to a higher impedance level to raise the characteristic impedances of the short-circuited stubs to an acceptable value. Note that the characteristic impedance of the middle shunt short-circuited stub can be raised to 80 Ω if the system impedance is raised from 50 Ω to 389.426 Ω. Doing this leads to the element values shown in the bandpass circuit of Figure 3-30.

Step 9: Scaling to a 50 Ω System Impedance

The previous step raised the system impedance (the required source and load impedances) to an unreasonably high level (389.426 Ω). For the filter to operate in a 50 Ω system, input and output impedance inverters are required to scale the source and load back to 50 Ω. The resulting circuit is shown in

[3] What is reasonable for the width of a microstrip line is subjective and based on experience. With a substrate having $\varepsilon_r = 10$, the width required for a characteristic impedance, Z_0, of 30–80 Ω is reasonable. A line with $Z_0 < 30\ \Omega$ will be very wide, use too much area, and potentially lead to multi-moding. A line with $Z_0 > 80\ \Omega$ will be narrow, close to the maximum Z_0 that can be realized in a technology, have manufacturing tolerance issues, and have large radiation. The range can be extended to 20–100 Ω but typically with degraded performance. Also see Example 3.4 of [29] for a microstrip design guideline.

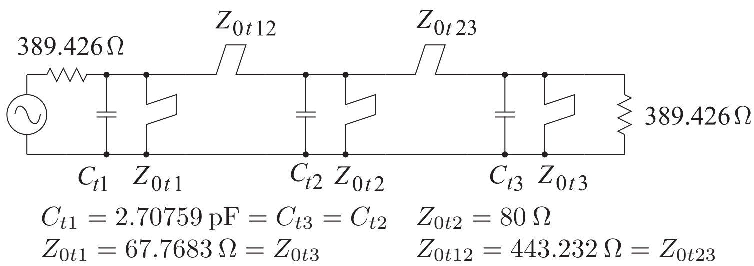

Figure 3-30: Step 8: Bandpass filter approximation.

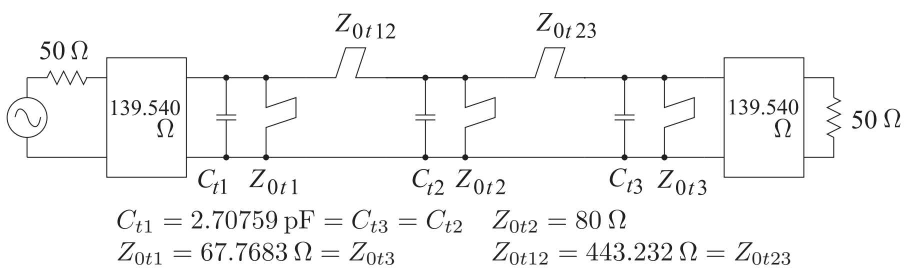

Figure 3-31: Step 9: Bandpass filter approximation.

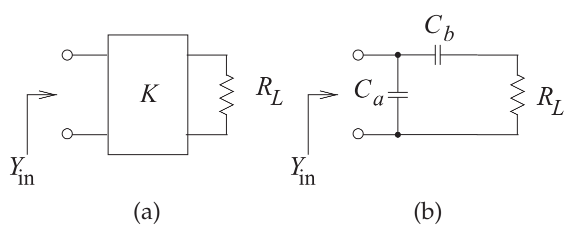

Figure 3-32: Inverter equivalence: (a) resistively-terminated impedance inverter; and (b) its equivalent capacitor network. Here $Z_{\text{in}} = 1/Y_{\text{in}} = 389.426\ \Omega$, $R_L = 50\ \Omega$, and $K = 139.540\ \Omega$.

Figure 3-31 with input and output inverters of impedance $\sqrt{50 \times 389.426} = 139.540\ \Omega$.

3.4.1 Realization of the Input/Output Inverters

At this stage the design is as shown in Figure 3-31, where the inverters at the input and output remain to be synthesized. There are many possible realizations of the inverters. Focusing on just the output inverter with a load R_L, as shown in Figure 3-32(a), it will be shown here how this can be realized using the capacitive network of Figure 3-32(b).

The input admittance of the inverter plus load resistor of Figure 3-32(a) is

$$Y_{\text{in}} = \frac{R_L}{K^2}, \tag{3.46}$$

and the input admittance of the circuit in Figure 3-32(b) is

$$Y_{\text{in}} = sC_a + \frac{1}{1/(sC_b) + R_L}. \tag{3.47}$$

Thus, equating the real parts of Equations (3.46) and (3.47),

$$\Re\left(Y_{\text{in}}\right) = \frac{R_L \omega^2 C_b^2}{R_L^2 \omega^2 C_b^2 + 1} = \frac{R_L}{K^2}, \tag{3.48}$$

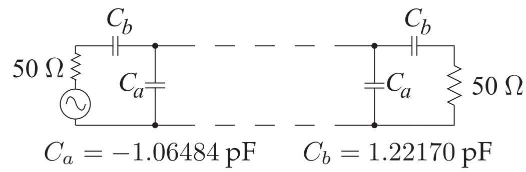

Figure 3-33: The external inverters of the prototype shown in Figure 3-31 replaced by capacitive networks.

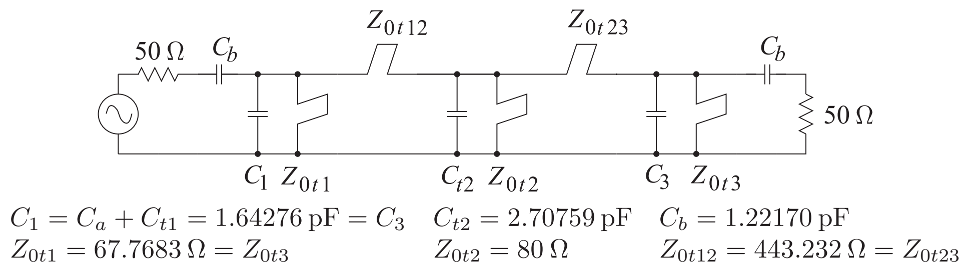

Figure 3-34: Step 10: The bandpass filter approximation combining the capacitive equivalent of the inverters with the first and last capacitors in the circuit of Figure 3-31.

and equating the imaginary parts yields

$$\Im\left(Y_{\text{in}}\right) = \omega\left[C_a + \frac{C_b}{1+(\omega C_b R_L)^2}\right] = 0. \tag{3.49}$$

Thus
$$C_b = \frac{1}{\omega K\sqrt{1-R_L^2/K^2}}, \quad C_a = \frac{-C_b}{1+(\omega C_b R_L)^2}, \tag{3.50}$$

and the inverters shown in Figure 3-31 can be replaced by the capacitive networks shown in Figure 3-33. This capacitive network is not a general replacement of an inverter. It only works when the inverter is terminated in a resistor. Note that C_a is negative, and this is absorbed in the first and last resonators so that the final lumped-distributed realization is as shown in Figure 3-34. This is the electrical design of the bandpass filter in a form that can be realized using the combline connection of coupled lines.

3.4.2 Implementation

The filter designed in the previous section can be implemented using three parallel microstrip lines, as shown in Figure 3-35(a), where the three capacitors of the electrical design in Figure 3-34 appear directly in Figure 3-35(a). The double Pi connection of stubs shown in Figure 3-34, and again in Figure 3-36(a), becomes the three coupled lines shown in Figure 3-36(b).

Derivation of Physical Dimensions

The task now is to determine the dimensions of the three parallel microstrip lines. The dimensions to be determined are shown in Figure 3-36(b) and are the length of the lines, L, the widths of the three lines, w_1, w_2, and w_3, and the gaps s_1 and s_2. The approach is to consider that the three parallel lines form two coupled-line pairs with each pair of coupled lines implementing a Pi network of stubs. The physical design procedure is outlined in Figure 3-36 with one of the lines shared. This, of course, is an approximation but a fairly accurate one. The physical synthesis of a pair of coupled lines is outlined in Figure 3-37 where the parameters of the Pi model, Figure 3-37(a), lead to the parameters of the transmission lines in the combline model, Figure 3-37(b). This then leads to the parameters defining the pair of coupled lines, Figure 3-37(c), in particular the even and odd-mode characteristic impedances, Z_{0e} and Z_{0o} and the system impedance Z_{0S}.

Using the quantities in Figure 3-37(a) and rearranging Equations (3.14)–(3.16), the parameters of the coupled-line model in Figure 3-37(b) are obtained as follows:

$$n = 1 + \frac{Z_{012}}{Z_{011}}, \quad Z_{02} = nZ_{012} \quad \text{and} \quad Z_{01} = n\left(\frac{Z_{011}Z_{022}}{Z_{011} + Z_{022} + Z_{012}}\right). \quad (3.51)$$

For the left pair (and also for the right pair because of symmetry)) of coupled lines in Figure 3-36(d), $Z_{012} = Z_{0t12} = 443.232\ \Omega$, $Z_{011} = Z_{0t1} = 67.7683\ \Omega$,

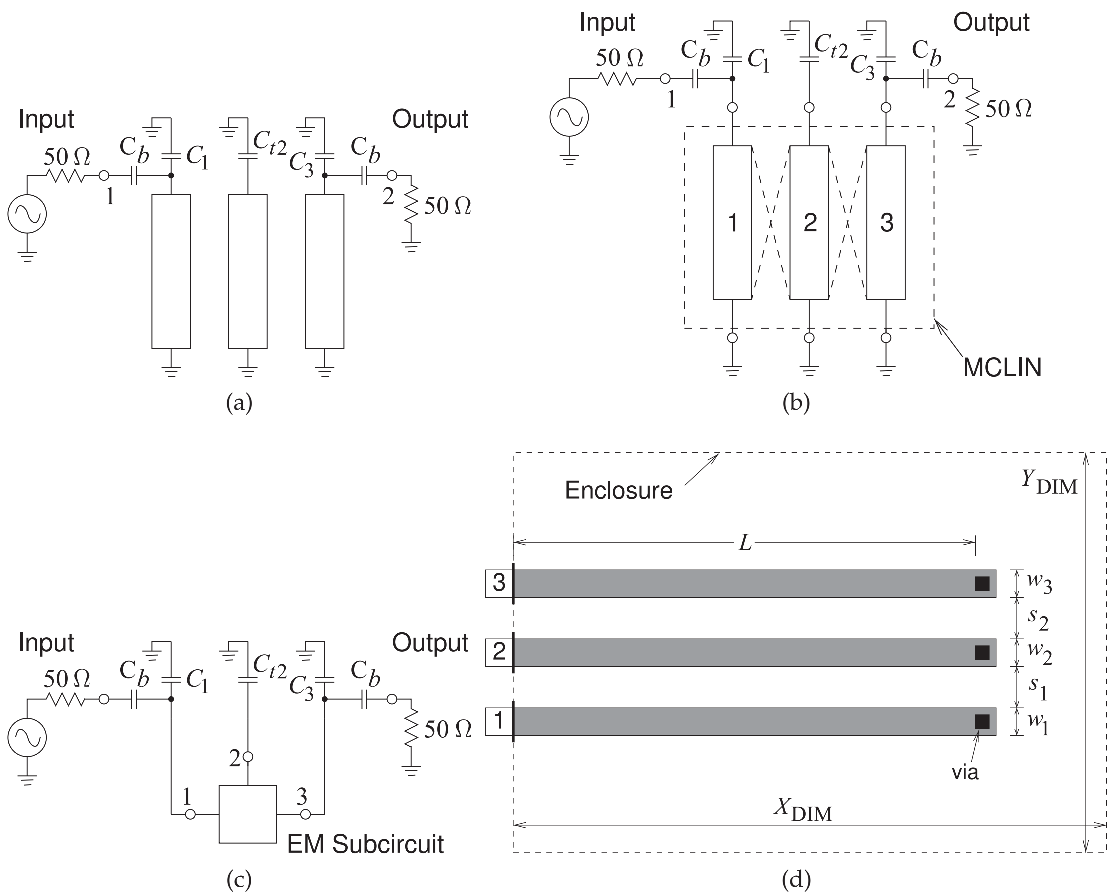

Figure 3-35: Physical layout of the combline bandpass filter designed in Section 3.4.1: (a) with discrete capacitors; (b) with a microstrip coupled transmission line element (MCLIN); (c) with an EM subcircuit block; and (d) the EM subcircuit block with layout to be simulated in an EM simulator. Details: 6 μm gold metalization, 635 μm thick alumina substrate with $\varepsilon_r = 10$, 400 μm × 400 μm tantalum vias, and the EM enclosure has perfectly conducting walls with $X_{\rm DIM} = 22$ mm, $Y_{\rm DIM} = 20$ mm, and height = 5.635 mm.

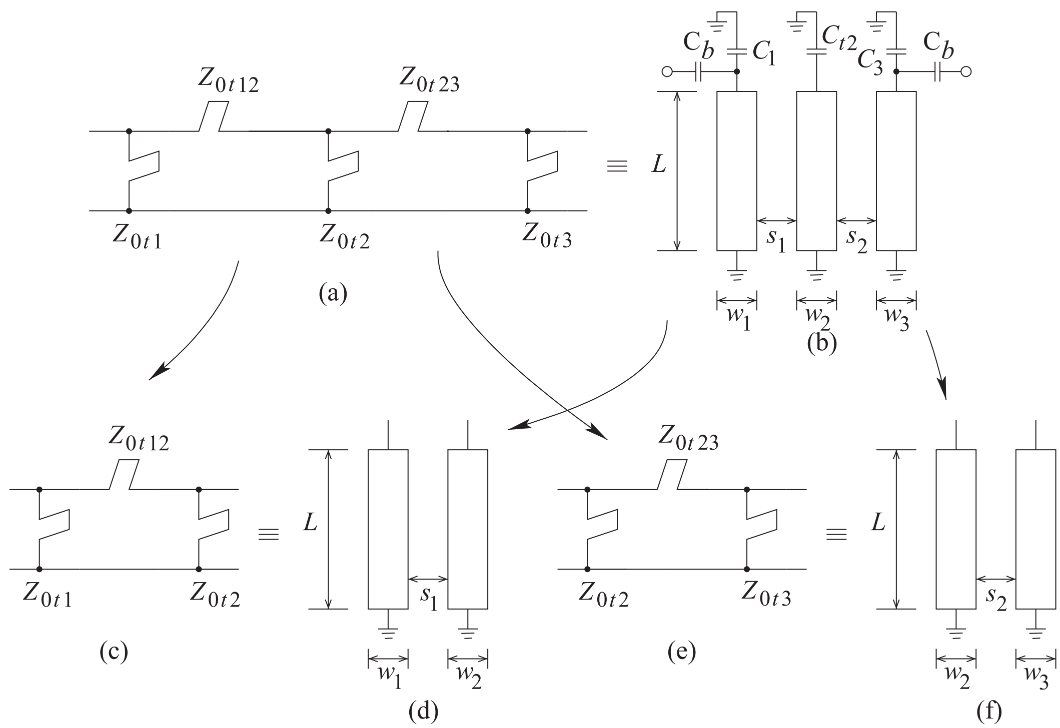

Figure 3-36: Physical design of the third-order combline bandpass filter. The double Pi network in (a) is partitioned into two Pi networks in (c) and (e). Similarly the three coupled microstrip lines in (b) are partitioned into two pairs of coupled lines in (d) and (f). Then physical design of the filter involves transforming the electrical design in (c) into the physical design in (d). Similarly the circuit in (e) is transformed into the layout in (f). With a shared central stub, the electrical circuit in (a) becomes the three coupled-line realization in (b).

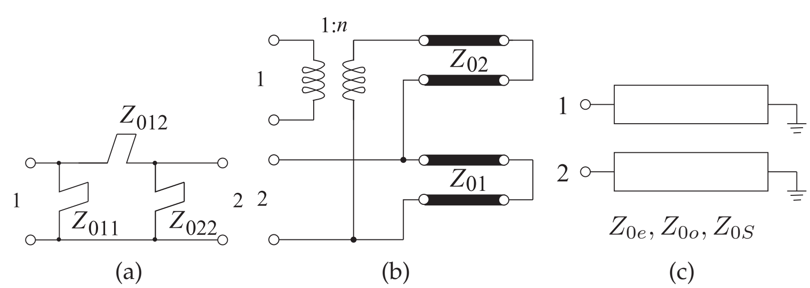

Figure 3-37: Equivalent circuits for a combline section (from Figure 3-13).

$Z_{022} = Z_{0t2} = 80\ \Omega$ and so[4]

$$n = 1 + \frac{Z_{012}}{Z_{011}} = 7.540, \quad Z_{02} = 3342\ \Omega, \quad \text{and} \quad Z_{01} = 69.17\ \Omega. \qquad (3.52)$$

[4] Note that the precision has been reduced. It was necessary to retain high precision during the electrical synthesis but the physical dimensions do not need the same precision.

The physical parameters of the coupled line pair in Figure 3-37(c) are derived using the results in Section 5.9.6 of [29]. Thus

$$K = 1/n = 0.1326. \tag{3.53}$$

From Equations (5.197) and (5.198) of [29] two estimates of the system impedance, Z_{0S}, are obtained:

$$Z_{0S,(3.54)} = Z_{01}\sqrt{1-K^2} = 68.56\ \Omega \tag{3.54}$$

$$Z_{0S,(3.55)} = Z_{02}\frac{K^2}{\sqrt{1-K^2}} = 59.30\ \Omega. \tag{3.55}$$

These two values of Z_{0S} are different and this is because the Pi arrangement of stubs is not symmetrical (i.e., in Figure 3-37(a) $(Z_{011} = 67.7\ \Omega) \neq (Z_{022} = 80\ \Omega)$).[5] The assumption behind the development of Equations (3.3) and (3.4) are that the pair of coupled lines is symmetrical. The only reasonable choice is to use the geometric mean of the two values. So

$$Z_{0S} = Z_{0S,\mathrm{mean}} = \sqrt{Z_{0S,(3.54)}Z_{0S,(3.55)}} = 63.77\ \Omega. \tag{3.56}$$

Then, from Equation (5.202) of [29],

$$Z_{0o} = Z_{0S}\sqrt{\frac{n-1}{n+1}} = 55.80\ \Omega, \quad Z_{0e} = \frac{Z_{0S}^2}{Z_{0o}} = 72.87\ \ \Omega, \text{ and } \quad \frac{Z_{0e}}{Z_{0o}} = 1.306. \tag{3.57}$$

The next step is to choose a substrate and realize the physical dimensions of the coupled lines. It is important that there be dimensional stability and that there be no multimoding. The best substrate for dimensional stability is a hard substrate like alumina, sapphire, or glass. Soft substrates like FR4 or teflon are too variable to be useful for filters. Alumina is particularly attractive as it is very hard and dimensions are reproducible. Alumina shrinks when it is processed but the amount of shrinkage is well controlled and reproducible. So once a design has been physically tuned, typically by drilling out part of the dielectric to change the effective permittivity, filters can be reliably reproduced and require only a small amount of adjustment. Alumina is polished to a well defined thickness and with a relative permittivity of around 10 a 50-Ω microstrip line has a width approximately equal to the thickness of the substrate. Having equal dimensions is a good thing to have for manufacturability. The thickness of the substrate must be decided on at this stage in design. A thicker substrate is less likely to crack during handling however a thicker substrate is more likely to support multimoding. Here a $(h =)\ 635\ \mu\mathrm{m}$-thick alumina substrate with $\varepsilon_r = 10$ is chosen and calculations (not shown here) indicate that there will not be multimoding at the filter's operating frequencies.

Physical dimensions could be derived by iteratively solving for Z_{0e} and Z_{0o} using the formulas in Section 5.6 of [29]. As an approximation, here the

[5] Thus error is being introduced at this step. In reality the final manufactured filter will need to be tuned anyway as the filter will require tolerances of about 0.1% or better and the best manufactured dimensional tolerance is usually about 1%. Also material parameters are usually not known to better than 1%. So this is an error that must be accepted.

physical dimensions are derived from Table 5-3 of [29]. Table 5-3 of [29] is for a system impedance, Z_{0S}, of $50\ \Omega$ and not the $63.77\ \Omega$ found here. Thus there will be an error, but it can be expected that there will be error in any case and these can be resolved using optimization in a simulator. From Table 5-3 of [29], the initial physical dimensions of the pairs of lines are

$$u = 0.93, w = uh = 591\ \mu\text{m}, \quad \text{thus with rounding} \ \ w_1 = w_2 = w_3 = 600\ \mu\text{m} \tag{3.58}$$

$$g = 1.0, s = gh = 635\ \mu\text{m}, \quad \text{thus with rounding} \ \ s_1 = s_2 = 650\ \mu\text{m} \tag{3.59}$$

The rounding has been done as for EM simulation the lines will be laid out on a regular grid and a $50\ \mu\text{m}$ grid is reasonable.

Scaling of Line Width

At this stage the error made with the characteristic impedance of the microstrip line should be considered. While any error can be corrected when optimizing the final design, making some correction at this stage will reduce the final adjustments needed. Three system impedances have been derived, $Z_{0S,(3.54)} = 68.56\ \Omega$, $Z_{0S,(3.55)} = 59.30\ \Omega$, and the geometric mean $Z_{0S,\text{mean}} = 63.77\ \Omega$. This divergence is one source of error. Another source of error is that a table for a $50\ \Omega$ system impedance was used to determine the coupled-line parameters. Note that the electrical design is exact and the tuning of the physical design will attempt to match the response of the physical circuit to that of the electrical design. However some initial corrections will reduce the amount of tuning that needs to be done.

Scaling for the higher actual system impedance ($63.77\ \Omega$ versus $50\ \Omega$) means using higher impedance microstrip lines (which will be narrower) and higher coupling impedance (requiring a greater separation of the lines). There are three possible characteristic impedance to scale to and a design decision needs to be made. Should the lines be scaled from $50\ \Omega$ to $54.2\ \Omega$, $68.6\ \Omega$, or $61.9\ \Omega$? The most conservative approach is to scale from $50\ \Omega$ to $54.2\ \Omega$, a factor of 1.08. Here only adjustment of the line widths will be considered and two correction approaches will be described. The first is based on the rule of thumb described in Example 3.4 of [29] which indicated that the characteristic impedance of the microstrip lines is approximately proportional to $1/\sqrt{w}$. So the line width should be reduced by a factor of $1.08^2 = 1.17$ to shift the characteristic impedance. Thus the line width should be reduced from $600\ \mu\text{m}$ to about $600\ \mu\text{m}/1.17 = 512\ \mu\text{m}$ or $500\ \mu\text{m}$ after rounding.

A second approach to correction is based on Table 3-3 of [29]. For $\varepsilon = 10$ and using the more conservative system impedance (i.e. $55.8\ \Omega$ which is closest to $50\ \Omega$), a better choice for u is to replace $u = 0.93$ by $u = 0.78$ and, after rounding, $w_1 = w_2 = w_3 = 500\ \mu\text{m}$. This cannot be expected to completely correct for the error, but it should be closer than the choice of $600\ \mu\text{m}$.

Scaling the system impedance should also require that s be increased but there is not a simple guideline to follow and so this will be skipped. Another reason for needing to increase s is that there is more coupling in our coupled line system than that predicted by considering two pairs of coupled lines. For example, there is coupling from lines 1 directly to line 3. To reduce the coupling s will need to be increased, perhaps significantly. Another source

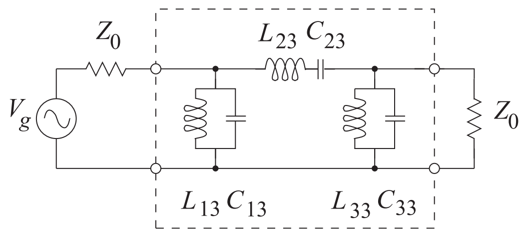

Figure 3-38: Lumped-element bandpass filter in a 50 Ω system. (Derived by multiplying the impedances in Figure 3-21 by 50.)
$Z_0 = 50\ \Omega$,
$C_{13} = C_{33} = 27.107$ pF,
$L_{13} = L_{33} = 934.47$ pH,
$C_{23} = 288.54$ fF, $L_{23} = 87.787$ nH.

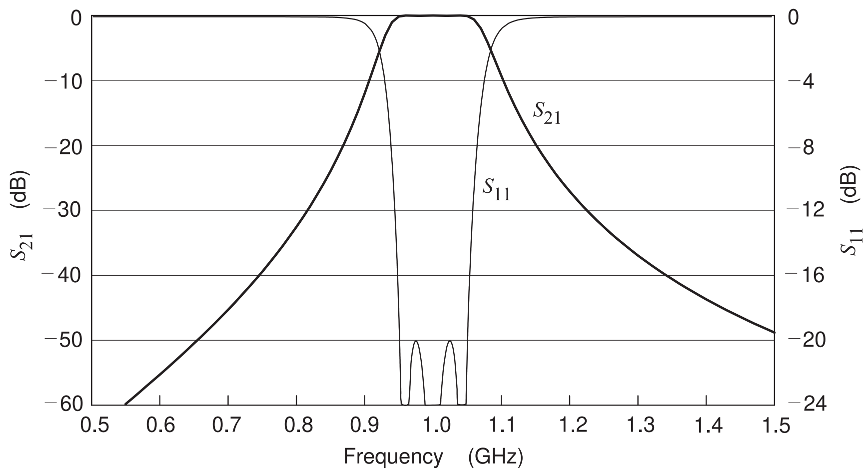

Figure 3-39: Return loss and insertion loss for the filter modeled using the lumped-element model.

of increased coupling is that the phase velocities of the even and odd modes differ. This tends to increase coupling. The adjustment of s is left to tuning of the physical design in an EM simulator.

Line Lengths

The stubs are one-eighth wavelength long at the center frequency of the filter. Thus the coupled lines are also one-eighth wavelength long. From Table 5-3 of [29], the effective relative permittivity of the even mode is $\varepsilon_{ee} = 7.24$ and for the odd mode is $\varepsilon_{eo} = 5.95$. These are quite different so the best that can be done is to use the geometric mean. Thus the effective relative permittivity is $\varepsilon_e = \sqrt{\varepsilon_{ee}\varepsilon_{eo}} = 6.56$. Thus at 1 GHz the line length $L = \lambda_8/8 = \lambda_0/\sqrt{\varepsilon_e} = (30\ \text{cm})/(8\sqrt{6.56}) = 14.64\ \text{mm}$ (14.65 mm with rounding). The use of a single effective permittivity in determining the lengths of the lines is perhaps the largest error and will result in the resonant frequency of each of the resonators, consisting of a capacitor (either C_1, C_{t2}, or C_3) and the $\lambda/8$-long line, being shifted from 1 GHz. The resonators can be re-centered by adjusting the capacitors. Adjusting the capacitance values also corrects for error in the widths of the lines since the main effect of an error in the width of a line is an error in its characteristic impedance and hence the input impedance of the resonator stub.

Microwave Circuit Simulation

Before simulating the combline filter the lumped-element bandpass filter will be considered to provide a benchmark. The 50-Ω lumped-element bandpass filter is shown in Figure 3-38. The responses of this filter is shown in Figures 3-39, 3-40, and 3-41. These responses provide a reference as the coupled-line

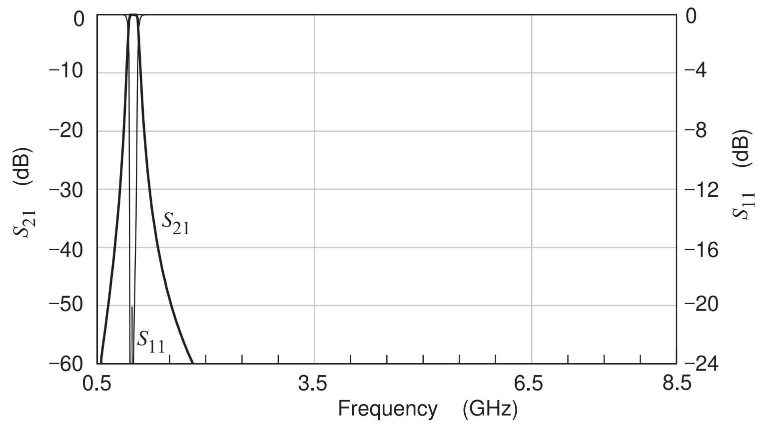

Figure 3-40: Wideband insertion loss and return loss for the filter modeled using the lumped-element model.

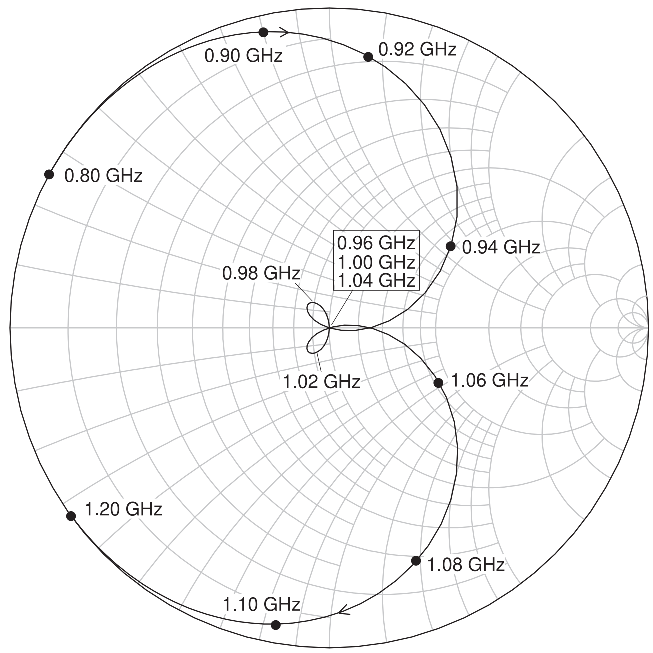

Figure 3-41: Plot of S_{11} on a Smith chart for the lumped-element bandpass filter. The zeros of the S_{11} response, and hence the poles of the S_{21} response, are at 0.96, 1.00, and 1.04 GHz. The looping near the origin is characteristic of Chebyshev filters.

filter design is optimized.

Figure 3-35(a) shows the combline filter to be modeled in a microwave circuit simulator. In a microwave simulator the filter can be modeled using a coupled microstrip element (known as the MCLIN element) or using EM simulation of an actual layout. The first set of results that will be presented uses the coupled microstrip element line model, the MCLIN element, and the filter model is as shown in Figure 3-35(b). The results of the circuit simulation are shown in Figure 3-42. The curves (a) are responses for a gap of $s = 650$ μm. The passband is too wide and this is reduced by increasing s to 1150 μm yielding curves (b). The effect of loss is seen with S_{21} less than 0 dB in the passband. The S_{21} response has a slight slope down in the passband and the S_{11} response does not show the three zeros seen in the lumped-element response, see Figure 3-39.

Plotting the S_{11} response of the MCLIN-based filter on a Smith chart, see Figure 3-43, provides more insight into what is happening. This should be contrasted to the S_{11} response of the lumped-element filter shown in Figure

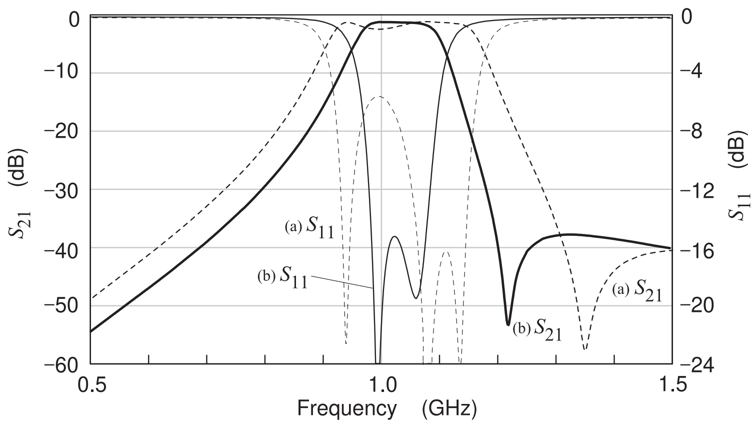

Figure 3-42: Insertion loss and return loss for the filter modeled using the MCLIN element with a line length of $L = 14{,}650$ µm and line widths $w_1 = w_2 = w_3 = 500$ µm. $C_1 = C_3 = 1.6428$ pF, $C_{t2} = 2.7076$ pF, and $C_b = 1.2217$ pF. For curves (a) $s_1 = s_2 = 650$ µm and for curves (b) $s_1 = s_2 = 1150$ µm.

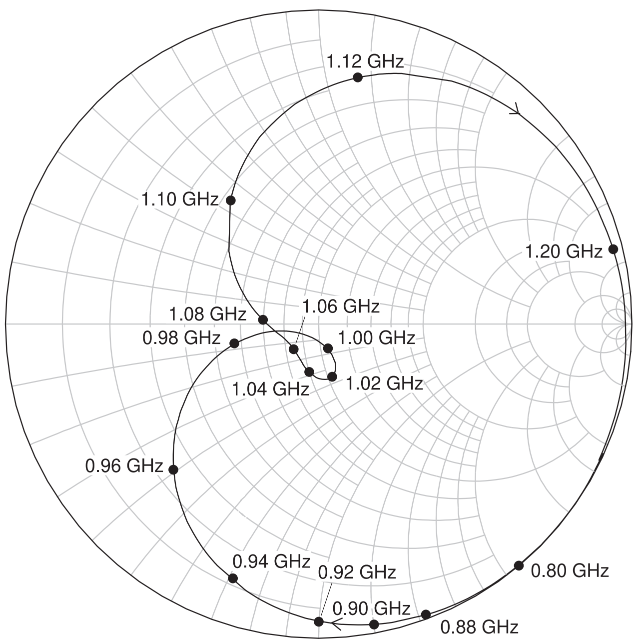

Figure 3-43: Plot of S_{11} on a Smith chart for filter modeled using the MCLIN element and gaps of $s_1 = s_2 = 1150$ µm and a line length of $L = 14{,}550$ µm and line widths $w_1 = w_2 = w_3 = 500$ µm. $C_1 = C_3 = 1.6428$ pF, $C_{t2} = 2.7076$ pF, and $C_b = 1.2217$ pF.

3-41. Recall that the lumped-element filter is the ideal electrical design. The looping of S_{11} at the origin in Figure 3-41 indicates that the ideal electrical response has three zeros as the locus of S_{11} passes through the origin three times. This behavior corresponds to the poles of the transmission response but these poles cannot be seen in the S_{21} response. Consequently in optimizing a filter the designer focuses on the S_{11} response.

Again consider the S_{11} responses of the two filters plotted on Smith charts (i.e. Figures 3-41 and 3-43). The S_{11} response of the lumped-element filter has two small loops corresponding to peaks in the in-band $|S_{11}|$ response seen in the rectangular plot of Figure 3-39. In contrast, the locus of S_{11} of the MCLIN-based filter does not go through the origin, see Figure 3-43, and there is one loop although the hint of a second loop is seen at 1.06 GHz. The performance is close to that required but optimization is necessary. In manually optimizing, also called tuning, the design of the MCLIN-based filter, both the rectangular and Smith chart plots should be overlaid with the lumped-element response. By adjusting C_1, C_{t2}, and C_3 (by 6%, 16%,

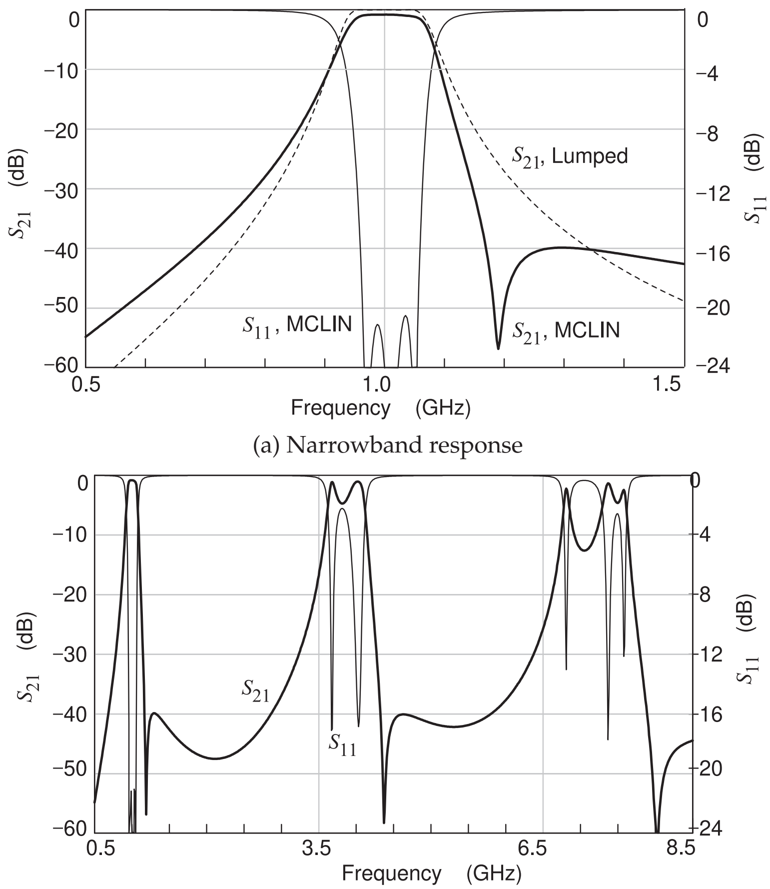

(b) Wideband response

Figure 3-44: Insertion loss and return loss for the filter modeled using the MCLIN element and gaps of $s_1 = s_2 = 1150$ µm and a line length of $L = 14{,}550$ µm and line widths $w_1 = w_2 = w_3 = 500$ µm. $C_1 = C_3 = 1.9076$ pF, $C_{t2} = 2.8748$ pF, and $C_b = 1.2217$ pF.

and 6% respectively), the resonant frequencies of the resonators are centered at 1 GHz and the filter response is also centered at 1 GHz[6]. The result of this tuning is shown in Figures 3-44 and 3-45 indicating that the required performance has been obtained.

In Figure 3-44(a) the MCLIN-based filter response is compared to the lumped-element response. The bandwidths of the MCLIN and lumped-element implementations are closely matched. The MCLIN implementation has the steep skirts resulting from the Chebyshev prototype. The Smith chart plot of S_{11} of the MCLIN-based filter is shown in Figure 3-45. The loops seen with the lumped-element response, in Figure 3-41, are seen but now there is an additional rotation with respect to frequency. This is because the MCLIN-based filter has additional transmission-line delays and hence frequency-dependent phase shift. Also the S_{11} response in Figure 3-45 is rotated by $180°$ from the S_{11} locus for the lumped-element filter (see Figure 3-41). This is because of the additional inverter at the input of the distributed filter design.

Some gross features are seen in the combline response that are not seen in the ideal electrical response. Referring to Figure 3-44(a), these include the additional zero seen in the S_{21} response at 1.2 GHz, the steeper skirt above

[6] Approximately, the resonant frequency of a resonator is inversely proportional to $\sqrt{C}$. So increasing the capacitances will reduce the center frequency of the filter.

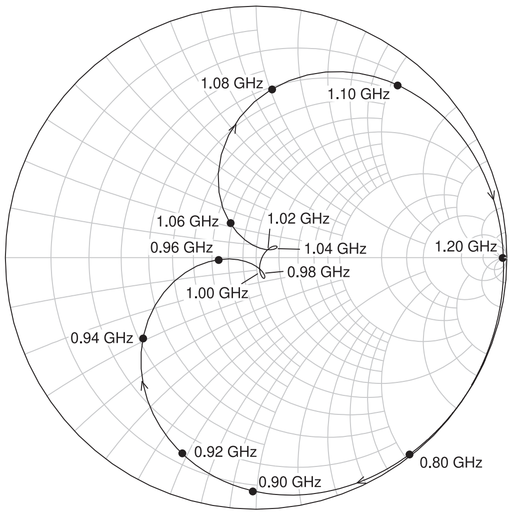

Figure 3-45: Plot of S_{11} on a Smith chart for filter modeled using the MCLIN element and gaps of $s_1 = s_2 = 1150$ µm and a line length of $L = 14{,}550$ µm and line widths $w_1 = w_2 = w_3 = 500$ µm. $C_1 = C_3 = 1.9076$ pF, $C_2 = 2.8748$ pF, and $C_b = 1.2217$ pF.

the 1 GHz passband, and the less-steep skirt below the passband. These are related. These features are common to PCL designs that use a combline. The origin of this behavior is the additional transmission path directly from the first line to the last line of the filter, the 1-3 coupling. During design the only transmission path considered was from line 1 to line 2, and then from line 2 to line 3, the 1-2-3 coupling. Apparently, at 1.2 GHz the 1-3 and 1-2-3 signals have the same magnitude but opposite phase and so cancel producing the S_{21} zero. Above the passband the signals on the two paths destructively interfere causing the steeper skirt. Below the passband the 1-3 and 1-2-3 signals constructively interfere and reduce the steepness of the filter skirt. The additional zero can be exploited to significantly reduce the level of a particular signal such as a local oscillator or a signal in a neighboring communication band. If the reduced filter skirt below the passband is not acceptable, then another arrangement of coupled lines should be used.

Figure 3-44(b) is a wideband response of the MCLIN-based filter and shows the spurious passbands that occur with most transmission-line based networks. In this case the properties of the lines are the same at $\lambda/8$, $5\lambda/8$, and $9\lambda/8$. So, by just considering the transmission lines alone it would be expected that there would be spurious passbands at 5 GHz and 9 GHz. The spurious passbands are lower because the impedances of the capacitances reduce at the higher frequencies, resulting in the passbands at four times and seven times the center frequency of the filter. In practice, a simple lowpass filter eliminates the spurious passbands. Often parasitics in the system do this without specific circuitry. Also, appropriate choice of matching networks can provide adequate elimination of the spurious passbands.

Before finalizing the filter layout, a more accurate EM simulation is required instead of using the MCLIN element. The EM simulation captures more subtle effects than can be included in the MCLIN model. The layout of the parallel coupled lines is shown in Figure 3-35(d) and the connection to incorporate these in a complete circuit simulation is shown in Figure 3-35(c). The results of the EM-based simulation are shown in Figures 3-46 and 3-47. It can be seen that the bandwidth of the filter reduces. Additional optimization would result in the EM-based filter response more closely matching the ideal electrical response.